# BRILLOUIN SPECTROSCOPY OF MACROMOLECULAR SOLUTIONS

Thesis for the Degree of Ph. D. MICHIGAN STATE UNIVERSITY DOUGLAS EDWARD NORDHAUS 1973



# This is to certify that the

#### thesis entitled

BRILLOUIN SPECTROSCOPY OF MACROMOLECULAR SOLUTIONS

presented by

DOUGLAS EDWARD NORDHAUS

has been accepted towards fulfillment of the requirements for

Ph.D degree in CHEMISTRY

Date JUNE 13, 1973

O-7639



#### **ABSTRACT**

BRILLOUIN SPECTROSCOPY OF
MACROMOLECULAR SOLUTIONS

Ву

Douglas Edward Nordhaus

Brillouin light scattering was evaluated as an experimental method for measuring the molecular weights of macromolecules. The thermodynamic theory of Miller was utilized in the calculations while its limitations were evaluated with the aid of the linearized hydrodynamic equations of Mountain as applied to a thermally relaxing liquid.

An instrumental procedure involving parameters associated with the optical quality was developed to experimentally separate the Rayleigh and Brillouin peaks over a range of scattering angles from 45 to 135 degrees. Brillouin spectra of benzene were taken and the isotropically scattered light identified, separated and measured. A good correspondence was found between the ratio  $J_{\rm V}$  obtained from the experimental measurements and from the calculations using Mountain's theory. This fact indicates that only isotropically scattered light was measured and that the correct spectral base line was selected.

An extensive cleaning and filtering procedure was also developed to give consistent scattering measurements from

sample solutions and some parameters of benzene were measured including a relaxation line, the "Mountain" line.

Brillouin spectra of macromolecular solutions were taken and it was found that for dilute solutions of polystyrene in benzene the solute did not affect the solvent parameters  $v_0$ ,  $v_\infty$ , and  $\tau$  to any measurable extent. This indicated that Miller's theory can be effectively applied to this solvent and solute combination. Six macromolecules, used as molecular weight standards and with different molecular weights, were measured with Brillouin scattering and the molecular weights calculated using Miller' theory. The final values compared well with other techniques previously used such as photometric light scattering and viscosity measurements, although the concentrations were about one order of magnitude smaller than needed for photometric measurements and the precision slightly lower.

A new sample scattering cell was designed for angular measurements from large macromolecules to eliminate reflected light from the back of the cell. This cell was subsequently used in the extrapolation of the scattered intensity measurements to zero concentration and zero scattering angle for large macromolecules and also for the measurement of the angular dependence of the Brillouin peak widths for the solvent benzene.

# BRILLOUIN SPECTROSCOPY OF MACROMOLECULAR SOLUTIONS

Ву

Douglas Edward Nordhaus

#### A THESIS

Submitted to
Michigan State University
in partial fulfillment of the requirement
for the degree of

DOCTOR OF PHILOSOPHY

Department of Chemistry



# TO MY PARENTS

Dr. and Mrs. E. A. NORDHAUS

#### **ACKNOWL** EDG EMENTS

The author wishes to express his deep appreciation to Professor J. B. Kinsinger for his guidance and patience during the preparation of this thesis and to the Chemistry Department of Michigan State University for its financial support.

Appreciation is also extended to Henry Yuen and Bill Toth for the many hours of stimulating discussion and their invaluable aid.

The author is particularly grateful to his parents for their continued encouragement and understanding.

#### TABLE OF CONTENTS

LI	ST OF TABLES	vi
LI	ST OF FIGURES	vi
ı.	INTRODUCTION	
	A-Historical Discussion	1 4
II.	THEORY	
	A-Light Scattering.  1-Time Independent Scattering Theory.  a-Scattering Processes.  b-Fluctuations.  c-Thermodynamic Theory.  2-Time Dependent Scattering Theory.  a-Pure Liquids.  (1) Fluctuations.  (2) Ideal Case.  (3) Relaxing Case.  b-Solutions.  (1) Mountain's Theory.  (2) Miller's Theory.  (3) Angular Corrections  3-Discussion.  B-Viscosity.  1-Theory.  2-Molecular Weight Determinations.	66 66 77 91 11 11 15 20 26 28 36 37 39 40
III.	EXPERIMENT  A-Light Scattering	43
	1-Instrument a-Laser. b-Interferometer c-Aperatures and Optics. d-Alignment e-Detection and Recording 2-Scattering Cell. a-Shape. b-Size. c-Holder	43 43 45 50 52 53 53 63 63

	3-Materials and Preparation	65
	a-Polystyrenes	65
	b-Solvents	65
	c-Filtration	66
	d-Glassware	67
	e-Solutions	69
	4-Spectra	69
	a-Shapes	69
	b-Baseline	71
	c-Peak Areas	73
	5-Spectral Analysis	75
	a-Solvents	75
	(1) Mirror Separation	75
	(2) Angular Measurements	77
	(3) Polarization Measurements	83
	(4) Experimental Values	83
	b-Solutions	87
	(1) Peak Widths and Frequency Shifts	87
	(2) Molecular Weight Determination	91
	6-Discussion	101
	B-Viscosity	105
	1-Constant Temperature Bath	106
	2-Viscometer	106
	3-Solutions	108
IV.	SUMMARY and CONCLUSIONS	113
	BIBLIOGRAPHY	115
	APPENDIX	119

# LIST OF TABLES

TABLE	DESCRIPTION	Page
2.	Identification of When Brillouin Peak Overlap Occurs	74 88 94 95
	LIST OF FIGURES	
FIGUR	E DESCRIPTION	Page
	Rayleigh-Brillouin Spectrophotometer Brillouin Spectrum of Benzene-Three	44
3.	Consecutive Orders, Intensity vs Frequency Cylindrical Scattering Cell-Original and Filled Brillouin Spectrum of Benzene-45 Degrees	49 55
	Scattering Angle, Intensity vs Frequency Brillouin Spectrum of Benzene-135 Degrees	56
	Scattering Angle, Intensity vs Frequency Brillouin Spectrum of Benzene-90 Degrees	57
	Scattering Angle, Intensity vs Frequency Brillouin Frequency Shifts from Benzene-Relative	58
	Angular Dependence of Incident and Reflected Light Brewster Light Scattering Cell	60 62
9.	Light Scattering Cell Holder	64
	Refluxing Column for Scattering Cell Relative Dependence of Brillouin Peak Separation	68
12	on Interferometer Mirror Spacing for Benzene Relative Brillouin Peak Separation for Benzene	76
13.	and a Polystyrene Solution	79 81
14.	Angular Dependence of the Scattering Ratio J for Benzene	82
15.	Concentration Dependence of Rayleigh and Brillouin Peak Half-Widths for Polystyrene in Benzene-(A) Brillouin, (B) Rayleigh,	90
16.	(C) True Brillouin Half-Width	90
	Benzene (A) $\overline{M}_W = 48,000$ , (B) $\overline{M}_W = 78,400$ , (C) $\overline{M}_W = 124,000$ , (D) $\overline{M}_W = 194,000$ , (E) $\overline{M}_W = 260,000$	93 00.

		Page
17.	Molecular Weight Measurement of Polystyrene in Benzene. $\overline{M}_{W} = 1.85 \times 10^{6}$	97
18.	Brillouin Spectrum of Polystyrene in Benzene at 45 Degrees Scattering Angle,	
	$c_2 = 0.038\%, \overline{M}_W = 1.85 \times 10^6$	98
19.	Brillouin Spectrum of Polystyrene in Benzene at 90 Degrees Scattering Angle,	
	$c_2 = 0.038\%, \overline{M}_W = 1.85 \times 10^6$	99
20.	Brillouin Spectrum of Polystyrene in Benzene at 135 Degrees Scattering Angle,	
	$c_2 = 0.038\%, \overline{M}_W = 1.85 \times 10^6$	100
22. 23.	Constant Temperature Water Bath	107 110 111 112
<b>24.</b>	Viscosity of Polystyrene in Benzene at 30.0°C	1.

#### I.Introduction

#### A-Historical Discussion

Scattered light has excited man's imagination for thousands of years as seen by his frequent attempts to explain common phenomena such as the origin of the blue sky and the red sunset. Experimentally Tyndall [1] produced the scattering effect of a "blue sky" by passing a beam of white light through a tube of small suspended particles from the mixed vapors of butyl nitrate and hydrochloric acid. Unfortunately his attempts to explain this scattering process were unsuccessful as were the attempts of many others before him, but in 1871 a theoretical paper based on his work was written by Lord Rayleigh [2] which correctly identified the process as one of diffraction. Using this theory, one could predict other properties from scattering such as the angular dependence of the scattered intensity from horizontally polarized incident light and the dependence of the intensity on the fourth power of the wave-length. Thus Lord Rayleigh initiated the science of light scattering as it is presently known.

Since Rayleigh's original theory [3,4] dealt only with small, simple, and noninteracting particles, others made an effort to extend his theory to solids and liquids. These attempts met with many difficulties since in a liquid the positions and interactions of individual particles are interdependent and thus can not be simply summed as had previously been done; thus Lord Rayleigh's theory had to be modified or

completely changed.

In a liquid, the physical properties at equilibrium are practically always equal to their mean values with great accuracy, although small deviations from these mean values do occur and can be described by fluctuation theory. Einstein [5] utilized the idea of fluctuations in a liquid to modify Rayleigh's earlier theory and calculated light scattering intensities for liquids and solutions.

All the theoretical work on light scattering processes up to this time, including Einstein's theory, dealt only with the intensity of the scattered light and entirely neglected any frequency dependence. This deficiency was finally remedied in a paper by Brillouin [6] who predicted that light is actually inelastically scattered from a liquid because of the presence of thermally excited acoustic or pressure waves. The incident light shifted in frequency due to this inelastic scattering is related directly to the velocity of the thermal waves in the liquid. Gross[7] experimentally verified this theory a short time later, but the experimental techniques were so difficult and the accuracy so poor that few experiments were ever attempted [8]. Most researchers instead directed their attention either to Raman scattering or to elastic light scattering.

The study of elastic light scattering developed rapidly and led to solution studies of polymers in which Debye [9] made an important contribution. By measuring the extra scattering from a solution over that of the same pure liquid,

he could count the number of molecules per unit volume and so determine the molecular weight of a macromolecule. But with macromolecules, the intensity of vertically polarized scattered light varies with the scattering angle, whereas for small molecules no variation is noticeable. To correct for this angular dependence and another effect due to the non-ideal behavior of solutions, Zimm [10] and his co-workers devised a double extrapolation plot to zero concentration and zero scattering angle in order to obtain a correct molecular weight for large macromolecules. Since then the theoretical development and experimental techniques have changed only slightly [11].

In the early 1960's the development of a powerful new optical source, the laser [12], now made Brillouin scattering a viable technique [13,14] in the study of liquids and solutions. The major advantages that this new source offered included both a very high intensity of polarized light and a very narrow frequency distribution. Those two properties were the main deterrents to obtaining good Brillouin spectra earlier, since it was necessary to separate three closely spaced peaks. When intensity is plotted against frequency, the Brillouin spectra of liquids are very simple consisting of a central peak resulting from elastically scattered light, the Rayleigh peak, and two symmetrical frequency shifted peaks on either side of the Rayleigh peak resulting from inelastically scattered light. It was observed that a macromolecule

added in small quantities to a pure liquid greatly increased the total amount of scattering from a liquid but this change was noticeable only in the intensity of the central peak [15,16]. The two frequency shifted side peaks related exclusively to the solvent and were unaffected by the solute. Thus, the increased scattering of a solution could be measured by relating the increased intensity of the central peak to the constant intensity of the two shifted peaks which could thereby act as internal standards.

A theory for the ratio of the intensity of the central peak to the frequency shifted peaks or Brillouin peaks,  $^{\rm I}{\rm c/_{2I}_{B}}$ , was developed by Miller [17] using strictly thermodynamic arguments. Subsequently it was applied to determine the molecular weight of a macromolecule in the same manner as Debye previously had done with elastic light scattering, but the primary assumptions made were never experimentally verified. Simultaneously Mountain [18,19] developed a theory which calculated the total frequency spectra of scattered light in the Brillouin-Rayleigh region in liquid mixtures. This theory included relaxation effects due to the solvent which can modify the Brillouin spectra sufficiently to render Miller's theory valid only under restricted circumstances.

#### **B-Purpose**

This thesis will examine experimentally the theory of Miller [17] for determining the molecular weights of macromolecules in solution, using Brillouin light scatter-

ing. The limitations which must be observed will be analyzed in the context of Mountain's theory [19] for solutions in thermally relaxing liquids, and experimentally verified where possible. A comparison between molecular weights obtained from Brillouin light scattering and other methods for a series of high molecular weight polystyrenes will be made along with a general comparison of this method with regular elastic light scattering [11] to evaluate major advantages and disadvantages.

#### II-Theory

#### A-Light Scattering

# 1-Time Independent Scattering Theory

#### a-Scattering Processes

Light scattering is a general phenomenon which occurs whenever electromagnetic radiation in the visible region interacts with matter. If a particle is small compared with the wave-length of light and sufficiently isotropic to be polarized in the direction of the incident electric vector, the exciting field will induce a dipole moment in the particle as it interacts with the field [20]. This dipole oscillates in phase with the original radiation and becomes a secondary source of energy, which emits light in all directions with the same frequency as that of the incident radiation. This induced dipole moment vector  $\mathbf{p_i}$ , is a function of the polarizability tensor  $\alpha_{\mathbf{i},\mathbf{j}}$  of a particle since the induced dipole is dependent on the shape of the particle and on the amplitude of the exciting radiation vector  $\mathbf{E_i}$ .

$$P_{i} = \alpha_{i,j} \cdot E_{i}$$

This is an expression for the dipole induced in a particle by a radiation field and can be used in Maxwell's electromagnetic equations to obtain a scattering equation for independent particles which are small compared to the wave-length of light. Unfortunately this theory specifically

applies to a dilute gas since in a liquid a particle is not independent of other particles in its position or properties.

A different and more practical approach to calculating the scattered intensity from a liquid is to consider it as a continuum instead of a collection of individual atoms. If the liquid is dense and homogeneous, the scattered intensity should be zero because the phases of the radiation scattered by each particle destructively interfere with each other. However, a pure liquid does scatter light. This is the result of optical inhomogeneities or fluctuations within the liquid which are due to the random thermal motions of the molecules [5].

#### b-Fluctuations

A statistical thermodynamic approach is taken to describe the fluctuations present in a liquid but the models require the system to be both isotropic and continuous. These conditions imply that the polarization vector of the incident light is not rotated during the scattering process (isotropic media) and the mean free path of the molecules in a liquid is much shorter than the wavelength of light in the media.

In a pure liquid, fluctuations are very small changes in the average value of some property of a liquid, for example fluctuations in the density. If these fluctuations affect the dielectric constant, light passing through the liquid will be scattered and the intensity will depend on

the extent to which the fluctuations are coupled to the dielectric constant. Because of the fluctuations, the dielectric constant can be separated into an average value,  $\mathbf{\epsilon}_0$ , and a fluctuating part  $\Delta \mathbf{\epsilon}_{i,j}$ . [20] This latter term accounts for the total optical inhomogeneities in a liquid and the total light scattered. We can now write the dielectric constant as follows:

$$\epsilon_{i,j} = \epsilon_0 \delta_{i,j} + \Delta \epsilon_{i,j}$$

The second term can be further divided into two terms, the isotropic part,  $\Delta \mathbf{E}$ , and the anisotropic part  $\Delta \mathbf{E}_{\text{i.i.}}^{\prime}$ .

$$\Delta \epsilon_{i,j} = \Delta \epsilon \cdot \delta_{i,j} + \Delta \epsilon'_{i,j};$$

$$\sum_{i=1}^{3} \Delta \boldsymbol{\epsilon'}_{i,i} = 0$$

The first term on the right side is due to isotropic fluctuations and is simply described by a set of statistically independent thermal variables such as density and temperature or entropy and pressure. The anisotropic part  $\Delta \mathcal{E}'_{i,j}$ , has not been fully described by theory but appears to be partly due to fluctuations in the orientation of anistropic molecules. Since there is no agreement on its evaluation [21], we set  $\Delta \mathcal{E}'_{i,j}$  equal to zero for our theoretical and experimental development.

#### c-Thermodynamic Theory

The intensity of the scattered light can be obtained by beginning with Maxwell's electromagnetic equations [19] and using the assumption that only first order terms are necessary to describe the scattering. The total scattering volume in a liquid V, is divided into a number of small parts  $V^*$ , in such a way that each of the parts contains a sufficient number of atoms to be independent of the others, yet small compared to the wave-length of light. The fluctuations in the dielectric constant of each volume  $\Delta \mathbf{E}_{V^*}$ , are related to  $\Delta \mathbf{E}$  for the total scattering volume since both have the same density dependence. Maxwell's equation for the scattered intensity is

$$I_{\text{scatt}} = I_0 \frac{\pi^2 v}{\lambda^4 r^2} \sin^2 \theta < (\Delta \mathcal{E})^2 > \frac{4}{\sqrt{2}}$$

The components of this equation are V, the scattering volume, L, the distance between the scattering volume and the detector,  $\lambda$ , the wave-length of the incident light in the medium,  $\theta$ , the viewing angle for the scattered light, and  $<(\Delta \, \boldsymbol{\xi}\,)^2>$ , the average value of the square of the fluctuations in the dielectric constant. This is the time independent scattering equation for which the values of all the terms can be measured except for the last term  $<(\Delta \, \boldsymbol{\xi}\,)^2>$ .

Einstein derived the value of this last term using statistical thermodynamics by separating the fluctuations in the dielectric constant into two statistically

independent parts.

$$\Delta \mathbf{\mathcal{E}} = \left(\frac{\partial \mathbf{\mathcal{E}}}{\partial \mathbf{S}}\right)_{\mathbf{P}} \Delta \mathbf{S} + \left(\frac{\partial \mathbf{\mathcal{E}}}{\partial \mathbf{P}}\right)_{\mathbf{S}} \Delta \mathbf{P}$$

In Brillouin spectroscopy, it is possible to separate experimentally these two contributions [7] since the part of the scattered light due to the pressure fluctuations  $\Delta P$ , is shifted in frequency sufficiently to separate it from the entropy fluctuations,  $\Delta S$ . Consequently an intensity ratio of the nonfrequency shifted light to that of the shifted components (there is both a positive and a negative frequency shift) is related to the ratio of the entropy and pressure fluctuations.

$$\frac{\mathbf{I}_{\mathbf{C}}}{2\mathbf{I}_{\mathbf{B}}} = \frac{\left(\frac{\partial \mathbf{E}}{\partial \mathbf{S}}\right)_{\mathbf{P}}^{2} < (\Delta \mathbf{E})^{2} >_{\mathbf{P}}}{\left(\frac{\partial \mathbf{E}}{\partial \mathbf{P}}\right)_{\mathbf{S}}^{2} < (\Delta \mathbf{E})^{2} >_{\mathbf{S}}}$$

This relation has been reduced by Landau and Placzek [22] to a very simple form by using the assumption that

$$\left(\frac{\partial \mathbf{E}}{\partial \mathbf{P}}\right)_{\mathbf{T}} = \frac{-\beta_{\mathbf{T}}}{\alpha} \left(\frac{\partial \mathbf{E}}{\partial \mathbf{T}}\right)_{\mathbf{P}}$$

The Landau-Placzek ratio is defined as,

$$\frac{I_{C}}{2I_{B}} = \gamma - 1 \quad ; \quad \gamma = \frac{C_{P}}{C_{V}}$$

However, in the event that the thermodynamic parameters do vary with the measurement frequency, this thermodynamic derivation is not sufficiently accurate [23]. A variation with frequency often appears to be present in liquids because the measured Landau-Placzek ratio is usually larger than calculated and another parameter, namely the velocity of sound, which is related to the adiabatic compressibility, also increases when measured at increasing frequencies [22]. Thus a different theory is necessary which will lead to a better correspondence between theoretical and experimental results when a dispersion in these terms is present.

### 2-Time Dependent Scattering Theory

# a-Pure Liquids

#### (1) Fluctuations

The frequency shifted light due to pressure fluctuations is caused by molecular motions which, according to ...

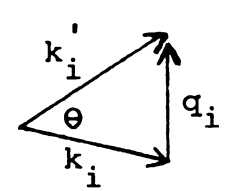
Debye's theory of heat in a solid [24], are a superposition of longitudinal and transverse waves of different frequencies. Liquids also contain these waves except that the transverse waves are almost nonexistent since the viscosity of a liquid is usually very low. Energy to excite the longitudinal waves is readily available in the liquid since the energy per phonon is much less than the energy available as heat.

Therefore at room temperature the frequency of the phonon,  $\Omega$  may have any value up to about  $10^{12}$  Hz.

Each propagating longitudinal wave is a periodic variation of the density and so will scatter light in a manner similar to the scattering of x-rays from the planes in a crystal in that both types of scattering must follow Bragg's law. This requires that the sum of the vectors for the incident wave  $k_i$ , the scattered wave  $k_i$ , and the sound wave  $q_i$  is equal to zero, or

$$k_{i}' = k_{i} + q_{i}. 10$$

Graphically, this is



The value of  $q_i$  is approximated by assuming that  $|k_i| = |k_i'|$ , since the scattered wave differs from the incident wave only by a very small amount. This assumption makes the vector triangle isosceles and therefore determines the value of the sound wave  $q_i$  when the scattering angle  $\theta$  is selected.

$$q_i = 2k_i \sin(\Theta/2) \qquad \qquad \underline{11}$$

The wave vectors for light and sound are respectively

$$k_i = 2\pi/\lambda$$
 and  $q_i = 2\pi/\lambda_s = 2\pi \nu_s/v_s$ , with  $\lambda$  and  $\lambda_s$ 

the wave-lengths of light and sound in the media,  $V_s$  the sound frequency, and  $v_s$  the sound velocity. Substituting in the above equation, we obtain equations for the characteristic properties of the sound wave. Letting  $\lambda = \lambda_0/n$ , with n the refractive index of the scattering media,

$$v_s = V_s \quad \lambda_0 / [2n \sin(\Theta/2)]$$
 12

$$\lambda_{s} = \lambda_{0} / [2n \sin(\Theta/2)]$$

$$V_s = \frac{v_s}{\lambda_0} [2n \sin(\theta/2)]$$
 14

The velocity of sound in a liquid can be calculated according to equation  $\underline{12}$  by measuring the frequency shift  $V_s$  of the Brillouin peaks, and substituting in the known values of the scattering angle, refractive index of the liquid and the wave-length of light in vacuo. In equation 13, the wave-length of the sound waves is dependent on the scattering angle and is of the same order of magnitude as the wave-length of the incident light waves, while the ultra high acoustic frequency of the waves can be calculated either from equation 14 or directly measured from the spectra. Examining equation 12 more closely and recognizing that at increasing scattering angles the scattered light is from sound waves of increasing frequency, we can measure the dispersion in the velocity of sound by simply changing the scattering angle. It will be noted here that the theoretical velocity dependence of the sound wave on the increasing scattering vector exhibits

a slight negative dispersion in light scattering and must be interpreted differently from acoustic propagation experiments [25].

The scattered light is considered to be shifted in frequency, either increasing or decreasing the original energy of the radiation, corresponding to the annihilation or creation of a phonon in the liquid. Since the phonon population is large at room temperature, the equilibrium population is maintained if energies of the incident light are less than 10<sup>5</sup> milliwatts per square centimeter [26]. This is still well in excess of the energies we use in laser scattering, indicating we are not disturbing the system during our measurements and hence are measuring liquids in thermal equilibrium.

The shortest pressure fluctuation that can be measured by Brillouin scattering is dependent on the incident wavelength of light.

$$(\lambda_s)_{\text{minimum}} = \lambda_0/2n$$
 15

This fluctuation is about  $10^{-5}$  cm. in length and has a frequency of  $10^{10}$  Hz. In terms of molecular sizes, these are very long fluctuations, so the scattered light can be interpreted as coming from coherent fluctuations in the pressure.

Associated with these pressure fluctuations are independent fluctuations in the entropy which cannot be included in Debye's purely mechanical description of heat motion because they do not propagate in the form of waves. In comparison to the coherent pressure fluctuations, entropy fluctuations occur only over a short range, and are related to the short range motions of the thermal diffusion process. Hence these are considered as incoherent processes. Thus Brillouin spectroscopy can be used to measure these two types of fluctuations but requires the scattered light to be sufficiently separated into two parts due to (1) frequency shifted light from pressure fluctuations and (2) light not shifted in frequency from entropy fluctuations. For an isotropic liquid in which the scattered light does not depend on the direction of the incident light vector  $\mathbf{k_i}$ , it has been established using Onsager's symmetry relations that the spectrum contains only those two frequency shifted lines [27].

# (2)-Ideal Case

Since the pressure and entropy fluctuations in a liquid are time dependent, these fluctuations can be calculated by adapting thermodynamic and hydrodynamic equations to the calculations. An approximate theory of the fluctuations employing both of these processes to account for the temporal dependence has been developed by Mountain to explain the frequency shifted light in the Rayleigh-Brillouin region [28]. Since this is a phenomenological theory which treats a liquid as a continuum, it should be strictly valid only for measurements at long wave-lengths and low frequencies. The fluctuations that scatter light are long,  $10^{-5}$ cm, compared with molecular sizes although the frequency,  $10^{10}$ 

is much higher than usually encountered in hydrodynamics. This theory should still apply up to frequencies close to the reciprocal of the collision time,  $10^{12}$  to  $10^{14}$  Hz [29,30,31]. This implies that some properties may have a significant frequency dependence, and for those cases a modified or completely different approach must be used.

Mountain's theory begins with the neutron scattering equation of van Hove [32] which has been modified for light scattering [33].

$$I(r_{i},t) = I_{0} \frac{\pi^{2} v}{\lambda^{4} L^{2}} \sin^{2}\theta \int \int \langle \Delta \mathbf{E}(r_{1},t_{1}) \cdot \Delta \mathbf{E}(r_{2},t_{2}) \rangle$$

$$\cdot e^{i \mathbf{W}(t_{2}-t_{1}) - ik_{i}(r_{2}-r_{1})} dr_{2} dr_{1} dt_{2} dt_{1}$$

$$\frac{16}{2}$$

The fluctuations in the dielectric constant are a function of the two statistically independent variables, density and temperature. Since the temperature fluctuations are small compared to those of the density [34], we can neglect the temperature fluctuations and obtain the resulting equation

$$I(r_{i},t) = I_{0} \frac{\pi^{2}v}{\lambda^{4}L^{2}} \sin^{2}\theta \left(\frac{\partial \mathbf{E}}{\partial \rho}\right)^{2}_{T} \int \langle \Delta \rho (r_{1},t_{1}) \Delta \rho (r_{2},t_{2}) \rangle$$

$$\cdot e^{i\mathbf{Q}(t_{2}-t_{1})-ik_{1}(r_{2}-r_{1})} dr_{2} dr_{1} dt_{2} dt_{1}$$

$$\frac{17}{2}$$

Introducing the Fourier-Laplace transform of the density fluctuations and letting  $r_j = r_2 - r_1$  and  $t_j = t_2 - t_1$ ,

we have

$$\rho(k_{i}, \omega) = \iint e^{ik_{i} \cdot r_{j}} - i\omega t_{j} \Delta \rho(r_{j}, t_{j}) dr_{j} dt_{j}$$

$$= \underbrace{18}$$

Now equation 17 can be written as

$$I(k_{i}, \boldsymbol{\omega}) = I_{O} \frac{\pi^{2} V}{\lambda_{T}^{4} 2} \left( \frac{\partial \epsilon}{\partial \rho} \right)_{T}^{2} \sin^{2} \theta \langle \rho(k_{i}, \boldsymbol{\omega}) \cdot \rho(-k_{i}) \rangle \qquad \underline{19}$$

where the last term in brackets is

$$\rho(k_{i}, \boldsymbol{\omega}) \cdot \rho(-k_{i}) = 2Re \int_{0}^{\infty} e^{-i\boldsymbol{\omega}t} \rho(k_{i}, t) \cdot \rho(-k_{i}) dt \qquad \underline{20}$$

Either of two different sets of independent variables can now be selected to calculate the time dependence of the fluctuations in the system; entropy and pressure, or density and temperature. Either set has inherent advantages and disadvantages in the calculations but the final equations are identical. We will follow Mountain's original derivation [28] using the latter set and begin with the linearized hydrodynamic equations. The deviation from equilibrium is assumed to be very small so that we can expand the mass density  $\rho$ , and the temperature T, about their equilibrium values  $\rho_0$ ,  $\sigma_0$ .

$$\rho = \rho_0 + \rho_1$$

$$T = T_0 + T_1$$

Using these terms, the linearized hydrodynamic equations are:

Equation of Continuity

$$\frac{\partial \rho_1}{\partial t} + \rho_0 \operatorname{div} v_i = 0$$

#### Navier-Stokes Equation

$$\rho_{0} \frac{\partial v_{i}}{\partial t} + \frac{v_{0}^{2}}{\gamma} \operatorname{grad} \rho_{1} + \frac{v_{0}^{2} \alpha \rho_{0}}{\gamma} \operatorname{grad} T_{1}$$

$$- (\frac{4}{3} \boldsymbol{\eta}_{s} + \boldsymbol{\eta}_{B}) \operatorname{grad} \operatorname{div} v_{i} = 0$$

$$\underline{23}$$

#### Energy Transport Equation

$$\rho_0 \, c_v \, \frac{\partial^T_1}{\partial t} - \frac{c_v \, (\gamma - 1)}{\alpha} \cdot \frac{\partial \rho_1}{\partial t} - \lambda' \, \text{grad grad } T_1 = 0$$

The components of these three equations are the thermal expansion coefficient  $\alpha$ , thermal conductivity  $\lambda'$ , ratio of specific heats  $\gamma = \frac{C_p}{C_v}$ , low frequency sound velocity  $V_0$ , and the shear and bulk viscosities  $\gamma_S$  and  $\gamma_B$  respectively. Since we have assumed only small deviations about the equilibrium values and a low viscosity, we can then neglect the transverse part of the velocity. This limits the following derivation to liquids where angular correlations between particles are not important. Also the concept of local thermodynamic equilibrium is assumed, so that the usual pressure and entropy terms can be replaced

with thermodynamic relations involving density and temperature.

According to Mountain's theory, these equations are now solved for the time dependence of the density fluctuations by first eliminating the velocity and obtaining two equations in the density and temperature. The space-time transforms of two equations are then taken and the resulting equations are solved in terms of the new variables. Subsequently the Laplace transform is taken and the ensemble average of the  $k^{\mbox{th}}$  component calculated over the initial values. Finally the frequency transform is calculated to give the final equation to describe the frequency dependence  $\omega$  , of the scattered light.

$$\begin{split} \text{I}(k,\omega) &= \text{I}_{0} \frac{\pi^{2} \text{V}}{\lambda^{4} \text{L}^{2}} \sin^{2} \theta \left( \frac{\delta \epsilon}{\delta \rho} \right)^{2} \rho_{0} \text{T} \beta_{\text{T}} \\ &+ \frac{1}{\gamma} \left[ \frac{\Gamma k^{2}}{(\Gamma k^{2})^{2} + (\omega + \nu_{0} k)^{2}} + \frac{\Gamma k^{2}}{(\Gamma k^{2})^{2} + (\omega - \nu_{0} k)^{2}} \right] \\ &+ \frac{2\lambda^{1} k^{2}}{(\Gamma k^{2})^{2} + (\omega + \nu_{0} k)^{2}} + \frac{\Gamma k^{2}}{(\Gamma k^{2})^{2} + (\omega - \nu_{0} k)^{2}} \\ &+ \frac{25}{(2 + 1)^{2} + (\omega + \nu_{0} k)^{2}} \end{split}$$

where

$$\Gamma = \frac{1}{2\rho_{O}} \left[ \frac{4}{3} \boldsymbol{\eta}_{S} + \boldsymbol{\eta}_{B} + \frac{\lambda^{1}}{C_{p}} (\boldsymbol{\gamma}-1) \right]$$
 26

The first term in the braces in equation  $\underline{25}$  represents the unshifted or Rayleigh peak while the other two terms represent the Brillouin doublet which is shifted in frequency by the amount  $v_0k$ . It is evident from equation  $\underline{25}$ 

that a ratio of the unshifted to the shifted components gives the Landau-Placzek ratio of vertically polarized light originally derived using only equilibrium thermodynamics and which we have mentioned earlier in equation 8.

$$\left(\frac{I_{C}}{2I_{B}}\right)_{V} = \gamma - 1$$

Mountain's theory gives results consistent with the thermodynamic treatment, since the final Landau-Placzek ratios are identical, although it does not account for any frequency dispersion in the experimental measurements.

#### 3) Relaxing Case

If we assume that the velocity dispersion is entirely due to a coupling between the molecular motions already described by Debye's theory and the internal degrees of freedom of the particles such as vibrational modes in a thermal relaxation process, as opposed to a structural relaxation process [35], the frequency spectrum of the scattered light can then be derived by using either an additional hydrodynamic equation for the internal degrees of freedom or a frequency dependent bulk viscosity [36]. The second alternative is more easily followed in the mathematical derivation although both modify the frequency shift and the width of the Brillouin peaks and also add a new unshifted mode in the spectrum [37] which we will refer to as the Mountain line after his theory.

To effect this change in the theory, the Navier-Stokes equation is modified by inserting an extra term to allow for a frequency dependent bulk viscosity; (the last term on the left side).

$$\rho_{0} \frac{\partial^{v}_{i}}{\partial t} + \frac{v_{0}^{2}}{\gamma} \operatorname{grad} \rho_{1} + \frac{v_{0}^{2} \alpha \rho_{0}}{\gamma} \operatorname{grad} T_{1}$$

$$- (\frac{4}{3} \boldsymbol{\eta}_{S} + \boldsymbol{\eta}_{B}) \operatorname{grad} \operatorname{grad} v_{i} - \int_{0}^{t} \boldsymbol{\eta}_{B}^{I} (t-t^{I}) \operatorname{grad} \operatorname{div} v_{i}(t^{I}) dt^{I} = 0$$

$$\frac{27}{3} \operatorname{grad} v_{i} + \frac{v_{0}^{2} \alpha \rho_{0}}{\gamma} \operatorname{grad}$$

The bulk viscosity thus has a frequency independent part  $\eta_B$  and a frequency dependent part  $\eta_B^I$ . The analysis proceeds in the same manner as in the ideal case except that the final equation is too detailed and the terms too interrelated to be able to identify specific expressions with properties of the material. Because of this complexity, a simplified approach is taken, even though the exact solution to the hydrodynamic equations is available for the fluctuations in the density. This simplification process is explained well by Mountain, who gives the final frequency dependent scattering equation from a relaxing liquid as follows:

$$I(k, \boldsymbol{\omega}) = I_O \frac{\pi^2 V}{\boldsymbol{\lambda}^4 R^2} \sin^2 \theta \left( \frac{\partial \epsilon}{\partial \rho} \right)^2 \rho_O T \beta_T \left\{ (1 - \frac{1}{\gamma}) \left[ \frac{\frac{\boldsymbol{\lambda}^1 k^2}{\rho_O C_P}}{\left( \frac{\boldsymbol{\lambda}^1 k^2}{\rho_O C_P} \right)^2 + \boldsymbol{\omega}^2} \right] \right\}$$

$$+ \left[ \frac{(v_{\infty}^2 - v_{0}^2) k^2 - (\frac{v^2}{v_{0}^2} - 1) \frac{v_{0}^4}{v^4 \boldsymbol{\tau}^2} + v_{0}^2 k^2 (1 - \frac{1}{\boldsymbol{\gamma}})}{\frac{v_{0}^2}{v^4 \boldsymbol{\tau}^2} + v^2 k^2} \right] \cdot \left[ \frac{\frac{2v_{0}^2}{v^2 \boldsymbol{\tau}}}{\frac{v_{0}^2}{v^2 \boldsymbol{\tau}^2} + v^2 k^2} \right]$$

$$+ \left[ \begin{array}{c} (1 - \frac{v_{O}^{2}}{v^{2}} (1 - \frac{1}{\gamma})) \cdot (v^{2}k^{2} + \frac{v_{O}^{2}}{v^{2}\tau}) - (v_{\infty}^{2} - v_{O}^{2})k^{2} \\ \hline - \frac{v_{O}^{4}}{v^{4}\tau} + v^{2}k^{2} \end{array} \right] \cdot$$

$$\left[\begin{array}{ccc} \Gamma_{\rm B} & \Gamma_{\rm B} \\ \hline \Gamma_{\rm B}^2 + (\boldsymbol{\omega} + vk^2)^2 & \Gamma_{\rm B}^2 + (\boldsymbol{\omega} - vk^2)^2 \end{array}\right]$$

The first term corresponds to the Rayleigh peak and is identical to those arising in the nonrelaxing case. This is the non-propagating decay of a fluctuation by thermal diffusion with the peak half-width at half-height.

$$\Gamma_{1/2}^{R} = \frac{\lambda^{I}}{\rho_{O}^{C_{P}}} k^{2}$$

Because of the dependence on the scattering vector k, this half-width should decrease with decreasing scattering angle,

since  $k^2 = \frac{8\pi^2 n^2}{\lambda_0^2}$  (1 - cos  $\theta$ ). This has been shown to be the

correct angular dependence by self-beating spectroscopy [38].

The second term corresponds to a nonpropagating decay that is coupled to the internal degrees of freedom of the molecules. This is a new peak, which is called the Mountain line, and it has a half-width

$$\Gamma = \frac{v_0^2}{v^2 \tau} .$$

The half-width is not dependent on the scattering vector as is the Rayleigh peak, but it does depend on the dispersion of the velocity of sound and on a single relaxation time ( $\tau$ ) of the liquid.

The third and fourth terms correspond to the propagating modes, the Brillouin peaks, and result from the moving sound waves. The frequency shift from the incident frequency (1) is  $\Delta$  (2) =  $v \cdot k$  and depends on the scattering vector

$$k = \frac{2\pi n}{\lambda_0} \sin(\Theta/2)$$
 31

Thus for a decreasing scattering angle the frequency shift will show a decrease. The half-width of this shifted term due to pressure fluctuations is

$$\Gamma_{1/2}^{B} = \left\{ \frac{1}{\rho_{0}} \left[ \frac{4}{3} \, \boldsymbol{\eta}_{S} + \, \boldsymbol{\eta}_{B} + \frac{\boldsymbol{\lambda}'}{C_{p}} \, (\boldsymbol{\gamma} - \frac{v_{0}^{2}}{v^{2}}) \right] \right\} k^{2} + \left( \frac{v_{\infty}^{2} - v_{0}^{2}}{1 + v^{2} \boldsymbol{\tau}^{2} k^{2}} \right) \left( 1 - \frac{\boldsymbol{\lambda}' \boldsymbol{\tau} k^{2}}{\rho_{0}^{C} v} \right) k^{2}$$

$$\frac{32}{2}$$

This half-width is also dependent on the scattering vector  $k^2$ , and decreases with a decrease in scattering angle, but the change is not linear as it is for the Rayleigh peak.

The ratio of the intensities of the central components to the shifted components is termed  ${\bf J}_{V}$  instead of the Landau-Placzek ratio because of the relaxation processes present, and is obtained from equation 28 .

$$J_{\mathbf{v}} = \frac{(1 - \frac{1}{\gamma}) \left(\frac{v_{0}^{4}}{v^{4}} + v^{2}k^{2}\right) + (v_{\infty}^{2} - v_{0}^{2}) - (\frac{v^{2}}{v_{0}^{2}} - 1) \left[\frac{v_{0}^{4}}{v^{4}} + v_{0}^{2}k^{2} (1 - \frac{1}{\gamma})\right]}{\left[1 - \frac{v_{0}^{2}}{v^{2}} (1 - \frac{1}{\gamma})\right] \left[v^{2}k^{2} + \frac{v_{0}^{2}}{v^{2}}\right] - (v_{\infty}^{2} - v_{0}^{2})k^{2}}$$

$$\frac{33}{\sqrt{2}}$$

At low phonon frequencies this reduces to the Landau-Placzek ratio, so for the case vk au << 1

$$J_{V} = \gamma - 1$$

At very large phonon frequencies equation 33 reduces to a slightly different but simpler form for the case  $vk\P>> 1$ .

$$J_{V} = \left(\frac{v_{\infty}^{2}}{v_{O}^{2}}\right) \gamma - 1$$
 35

Between these two extremes the more complex equation  $\underline{33}$  must be used to determine the ratio  $J_V$ , although it should be noted that the value  $J_V$  can be equal to or larger than the Landau-Placzek ratio but not smaller. This is true for all liquids examined to date.

The relaxation time  $\boldsymbol{\tau}$ , can be calculated from the velocity dispersion equation in Mountain's theory.

$$(vk\mathbf{7})^{2} = \frac{1}{2} \left[ (v_{\infty} k\mathbf{7})^{2} - 1 \right] + \frac{1}{2} \left[ ((v_{\infty} k\mathbf{7})^{2} - 1)^{2} + 4(v_{0} k\mathbf{7})^{2} \right]^{\frac{1}{2}}$$

The velocity of sound extrapolated to zero frequency  $v_0$ , is measured acoustically while the velocity of sound at infinite frequencies is approximated by using acoustic theory and assuming that only one relaxation mechanism with a single relaxation time contributes to the velocity dispersion [39], giving the equation

$$\frac{\mathbf{v}_{\infty}^2}{\mathbf{v}_{0}^2} = \left[\frac{\mathbf{c}_{\mathbf{p}} - \mathbf{c}_{\mathbf{I}}}{\mathbf{c}_{\mathbf{V}} - \mathbf{c}_{\mathbf{I}}}\right] \cdot \left[\frac{\mathbf{c}_{\mathbf{V}}}{\mathbf{c}_{\mathbf{p}}}\right]$$

$$\frac{37}{2}$$

The internal specific heat  $C_{\rm I}$ , is calculated from vibrational energy levels and their known degeneracies [39] from the equation

$$c_{I} = \sum_{i=1}^{N} g_{i}R x^{2} / e^{x} (1-e^{-x})^{2} ; x = \frac{h \mathbf{v}_{i}}{kT}$$
 38

The measured velocity v, with the corresponding incident vector k, is then substituted in the dispersion equation

to obtain 7, the relaxation time.

# b-Solutions

## 1) Mountain's Theory

The frequency dependence of light scattered from a solution [19] with the solvent a relaxing liquid, can be treated in a manner similar to the case of a pure relaxing liquid by including another equation to describe the mass diffusion due to the solute.

$$\frac{\partial^{C}_{2}}{\partial t} = D \left[ \nabla^{2}C_{2} + (\frac{kT}{T_{0}}) \nabla^{2}T + (\frac{kp}{\rho_{0}}) \nabla^{2}P \right]$$

$$\underline{39}$$

The components of this equation are the binary diffusion coefficient D, the thermal diffusion ratio  $\mathbf{k}_{\mathrm{T}}$ , and a term  $\mathbf{k}_{\mathrm{P}}$ , containing different thermodynamic quantities,

$$k_{p} = -\frac{P_{O}}{\rho_{O}} \frac{(\frac{\partial P}{\partial C_{2}})P,T}{(\frac{\partial \mu_{1}}{\partial c_{2}})P,T}$$

$$\frac{40}{\rho_{O}}$$

The solution of these equations has been approximated, as was done previously, even though an exact solution again is available. Nevertheless it is extremely complex, requiring at least a full page to reproduce in its entirety. Since we are principally interested in the intensity ratio  $J_{v}$ , the complex set is reduced to a much simpler set based on a thermodynamic ratio  $J_{v}^{T,soln}$ . derived by Miller [40]. We must first assume that the relaxation peak is narrower in width than the frequency shift of the Brillouin peaks, so

 $vk7 \ge 1$ . This is true experimentally since for benzene we find vk7 = 5.44. The complex equation is then reduced to the following form based on the ratio  $J_v^{T,soln}$ .

$$J_{V}^{\text{soln.}} = \frac{J_{V}^{T,\text{soln.}} [1 + A(k)] + B(k)}{1 - B(k) - J_{V}^{T,\text{soln.}} [A(k)]}$$
41

The two composite terms A(k) and B(k) are

$$A(k) = \frac{(v_{\infty}^2 - v^2)k^2 \tau^2 - (\frac{v_0}{v})^2 + (\frac{v_0}{v})^4}{(vk\tau)^2 + (\frac{v_0}{v})^4}$$
42

$$B(k) = \frac{(v_{\infty}^2 - v_{0}^2)k^2 \tau^2 - (\frac{v_{0}}{v})^2 + (\frac{v_{0}}{v})^4}{(vk\tau)^2 + (\frac{v_{0}}{v})^4}$$

$$43$$

These two terms are equal to zero for a very small wave vector k, (A(k) = B(k) = 0) and equation  $\underline{41}$  reduces to the following for vk? << 1

$$J_{V}^{\text{soln}} = J_{V}^{T, \text{soln}}$$

At the other limit of a very large vector k, A(k) = 0

and B(k) =  $1 - \left(\frac{v_0}{v_\infty}\right)^2$  and equation <u>41</u> reduces to the

following for  $vk \uparrow >> 1$ 

$$J_{v}^{\text{soln.}} = J_{v}^{T,\text{soln.}} \left(\frac{v_{\infty}}{v_{0}}\right)^{2} + \left(\frac{v_{\infty}^{2}}{v_{0}^{2}} - 1\right)$$
 45

Using our experimental spectra of benzene at a 90° scattering angle and the known values of k,  $v_0$ , and  $v_\infty$ , the value of A(k) = 0.00253 is small and relatively unimportant, although the second term B(k) = 0.2769 is too large to be neglected in our calculations. Thus the thermodynamic derivation of the ratio  $J_v^T$  cannot be used directly for benzene and its solutions but must be modified to account for the internal relaxation present.

# 2) Miller's Theory

A light scattering theory of solutions has been derived by Miller [40] which separates pressure fluctuations from entropy and concentration fluctuations. The derivation is similar to that described in the section on thermodynamic theory, but it also includes fluctuations in the concentration in deriving the average value of the fluctuation in the square of the dielectric constant  $<(\Delta \, \xi \,)^2>$ . Using the variables temperature T, pressure P, and number of moles of solute  $n_2$ , the scattering equation  $\underline{4}$  is

I<sub>scatt.</sub> = I<sub>O</sub> 
$$\frac{\pi^2 V}{\lambda^4 R^2} \sin^2 \Theta \left[ \left( \frac{\partial \mathbf{E}}{\partial T} \right)^2_{\mathbf{P}, \mathbf{n}_2} < (\Delta T)^2 > \frac{46}{2} \right]$$

$$+ 2\left(\frac{\partial \mathbf{E}}{\partial \mathbf{T}}\right)_{\mathbf{P},\mathbf{n}_{2}} \left(\frac{\partial \mathbf{E}}{\partial \mathbf{P}}\right)_{\mathbf{T},\mathbf{n}_{2}} < (\triangle \mathbf{T} \triangle \mathbf{P}) > + \left(\frac{\partial \mathbf{E}}{\partial \mathbf{P}}\right)_{\mathbf{T},\mathbf{n}_{2}}^{2} < (\triangle \mathbf{P})^{2} >$$

$$+\left(\frac{\partial \epsilon}{\partial n_2}\right)^2 < (\Delta n_2)^2 >$$

The cross terms,  $<(\Delta T \cdot \Delta T)>$ and $<(\Delta P \cdot \Delta T)>$  are zero, since the variables are statistically independent. Statistical thermodynamics is used to obtain the fluctuation averages and gives the final scattering equation

$$I_{\text{scatt.}} = I_0 \frac{\pi^2 v}{\lambda^4 L^2} \sin^2 \theta \left[ \frac{RT^2}{c_v} \left( \frac{\partial \epsilon}{\partial T} \right)_{P,n_2}^2 \right]$$

 $+ \frac{2RT^{2}\alpha}{\beta_{T}C_{V}} \left(\frac{\partial \boldsymbol{\xi}}{\partial T}\right)_{P,n_{0}} \left(\frac{\partial \boldsymbol{\xi}}{\partial P}\right)_{T,n_{0}} + \frac{RT}{V\beta_{S}} \left(\frac{\partial \boldsymbol{\xi}}{\partial P}\right)_{T,n_{0}}^{2}$ 

47

$$+ \frac{\operatorname{RT}(\partial \mathcal{E}/\partial n_2)^2}{(\partial \mu_2/\partial n_2)_{T,P}} \right]$$

The Brillouin peaks are due only to adiabatic pressure fluctuations, therefore, this contribution to the fluctuations in the dielectric constant is given as follows

$$<(\Delta \epsilon)^2>_{P,n_2} = \left(\frac{\partial \epsilon}{\partial P}\right)^2_{S,n_2} <(\Delta P)^2>$$
 48

From thermodynamics we obtain the equation

$$\left(\frac{\partial \boldsymbol{\xi}}{\partial \mathbf{p}}\right)_{S,n_2} = \left(\frac{\partial \boldsymbol{\xi}}{\partial \mathbf{T}}\right)_{P,n_2} \frac{\mathbf{T} \nabla \alpha}{C_p} + \left(\frac{\partial \boldsymbol{\xi}}{\partial P}\right)_{T,n_2}$$

$$\underline{49}$$

From statistical thermodynamics the pressure fluctuations are given as follows

$$<(\Delta P)^2> = {RT \over V\beta_s}$$
 50

Combining the above to obtain the contribution due to the adiabatic pressure fluctuations, the final equation obtained is

$$\langle (\Delta \boldsymbol{\xi})^2 \rangle = \frac{RT^2}{C_v} (1 - \frac{1}{\gamma}) \left( \frac{\delta \boldsymbol{\xi}}{\delta T} \right)_{P,n_2}^2$$

$$+ \frac{2RT^{2}\alpha}{\beta_{T}^{C}v} \left( \frac{\partial \xi}{\partial T} \right)_{P,n_{2}} \left( \frac{\partial \xi}{\partial P} \right)_{T,n_{2}} + \frac{RT}{V\beta_{S}} \left( \frac{\partial \xi}{\partial P} \right)_{T,n_{2}}^{2}$$

Since this part is included in equation 47, subtrac — tion gives the fluctuations contributing to the central peak. A ratio of the fluctuations contributing to the central peak to the fluctuations contributing to the Brillouin peaks is found as follows:

$$\frac{\mathbf{I}_{\mathbf{C}}}{^{2}\mathbf{I}_{\mathbf{B}}} = \frac{\langle (\Delta \boldsymbol{\xi})^{2} \rangle_{\mathbf{S}, \mathbf{n}_{2}}}{\langle (\Delta \boldsymbol{\xi})^{2} \rangle_{\mathbf{P}, \mathbf{n}_{2}}} = \frac{52}{\mathbf{E}}$$

$$\frac{RT^{2}}{C_{v}}\left(\frac{\partial \epsilon}{\partial T}\right)_{P,n_{2}}^{2} + RT \frac{\left(\partial \epsilon/\partial n_{2}\right)_{T,P}^{2}}{\left(\partial \mu_{2}/\partial n_{2}\right)_{T,P}^{2}}$$

$$\frac{\operatorname{RT}^{2}}{\operatorname{C}_{V}}(1-\frac{1}{\gamma})\left(\frac{\partial \boldsymbol{\epsilon}}{\partial \mathtt{T}}\right)_{\operatorname{P,n}_{2}}^{2}+\frac{2\operatorname{RT}^{2}\alpha}{\beta_{\operatorname{T}}\operatorname{C}_{V}}\left(\frac{\partial \boldsymbol{\epsilon}}{\partial \mathtt{T}}\right)_{\operatorname{P,n}_{2}}\left(\frac{\partial \boldsymbol{\epsilon}}{\partial \mathtt{P}}\right)_{\operatorname{T,n}_{2}}+\frac{\operatorname{RT}}{\operatorname{V}\beta_{\operatorname{S}}}\left(\frac{\partial \boldsymbol{\epsilon}}{\partial \mathtt{P}}\right)_{\operatorname{T,n}_{2}}^{2}$$

Values of  $(\frac{\lambda \xi}{\lambda p})$  are usually not available in the literative  $T, n_2$ 

ture, but by assuming that  $\mathbf{E} = n^2$ , and rearranging the denominator using a term  $\mathbf{X}$ , where

$$\chi = 1 + \frac{\beta T}{\alpha} \frac{(\partial n/\partial T)_{P}}{(\partial n/\partial P)_{T}}$$
53

for which excellent values are available from the literature [34], equation 52 reduces to

$$J_{V}^{T,soln} = \frac{\frac{RT^{2}}{C_{p}} \left(\frac{\partial n}{\partial T}\right)_{P,n_{2}}^{2} + RT \frac{\left(\frac{\partial n}{\partial n_{2}}\right)_{T,P}^{2}}{\left(\frac{\partial \mu_{2}}{\partial n_{2}}\right)_{T,P}}}{\frac{RT^{2}}{C_{p}} \left(\frac{1}{\gamma-1}\right) \left(\frac{\partial n}{\partial T}\right)_{P,n_{2}}^{2} \left[1 + \gamma \left(\frac{2x}{1-x} + \frac{\gamma_{x^{2}}}{(1-x)^{2}}\right)\right]}$$

Simplifying this equation further by letting

$$f = \frac{2x}{1-x} + \frac{\gamma_x^2}{(1-x)^2}$$
 55

and writing the solvent chemical potential in terms of the concentration of a macromolecule  $\mathbf{C}_2$ ,

$$\mu_1 - \mu_0 = -RTV_1 C_2 \left( \frac{1}{M} + A_2 C_2 + A_3 C_2^2 + \cdots \right)$$
 56

The ratio  $\mathbf{J_v}^{\mathbf{T}}$  for a real polymer solution is

$$J_{V}^{T,soln} \cdot = \left(\frac{Y-1}{1+Yf}\right) + \left(\frac{Y-1}{1+Yf}\right) \frac{c_{P}}{RT^{2}} \cdot \frac{(\partial n/\partial c_{2})_{T,P}^{2}}{(\partial n/\partial T)_{P,n_{2}}^{2}} c_{2}$$

$$\cdot \left(\frac{1}{\overline{M}_{W}} + 2A_{2}c_{2} + 3A_{3}c_{2}^{2} + \cdots\right)^{-1}$$

This is an exact thermodynamic ratio without approximations or relaxation effects adding to the central peak.

This equation can be reduced to a simpler and more easily handled form by setting the exact thermodynamic ratio for the pure solvent equal to  $\mathbf{J_v}^T$ .

$$J_{\mathbf{v}}^{\mathbf{T}} = \frac{\mathbf{\gamma}_{-1}}{1 + \mathbf{\gamma}_{f}}$$

Grouping other terms into a constant K, dependent on the solvent and solute system, we have

$$K = \frac{C_{P}}{RT^{2}} \frac{(\partial n/\partial C_{2})^{2}}{(\partial n/\partial T)_{P,n_{2}}^{2}}$$
 59

Now we can write equation 57 in a simplified form.

$$J_{v}^{T,soln} = J_{v}^{T} + J_{v}^{T} KC_{2} \left(\frac{1}{M_{w}} + 2A_{2}C_{2} + 3A_{3}C_{2}^{2} + ...\right)^{-1}$$
 60

If no relaxation or dispersion effects are present to form a significant Mountain line, the experimentally measured ratio  $J_v$  for the solvent is equal to the thermodynamic ratio  $J_v^T$ . The presence of thermal relaxation effects can be detected by an increased velocity of sound in the pure liquid at increasing frequencies and a larger experimental intensity ratio  $J_v$ , than calculated from thermodynamics as  $J_v^T$ . When these effects are present, equation 60 must be modified to use the experimental ratio  $J_v$ . This is accomplished by multiplying each term due to the pure liquid by the quantity  $({}^Jv/J_v^T)$  so that equation 60 may now be written as

$$J_{v}^{\text{soln.}} = J_{v} + J_{v} KC_{2} \left(\frac{1}{M_{w}} + 2A_{2}C_{2} + 3A_{3}C_{2}^{2} + \ldots\right)^{-1}$$
 61

If no relaxation or dispersion effects are present  $J_v = J_v^T$  and the original equation is recovered. Unfortunately

equation <u>61</u> is not entirely correct when dispersion is present, since to evaluate the molecular weight we need to measure the relative amount that the central peak is increased due to concentration fluctuations. This increase is dependent on the original amount of scattering present which is due only to entropy fluctuations and so should not include other effects such as the Mountain line.

Since Miller's calculations are based on the complete separation of fluctuations due to pressure from those due to entropy and concentration effects, the relative intensity of the central peak must be reduced to the thermodynamic value. This is accomplished by multiplying the measured ratio  $J_{\nu}$  by the term

$$\frac{J_{v}^{T} (J_{v} + 1)}{J_{v} (J_{v}^{T} + 1)}, \qquad \underline{62}$$

which is derived as follows: the thermodynamic ratio

 $J_{v}^{T} = \frac{I_{c}}{2I_{B}}$  is a ratio of the scattered intensity from entropy and concentration fluctuations  $I_{c}$ , to the intensity due to pressure fluctuations  $I_{B}$ , whereas the measured ratio

$$J_v = \frac{I_c}{2I_B}$$
 is the same except that  $I_c > I_c$  and  $I_B > I_B$ 

due to an extra relaxation peak, the Mountain line. Assuming that the total scattered intensity in each case is equal, the intensity of the Rayleigh and Brillouin peaks in terms of the ratios and the thermodynamic value from Miller's

equation is

$$I_{C} = I_{C'} \left( \frac{J_{V}^{T}(J_{V} + 1)}{J_{V}(J_{V}^{T} + 1)} \right) ; I_{B} = I_{B'} \left( \frac{J_{V} + 1}{J_{V}^{T} + 1} \right)$$

Therefore by multiplying the intensity of the central Rayleigh peak as measured in a spectra by the ratio

$$\frac{J_{\mathbf{v}}(J_{\mathbf{v}}^{T}+1)}{J_{\mathbf{v}}^{T}(J_{\mathbf{v}}+1)}$$
 we obtain the correct thermodynamic value and

equation 61 becomes

$$J_{v}^{\text{soln.}} = J_{v} + J_{v} \left( \frac{J_{v}^{T} (J_{v} + 1)}{J_{v} (J_{v}^{T} + 1)} \right) \quad KC_{2} \left( \frac{1}{\overline{M}_{w}} + 2A_{2}C_{2} + 3A_{3}C_{2}^{2} + \cdots \right)^{-1}$$

$$\underline{64}$$

Simplifying this expression by letting

$$B = \frac{(J_V + 1) \quad (Y - 1)}{Y(1 + f)}$$
 65

and rearranging, the final working equation becomes

$$\frac{BKC_2}{J_{y}^{soln} - J_{y}} = \frac{1}{\overline{M}_{w}} + 2A_2C_2 + 3A_3C_2^2 + \cdots$$
 66

If there is no dispersion present in the constants which characterize the solvent, then the measured ratios and thermodynamic ratios are equal and we find for the solvent

$$J_{v} = J_{v}^{T} = B = \frac{\gamma - 1}{1 + \gamma f}$$
 67

Therefore with no dispersion, equation <u>66</u> reduces to the thermodynamic expression 60.

## 3) Angular Correlations

Equation <u>66</u> is often modified by inserting an extra term  $P(\Theta)$ , the internal interference factor.

$$\frac{BKC_2}{J_{W}^{\text{soln.}} - J_{W}} = \frac{1}{\overline{M}_{W} P(\Theta)} + 2A_2C_2 + 3A_3C_2^2 + \cdots$$
 68

This term  $P(\theta)$ , is defined as [41]

$$P(\Theta) = \frac{1}{N^2} \sum_{\mathbf{x}} \sum_{\mathbf{y}} \frac{\sin(\mathbf{K} \cdot \mathbf{r}_{\mathbf{x}, \mathbf{y}})}{\mathbf{K} \cdot \mathbf{r}_{\mathbf{x}, \mathbf{y}}}$$
 69

where

$$K = \frac{4\pi n}{\lambda n} \sin(\Theta/2).$$

The relative amount of destructive interference which decreases the scattered intensity can be determined from the scattering at N different points which are pairwise separated by the distance  $r_{x,y}$ . If a solution is dilute, this destructive interference is calculated only from the separate scattering points within each molecule, since  $r_{x,y}$  is very large for widely separate random points and thus produces a very small interference effect at these distances. Therefore  $P(\theta)$  becomes a factor internal to the molecule, although only becoming a significant factor in reducing the scattered intensity if the size of the macro-

molecule exceeds about 1/20 of the wavelength of the light used. Consequently the molecular weight should be greater than about  $10^6$  g/mole for P( $\theta$ ) to be smaller than unity and significantly affect the molecular weight measurements.

## 3-Discussion

An analysis of the light scattered from a solution of macromolecules or even from a pure liquid is difficult to interpret completely without a precise liquid theory. Consequently we can only approximate the scattering with simplified models [42]. The two different theories we have used to evaluate Brillouin light scattering from solutions and pure liquids are (1) Miller's thermodynamic theory, and (2) Mountain's thermodynamic-hydrodynamic theory. Other theories similar in nature are available [42,43,44,45,46,47].

Both theories attempt to explain only the light scattered from isotropic fluctuations; so only the vertically polarized light  $V_{\rm V}$  or  $J_{\rm V}$  can be evaluated. In many liquids, a significant amount of the scattered intensity is not vertically polarized and therefore must be separated and eliminated from the measured value. Also, part of the remaining vertically polarized light is due to anisotropic fluctuations which may have broad frequency shifts such as is exhibited in the Rayleigh "wing" in benzene and also must be separated and eliminated from the analysis. Because much of the scattered light is not included, both of these theories are only approximations to the total scattering and should

only be treated as such.

Both theories also often contain simplifying assumptions to allow a clearer mathematical representation of the final result. Mountain's theory necessarily employs more approximations because of its complexity. The most significant approximations are in (1) describing extremely rapid fluctuations on the order of 10 10 Hz by hydrodynamic equations, (2) evaluating the fluctuations in the dielectric constant with only density fluctuations, and (3) using a single frequency dependent bulk viscosity to describe dispersion effects [46]. The first approximation mentioned above is Mountain's basic assumption and appears to result in a reasonable correspondence with experimental measurements. The second approximation neglects temperature fluctuations since they are small when compared with density fluctuations. Since the temperature fluctuations are about 0.2% of the density fluctuations for many liquids [34]. this approximation is often used in light scattering theory. The third approximation results in an entirely new peak which appears to be present.

The theory by Miller makes a basic assumption that fluctuations in entropy and concentration can be completely separated from fluctuations in the pressure in order to derive a ratio. In some solutions this separation is not possible if the solute affects the values of  $v_0$ ,  $v_\infty$  and  $\boldsymbol{\tau}$ , as has been seen in gas mixtures [31,48]. When this happens, a coupling between pressure and concentration fluctuations

occurs requiring a very complex expression such as Mountain has derived. It is also assumed in Miller's theory that the Brillouin peaks scatter an identical amount of light even after large macromolecules are added to the solvent. This assumption also appears to be valid for very dilute solu—tions in solvents where significant structural relaxation is not present. An evaluation of these assumptions with experimental data will be made when possible along with the ability of Brillouin scattering to determine accurate molecular weights of large macromolecules.

## **B-Viscosity**

## 1-Theory

A liquid which is under small shear stress will easily distort and flow, whereas a solid will show a fixed shear strain. This distortion and flow in a liquid is a result of adjacent molecules or molecular layers moving relative to each other, while the frictional forces between them reduces this relative motion. The rate that mechanical energy from a stress is transformed into heat J, by frictional resistance is [49]

$$J = \eta_0 q^2$$
 70

The uniform velocity gradient is q and the viscosity of a pure liquid  $\boldsymbol{\eta}_{\mathrm{O}}.$ 

The addition of a solute to a liquid will modify J by an amount  $\Delta J$ .

The relative change or specific viscosity,  $\boldsymbol{\eta}_{\text{sp}}$ , is written as

$$\frac{\Delta J}{J} = \eta_{sp} = \frac{\eta - \eta_{o}}{\eta_{o}}$$

If the solute consists of large rigid spheres, the specific viscosity depends on the volume of these spheres plus second order effects, and can be expressed as [49]

$$\eta_{sp} = 2.5 \left(\frac{v_e}{M_2}\right) c_2 + 12.6 \left(\frac{v_e}{M_2}\right)^2 c_2^2$$
73

#### 2-Molecular Weight Determinations

Experimentally we use an empirical equation which has the same form as above even though macromolecules in solution do not act exactly as large rigid spheres.

$$\frac{\eta_{\rm sp}}{c_2} = [\eta] + k' [\eta]^2 c_2 \qquad \underline{74}$$

The limiting viscosity number [  $\eta$ ], is related to the hydrodynamic volume  $V_e$ , for a mole of particles but varies with the size and shape of the particles, the solvent, solute and temperature. Also and most importantly, the hydrodynamic volume varies with the molecular weight

according to the well established theoretical equation of Flory [50].

$$[\eta] = \Phi_0 \left(\frac{\langle r_0^2 \rangle}{M}\right)^{\frac{3}{2}} M^{\frac{1}{2}} \alpha^3$$

The components of this equation are the molecular weight M, the average value of the square of the end-to-end distance <  ${\rm r_0}^2$  > , the expansion factor  ${\alpha}$ , and a universal constant  $\Phi_{\!_{\mathbf{O}}}$  . When a macromolecule is in a solvent at the theta temperature,  $\Theta$ , as defined by Flory, equation 75 reduces to a very simple form, where the constant K depends only on the specific solvent and solute

$$[\mathbf{\eta}]_{\Theta} = K M^{a} ; a = 1/2$$

This simple form can be used at temperatures higher than the theta temperature but then the constants and a must be experimentally determined, since they are not simply derived from theory.

If we define a viscosity average molecular weight as

$$\overline{\mathbf{M}}_{\eta} = \left[ \sum_{i=1}^{N} \mathbf{W}_{i} \mathbf{M}_{i}^{b} \right]^{\frac{1}{b}} , \qquad \underline{77}$$

we find that when b = 1.0, the viscosity average molecular weight equals the weight average molecular weight  $\overline{\underline{\mathbf{M}}}_{\mathbf{w}}$  . Since  $\overline{\mathtt{M}}_{\eta}$  is often a closer approximation to  $\overline{\mathtt{M}}_{\mathtt{W}}$  than the number average molecular weight  $\overline{M}_n$ , the constants K and a are usually determined by an experimental method such as elastic Photometric light scattering which permits determination of the weight average molecular weight. In the experimental section on viscosity we have used light scattering data from the literature to determine the constants K and a so as to experimentally evaluate the weight average molecular weights for a series of polystyrenes. These then are compared with experimental values calculated from Brillouin scattering experiments.

## III Experiment

# A-Light Scattering

#### 1-Instrument

An instrument to measure Brillouin light scattering, shown in Figure 1, was designed and constructed in the chemistry laboratory at Michigan State University [51].

Basically it consists of a laser, collecting and resolving optics, plus a detector and recorder which are constructed along two parallel tracks. The optical system, which is very sensitive to vibrations, is mounted entirely on a large, flat, acoustically isolated table to eliminate building vibrations which otherwise would force the system out of alignment.

One track of this system holds an argon ion laser and beam directing mirror, while the other holds the scattering cell and angular adjustment system, collecting lens, interferometer, resolving lens and detector. Each of these components will be described separately, although only briefly, since a more complete description can be found in the thesis of S. Gaumer.

#### a-Laser

The primary light source is a commercial Spectra Physics argon ion laser, model 165-03. Due to its high intensity and single frequency, the detection of Brillouin spectra is quite simple. Also because of stable output, vertical polarization and a single spacial mode configuration of the light

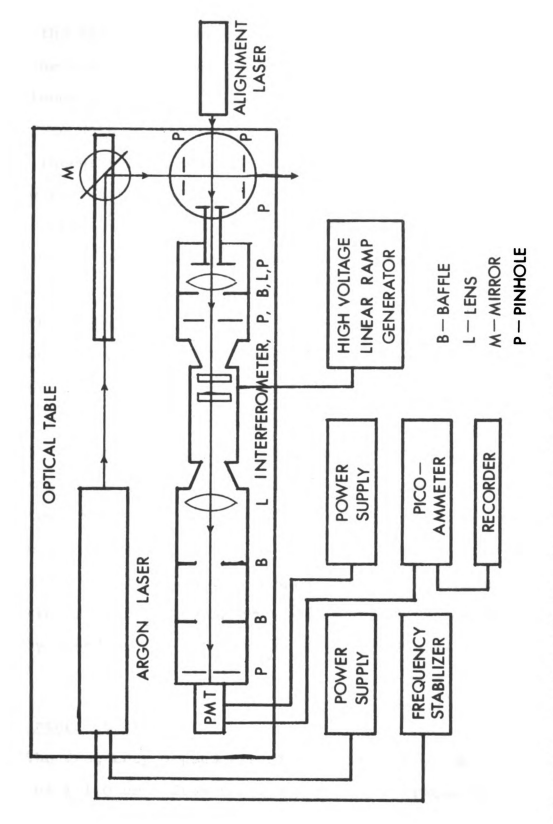


Figure 1. Rayleigh-Brillouin Spectrophotometer

beam, the spectra can be quantitatively analyzed. Besides these necessary features, there are also eight separate wave-lengths which can be used for light scattering, although only five (514.5, 496.5, 488.0, 476.5, 457.9 nm) have sufficient intensity to provide good spectra. The most commonly used wave-length is 514.5 nm with a corresponding single mode intensity of 400 mw. This intensity, lower than the maximum 800 mw, allows both a good stability of the light output and a longer usable laser lifetime.

The light beam is usually used with a vertical polarization vector although infrequently the vector is rotated horizontally for depolarization measurements. Consequently a good vertical alignment is necessary and can be quickly established by reflecting the "vertically" polarized beam from a glass plate located at the critical angle and adjusting the direction of the incident polarization to obtain a minimum reflection. Specific details of the stability of the light intensity, frequency drift, single mode selection and construction of internal laser components are readily found in the literature [51] and from the manufacturer.

### b-Interferometer

The frequency dependence of the scattered light in the range of  $\pm$  1.0 cm<sup>-1</sup> from the incident light frequency, the Rayleigh-Brillouin spectral region, is obtained with a commercial Fabry-Perot scanning interferometer, Lansing

Research model 30.205. Although this interferometer is a fine interference filter and allows only a very narrow frequency distribution of light to pass at one time, it still can be scanned over a small range of frequencies by varying the optical path length between two very flat mirrors ( $\lambda$ /100). The interferometer is the most sensitive component of the entire instrument and its alignment and operation are critical to the quality of the final Brillouin spectra. Thus, its operation and associated terminology will be discussed in more detail.

Before a specific frequency is passed through the two parallel interferometer mirrors, it must meet the interference condition given by an Airy function [52]:

$$I_{trans} = I_{incid} \left(\frac{T}{1-R}\right)^{2} \cdot \frac{1}{1 + \frac{4R}{(1-R)^{2}} \sin^{2} \frac{\delta}{\lambda}}$$
 78

where  $\delta = 2\pi n \mathcal{L} \sin \theta$ .

The light intensity transmitted through the mirrors depends on the incident intensity, the transmission T, and reflection R, coefficients of the mirrors, R = 98.5% for our mirrors, and on the optical path length  $\delta$ . When the interferometer is scanned to obtain a Brillouin spectrum, the optical path length  $\delta$  can be changed by varying either the refractive index n, between the mirrors, the angle  $\theta$ , between the mirrors and the incident light, or the separation  $\mathcal L$ , between the mirrors.

A piezoelectric transducer is used to move one mirror towards the other. This transducer is an anisotropic crystal which expands when a large voltage difference is applied across two opposite crystal faces. If this applied voltage is gradually increased, a mirror attached to one crystal face is slowly moved toward the other mirror and so allows the separation between the two parallel mirrors to decrease. Because this movement is very small, it cannot be mechanically changed with a micrometer screw with good precision, which is why a piezoelectric transducer is employed. Applying from zero - 1600 volts across the crystal faces will expand a four layered crystal 1.2  $\mu$  and scan almost five spectral orders. This voltage is linearly increased with time with a Lansing Research model 80.010 power supply. Unfortunately neither the lower voltage range nor the largest crystal expansion gives a linear expansion with increasing voltage. A linear range is only over a voltage range of -250 to -1500 volts. While this still allows four spectral orders to be scanned, we maintain a safety factor by selecting only the three central orders. The measured values from three orders are averaged in the final analysis for this gives a more consistent value than if only one order is selected.

Continuously increasing the applied voltage results in a series of repeating spectral orders in which one order immediately follows another. An example of three consecutive orders for benzene with the dark current baseline also

included is shown in Figure 2. The peaks are the time dependent intensity changes for an interference pattern originally in the form of a concentric series of rings.

Reducing the mirror separation forces the rings to converge toward a center until the interference condition given by the Airy function is met, then all the rings brighten simultaneously. Only the small central spot of this ring pattern is detected for reasons which will be explained in the section on Aperatures and Optics.

Specific terminology regarding the interferometer, which will frequently be used is described in detail below [52].

Free Spectral Range; 
$$f = \frac{c}{2n \lambda}$$
.

This is the frequency range that is scanned in one spectral order. It is inversely proportional to the mirror separation  $\lambda$ , the index of refraction n, of the media between the mirrors, and the velocity of light C.

Choosing a specific mirror separation for a spectrum must be done carefully so as to eliminate overlap of Brillouin peaks from adjacent orders yet identify the correct central peak associated with each Brillouin peak.

Our method for meeting these two objectives is given in the section on Spectral Analysis.

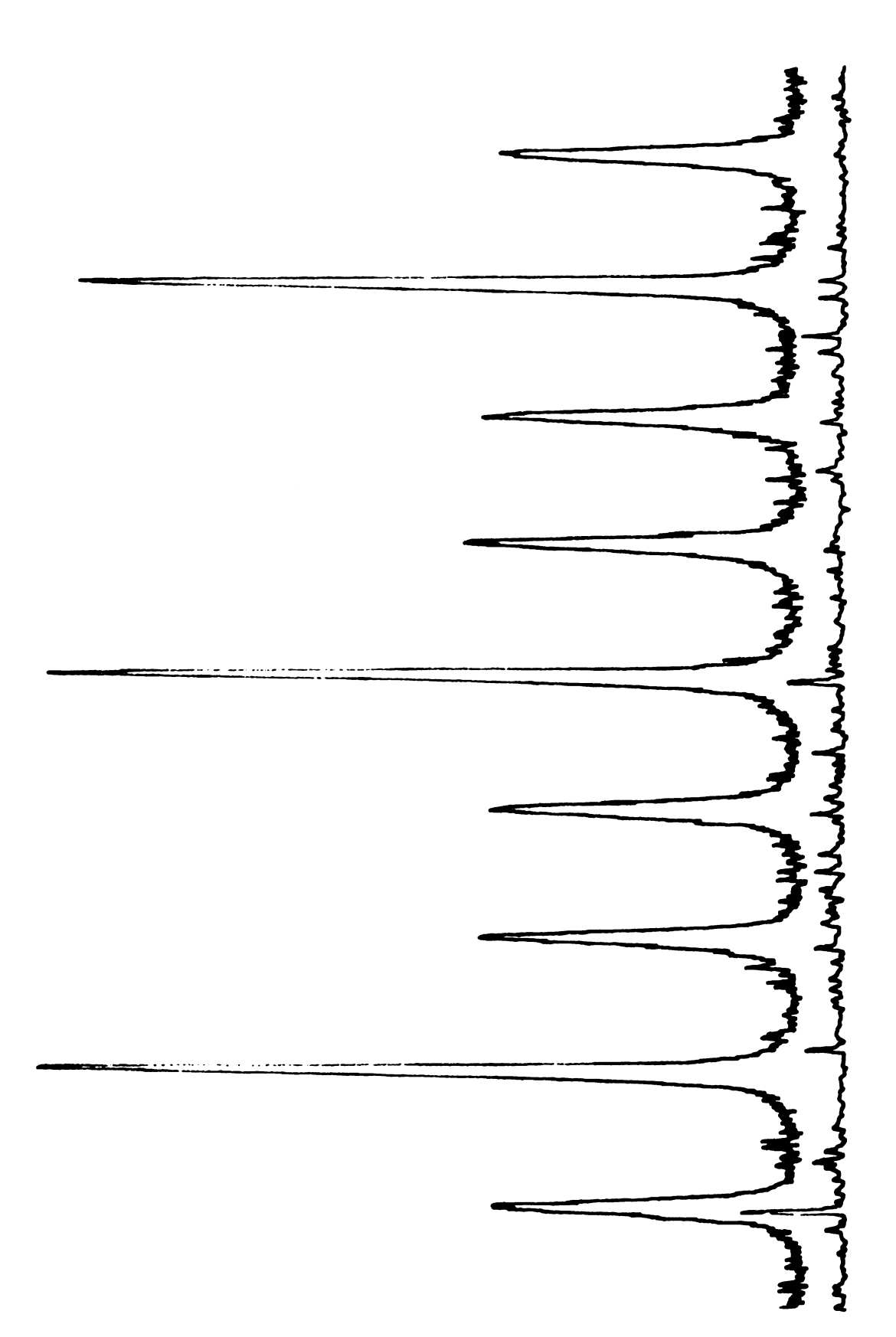


Figure 2. Brillouin Spectrum of Benzene-Three Consecutive Orders, Intensity vs Frequency

When a careful determination of Brillouin peak separation is necessary, as in sound velocity measurements, the small linear increase in the free spectral range due to a decreasing mirror separation must be corrected. This is done mathematically by determining the increasing distance between consecutive Rayleigh peaks and applying this correction to the Brillouin separations.

# Instrumental Band Width; $\delta \nu_{\text{B.W.}}$ .

This is the narrowest full peak width at half height passed by the interferometer when a perfectly monochromatic light beam is used as a source. As seen in the expression for the Airy function, it is dependent on the T and R coefficients for the mirror and is an instrumental constant of about 293 MHz for our particular instrument. The experimental value of the instrumental band width is also dependent on the alignment and reaches a minimum value with perfect alignment of the interferometer mirrors, parallel incident light, etc.

# c-Aperatures and Optics

The Brillouin scattering instrument contains two achromatic lenses and three pinholes to collect the scattered light and define its direction during analyzing and detection. Most of these components are aligned on precision optical rails inside two light tight boxes which help eliminate extraneous light from adding to the scattered

beam and also to keep the lenses as clean as possible. In the front of the first box closest to the scattering cell is a collimating tube which is blackened inside and supports a variable aperature at each end. The first aperature determines the acceptance angle of the diverging scattered light and the second determines the cone angle. We have found the best finesse (an experimental ratio of the width of the central peak to the separation between central peaks of consecutive orders) is obtained when the first aperature is 1.0 mm and the second 2.0 mm.

After passing through the two aperatures, the scattered light is gathered by the first lens and made parallel before entering the interferometer. The first lens (f = 50.0 cm) is positioned so its focal point is at the center of the scattering volume which is within the sample cell. An exact positioning of this lens is critical only to within ± 2 cm of the focal length because the scattered beam has a small divergence angle. A large aperature, 2.0 cm in diameter, is placed between the first lens and the front interferometer mirror to reduce light reflected off the front surface of the front mirror and prevent it from re-entering the beam path of the instrument.

A second lens (f = 100.0 cm) is positioned behind the interferometer and its focal point is placed on a small pinhole 2.0 mm in diameter, directly in front of the photomultiplier tube. Thus, only a central spot of the complete

ring pattern is detected. This will give a finesse at least two times better than if the complete pattern is used. The main reason for the increased finesse is that the two mirrors are not perfectly flat over their complete surface nor perfectly parallel. If only a small section of the surface of the mirrors is used to determine the interference pattern, as when a small spot is isolated from the ring pattern, a closer approximation to the ideal case of perfectly flat and parallel mirrors is possible, thus allowing a better finesse.

# d-Alignment

A complete experimental alignment procedure is provided in the appendix and is based on an extra stationary laser which is used only for alignment of the optical components. We use a Spectra-Physics model 125 helium neon laser which has a well defined, moderately intense beam to initially allow an interlocking set of pinholes to be accurately aligned. Then, sequentially, the mirrors and lenses are placed in the optical train and finely adjusted by matching the path of the reflected light from their front surfaces with the path of the incident beam. Only by a very careful alignment are good reproducable spectra possible and then only when realignments are made between each run.

# f-Detection and Recording

To detect the radiation, an E.M.I. 9558B photomultiplier

tube with a S-20 frequency response is supplied with -1,200 volts by a regulated high voltage power supply from KEPCO.

A low dark current is maintained by exposing the detector only to the low intensities of the scattered light, not the room light, and continuously cooling the cathode to only -10° C with a Products for Research, Model TE-104TS, refrigerated chamber. When lower cathode temperatures are used, moisture condenses on the front window of the detector and decreases the signal intensity obtained. The signal from the detector is then fed into a preamplifier with a variable current range, usually set at 0-10<sup>-9</sup> amps, and damping control set at 30% of the maximum value. The signal is then fed into a Keithly Model 417 picoamplifier, and finally to a Sargent Model SRC strip chart recorder where the final spectra is recorded. Specifications for each component are obtained from the manufacturers and from the literature [51].

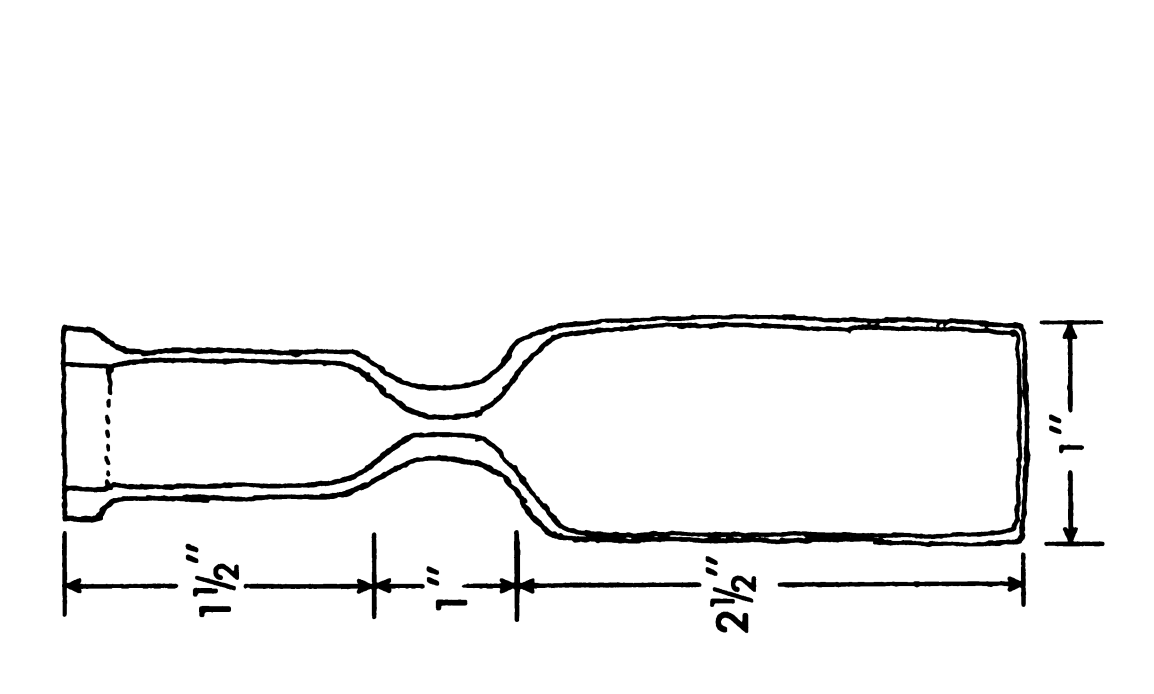
# 2-Scattering Cell

## a-Shape

A regular, rectangular light scattering cell with parallel entrance and exit windows is excellent for Brillouin scattering at 90 degrees to the incident beam since this shape allows the scattered light beam to be observed with a minimum of extraneous reflections from the surfaces of the cell. A cylindrical cell at least one inch in diameter is also satisfactory and much less expensive if the solutions are to be degassed and sealed. A design we incorporated

consists of a precision bore tube one inch in diameter and sealed to a 15 mm Fisher-Porter joint. A neck was formed in the tube about two inches below the joint while the bottom, about five inches below the joint was sealed and flattened for a base as seen in Figure 3. This cell was attached to a similar Fisher-Porter joint on the filter with a teflon gasket making an air tight system.

However, for scattering angles other than 90 degrees, an entirely different cell design is required. We have noted that for a scattering angle other than 90 degrees with a standard cylindrical light scattering cell, a small amount of light from the incident beam is reflected back from the glass-air interface at the point where the incident beam exits the cell. This reflected beam produces an extra set of small Brillouin peaks in the spectra with a frequency shift corresponding to the complementary scattering angle, while the Brillouin shift  $\Delta$  f 1 , is dependent on the scattering angle as seen from the previous equation 14. These small peaks can be seen very faintly in a vertically polarized, V., benzene spectrum at 45 degrees, Figure 4, and at 135 degrees, Figure 5, where the main Brillouin peaks and the reflected peaks exchange positions. In comparison with these two spectra, a Brillouin spectrum of benzene at 90 degrees, Figure 6, does not contain these separate reflected peaks. When the frequency shift of the small peaks is plotted with an equation for the complementary angle,



Cylindrical Scattering Cell-Original and Filled Figure 3.

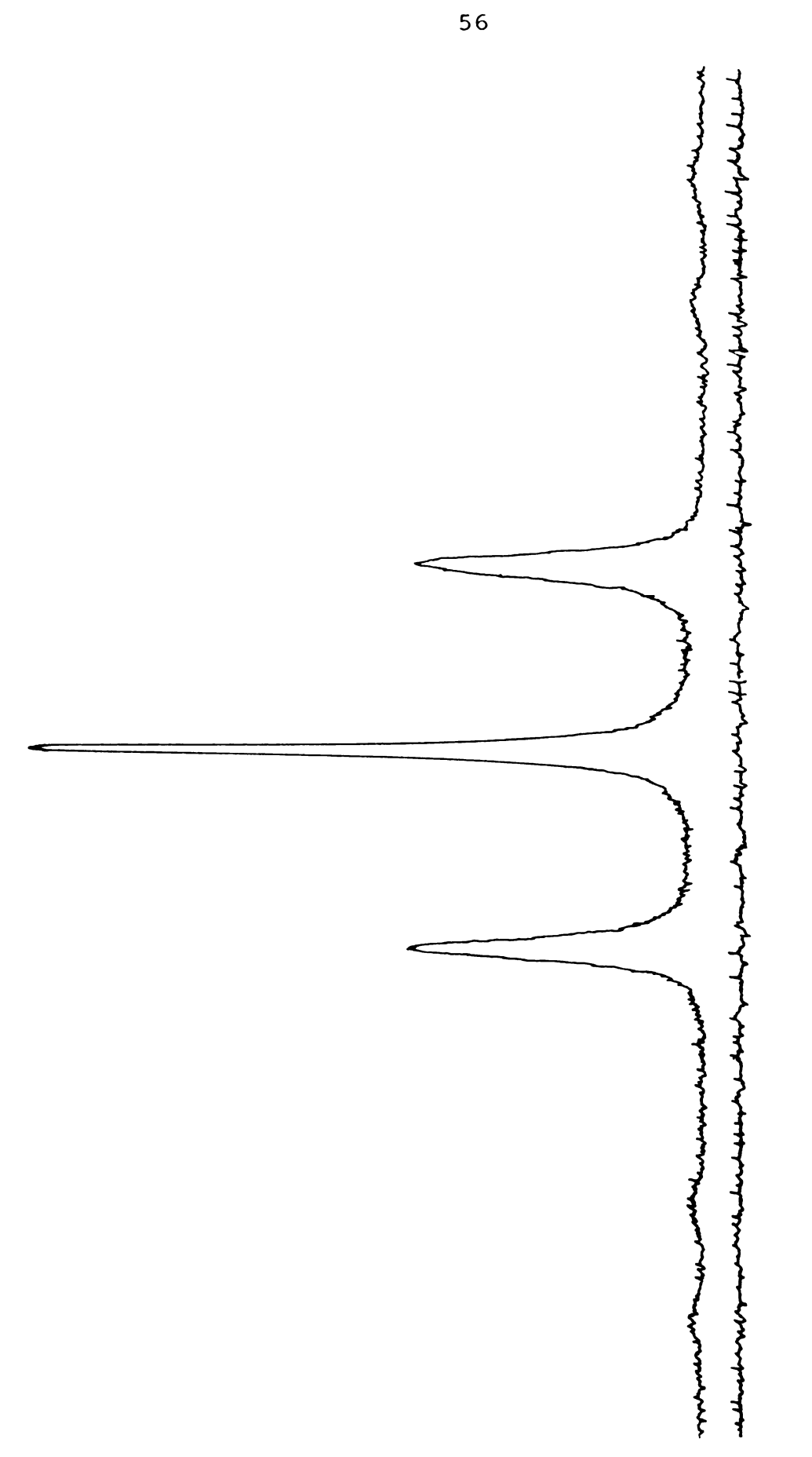


Figure 4. Brillouin Spectrum of Benzene-45 Degrees Scattering Angle, Intensity vs Frequency

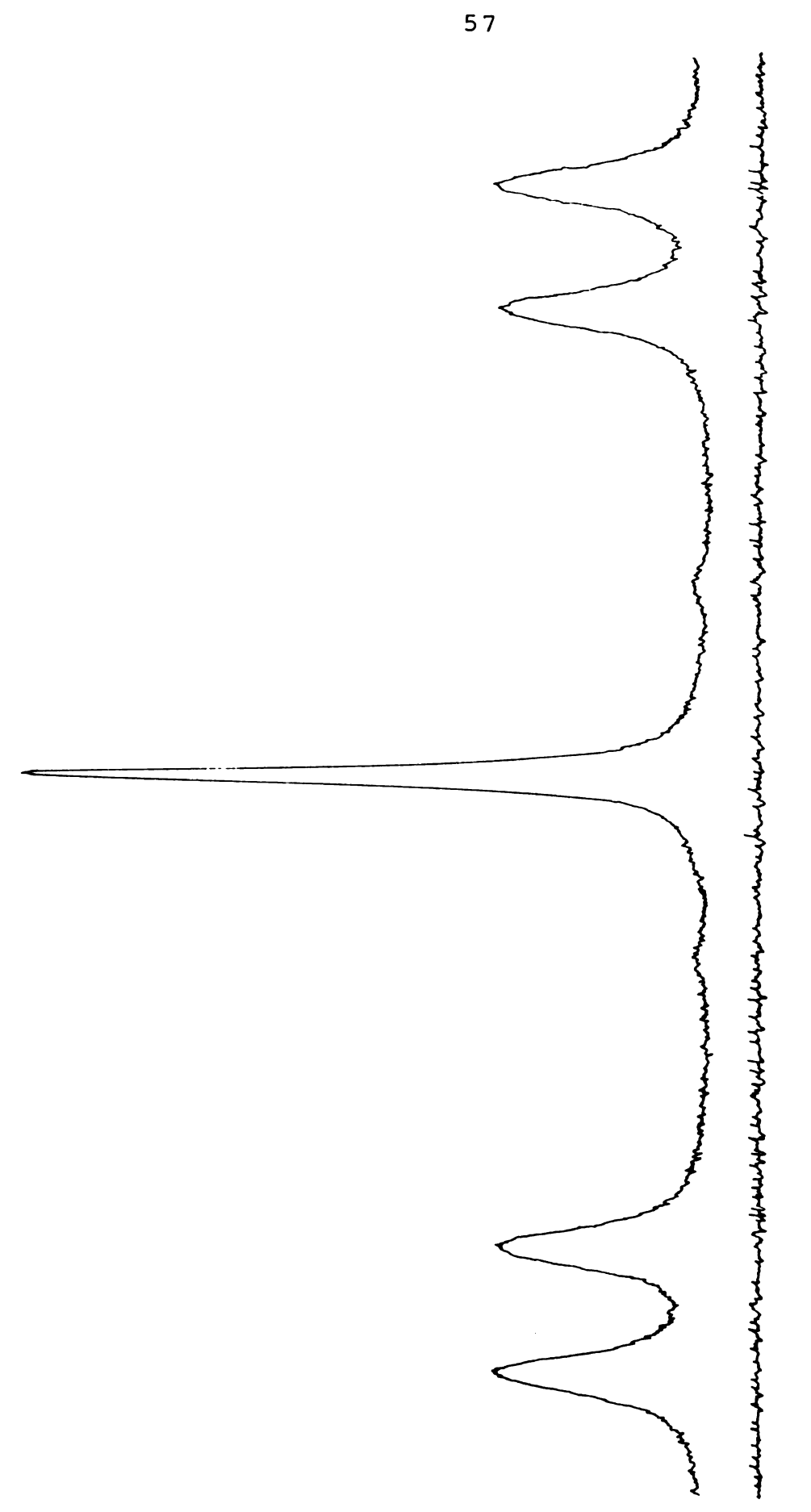


Figure 5. Brillouin Spectrum of Benzene-135 Degrees Scattering Angle, Intensity vs Frequency

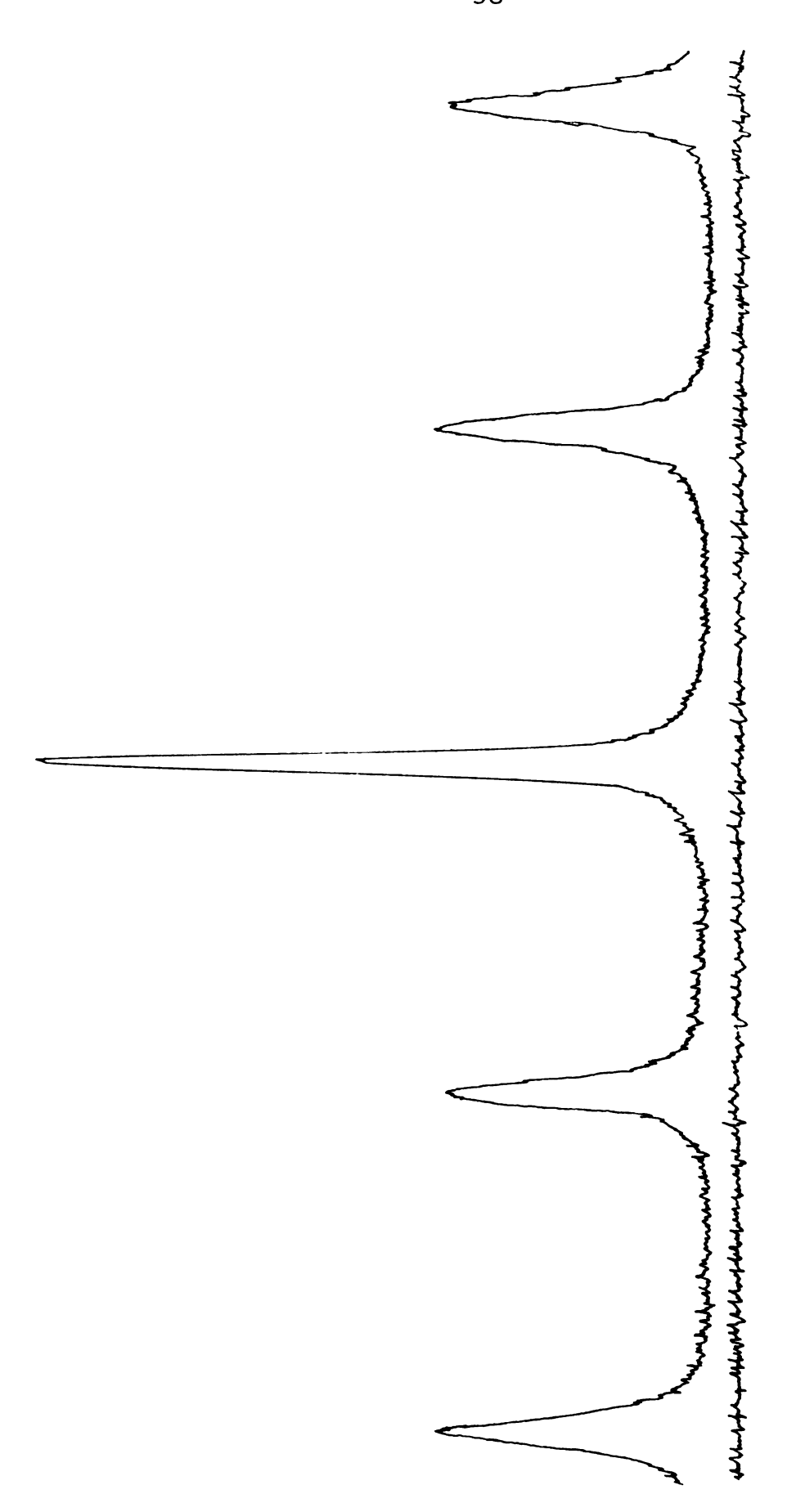
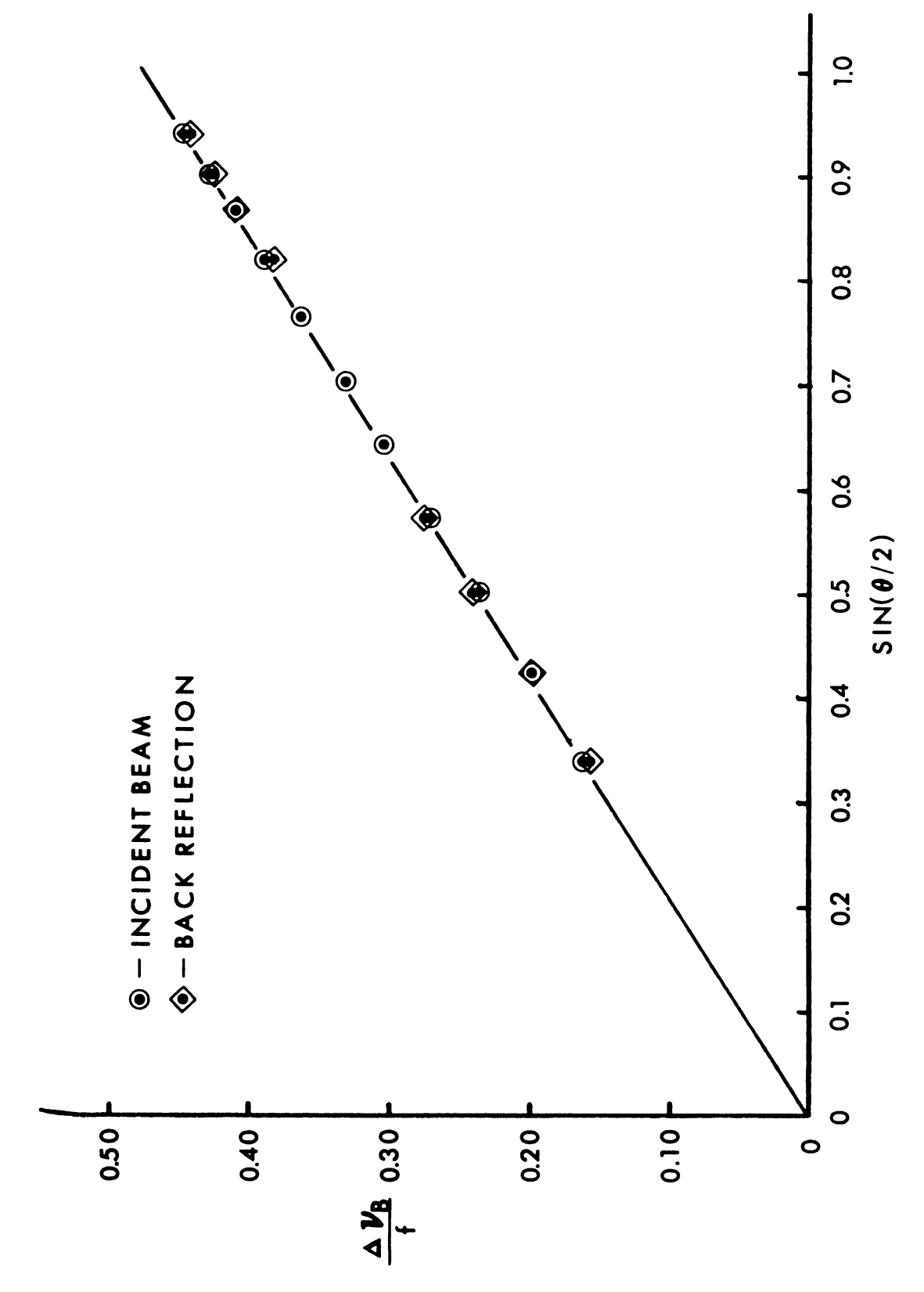


Figure 6. Brillouin Spectrum of Benzene-90 Degrees Scattering Angle, Intensity vs Frequency

$$\Delta V = \frac{2v_s}{\lambda_0/n} \sin(180 - \theta)/2 = \frac{80}{n}$$

the points correspond very well with the regular angular dependence as seen in Figure 7, indicating these peaks are from the same scattering volume. The intensity of small reflected Brillouin peaks are approximately 5% of the intensity of the main Brillouin peaks. This value corresponds well with a reflected intensity of 4%, calculated from the index of refraction for the interfaces benzene-glass plus glass-air perpendicular to the incident beam. Irregularities in the surfaces of the scattering cell and difficulties in accurately measuring the intensities of the small peaks easily account for the small difference between these two values.

These small peaks, which are due to the reflected beam, affect the use of the spectra by modifying the experimental ratio  $J_{\rm v}$  in two ways. First, these peaks can be separated from the regular Brillouin peaks by selecting a scattering angle other than 90 degrees. This separation is impossible for the central peak, therefore an accurate  $J_{\rm v}$  ratio must include the intensity from all four Brillouin peaks plus the central peak. Second, the location of the base line is difficult to determine since the extra two peaks generate a large uncertainty in its position because a consistent flat portion cannot be obtained. For these reasons we were obliged to design a different type of cell to eliminate the problems mentioned.



Brillouin Frequency Shifts from Benzene-Relative Angular Dependence of Incident and Reflected Light Figure 7.

The final design selected, which we call the Brewster cell, is shown in Figure 8. The flat entrance window allows a parallel beam to enter and exit while preventing the focusing that will occur within a cylindrical cell. Thus the incident beam in a cell with a flat entrance window is still parallel at the position of the exit window, whereas for a cylindrical cell the incident beam is expanding and produces more diverse reflections. The exit window is tilted at the calculated Brewster's angle for the glass-air interface instead of the benzene-glass interface since the first set of interfaces involves the largest refractive index change and therefore the largest reflection at this surface. At Brewster's angle, vertically polarized light will completely pass through a window while horizontally polarized light will be reflected. Since the incident light is vertically polarized, this angle will eliminate most of the back reflections which produce the two extra peaks. Brewster's angle for the glass-air interface is 34°8' from the perpendicular but because of the small refraction at the benzene-glass interface, the exit window is set instead at 33°30'. There still appears to be a small amount of light reflected from the benzene-glass-air surfaces but this light is not reflected directly back into the scattering volume but upward and out of this volume.

The Brewster cell solved one problem, namely the elimination of the small reflected peaks, but causes more extraneous light to be scattered because of the many angles in the cell, thus giving a higher "noise" level in the final

spectra. This undesirable feature fortunately is easily reduced by painting the outside of the cell with a flat black paint, but leaving entrance and exit surfaces free plus a narrow strip between these for the scattered light detection.

## b-Size

A study relating the effect of the scattering cell size to the final Brillouin spectra, shows that a cylind-rical cell of one inch diameter or larger should be used. Extraneous surface scattering which increases as the cell diameter decreases, adds only to the central peak, giving false  $J_v$  ratios for small cells. Our  $J_v$  ratios for benzene when taken with rectangular cells, the Brewster cell and a one inch in diameter cylindrical cell were all consistent, indicating that extraneous surface scattering was a minimum.

#### c-Holder

A sample cell holder, Figure 9, was designed so the Brewster cell or any other cylindrical cell could be removed from its original scattering position for filling, alignment, etc. and then be replaced to obtain reproducable spectra. The sample cell is secured to the holder with an "O" ring having the same size as the outside diameter of the cell. This "O" ring is located between two plates which can be tightened together with three small screws flattening the "O" ring slightly and thus holding the cell in place. The height and vertical alignment of the sample cell with respect to the table is adjusted with three supporting screws. To

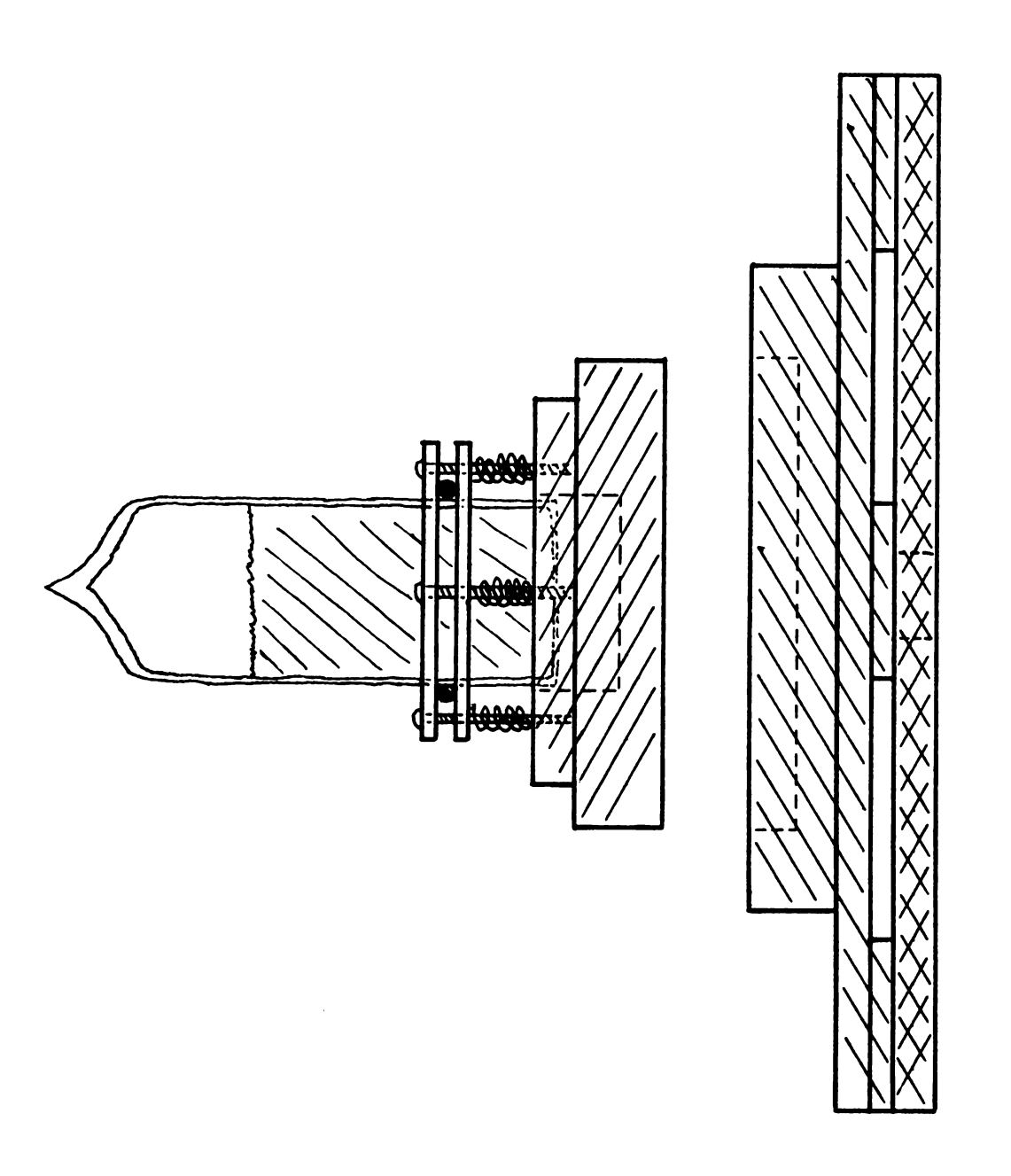


Figure 9. Light Scattering Cell Holder

increase the height of the cell, the supporting screws are all unscrewed the same amount, whereas if only one or two are unscrewed the vertical alignment is adjusted. This design also allows for the use of a temperature control block, previously available, by simply placing the control block over the cell and holder.

# 3-Materials and Preparation

#### a-Polystyrenes

All the polystyrene samples except one, were polymerized anionically and have a narrow molecular weight distribution. The exception, N.B.S. 706, was polymerized thermally and has a broad distribution. All appeared fluffy, except the two from N.B.S., and dissolved easily in benzene. The data characterizing each sample is listed in Table 3. When solutions of each sample were examined by ultraviolet and infrared spectroscopy, no evidence of impurities was found. Also, the molecular weight distribution was checked for a single peak in the ultracentrafuge using the technique of velocity-sedimentation. All solutions showed a single peak when run at a concentration of 16 mg/ml in benzene, confirming a single molecular weight distribution.

## b-Solvents

Chromatographic quality benzene, 99.83 mole percent pure from Matheson, Coleman and Bell, was used to make the polymer solutions. The largest impurities were water,

determined to be 0.13% by the Karl Fisher method, and a low boiling unknown of 0.04% determined by gas chromatog-raphy. These impurities were reconfirmed with mass spectroscopy and gas chromatography, while no other higher molecular weight or higher boiling point impurities were present.

## c-Filtration

All polymer solutions were filtered before use in Brillouin scattering. Since large particles other than the polymer particles, like dust, scatter light they can add a significant amount to the total scattering. Consequently if dust particles are present, the final spectra cannot give quantitative information for our calculations. A filtering apparatus was constructed consisting of two filters arranged in series with the sample cell so that when a solution is filtered into a sample cell, contact with the air and dust is eliminated. The first filter in the series consists of an ultrafine Pyrex sintered glass filter with a pore size of  $0.9-1.4\mu$ , while the second is a Solvenert Millipore filter with a pore size of  $0.25\,\mu$ . The construction of the filter is described in the literature [54].

It is possible to connect the filtering appartus with the sample cell in two different ways, depending on whether or not the sample cell is to be reused. The cylindrical cells were connected easily to the filtering apparatus with two Fisher-Porter joints and a teflon gasket making a sealed system. The reusable Brewster cells however, could only be filled using the filter when these cells are placed in a dust free enclosed box.

A clean, dust free, covered cell is placed inside the box and a continuous flow of filtered air is passed through the box to eliminate dust present in the air. The cell was uncovered, rinsed five times with filtered solvent and four times with solution before being filled with solution and recovered. Neither the solvent nor solutions at any time showed "speckle scattering" from large dust particles when placed in an intense laser beam.

## d- Glassware

All glassware in contact with solvent or solutions, including flasks, filters and scattering cells are carefully cleaned before use. The cleaning procedure includes first annealing the glassware overnight in a glass oven at 580°C to burn off all dust, solvent and adhering polymer, then washing with aqua regia. The acid is completely rinsed off with distilled water followed by a final rinse with conductance water and final drying in a hot air oven to give a spotless piece of glassware.

To assure that the Brewster cell was completely dust free, it was attached to a siphon, suspended in a special column and refluxed with the solvent to be used, Figure 10. After being flushed out overnight, it was capped while in the column under reflux conditions, then cooled and placed in the dust free box to be rinsed and filled as already

described.

#### e-Solutions

All solutions were initially made on a weight basis, e.g., weight of solute to weight of solvent, then filtered into a scattering cell according to a procedure described previously. About 10 ml of the solution was filtered into the cell while the remaining 70 ml was filtered into a volumetric flask. This latter amount was divided into two parts and evaporated to dryness in a hot air oven for two hours to give the weight of polymer present and the value of the final concentration in terms of grams of polymer to grams of solvent. Small concentration deviations often occured between the two aliquots because only small amounts of polymer were left after evaporation; frequently ten milligrams or less. Even so the final concentrations were always higher than what was initially made by about 3%, possibly due to solvent evaporation during transfer and handling. Finally the concentrations were multiplied by the density of the solvent at the temperature of the scattering experiment to obtain the concentration in grams per milliliter.

# 4-Spectra

#### a-Shapes

The Brillouin spectrum for a nonrelaxing liquid consists simply of three Lorentzian shaped peaks [28]. For the usual case of a relaxing liquid, the line shapes are more

complex [55], involving the superposition of two or more peaks, the overlap of adjacent peaks and instrumental distortion [18]. To identify the actual shapes present in our spectra of benzene we took 99 points from each of the three peaks and fit them with a least squares computer program to both exponential and Lorentzian equations. A reasonable fit was obtained with the Lorentzian shape for all three peaks while an exponential shape had a very poor fit. On a closer point by point examination of the central peak, the experimental points fit with the Lorentzian equation were broader at the bottom 20% than the equation predicts from the best curve fit indicating a second broader peak might also be present. When two Lorentzian equations were used to fit the points in the central peak, one for the top 80% and the other for the bottom 20%, an excellent fit was obtained for each section. This fact tends to support Mountain's theory for the existence of a relaxation peak with a different halfwidth located under the central peak. To determine if this relaxation peak should have a half-width large enough to be measured with a scanning interferometer, we use Mountain's equation 29, where the half-width of this peak is

$$\Gamma_{1/2}^{M} = \frac{v_0^2}{v^2} (\frac{1}{7}) .$$
 81

Using literature values [20] at 22.6° C for  $v_0 = 1312$  M/sec. and  $T = 2.4 \times 10^{-10}$  sec. and from our own measurements of the Brillouin shift for benzene v = 1533 M/sec., we find the half-width  $\Gamma_{1/2}^{\rm M}$  = 3.05 x 10<sup>9</sup> Hz. Thus, this peak is wide enough to be detected and should slightly overlap the Brillouin peaks which have a splitting of  $\Delta V$  = 8.94 x 10<sup>9</sup> Hz.

The Brillouin peaks, when curve fit by a least squares computer program, are definitely not symmetrical about the maximum intensity [56]. But when each Brillouin peak was divided into a "left half" and "right half" and curve fit, both halves had good Lorentzian shapes although differing in their half-widths. The half-width of the lower frequency shift side, the side toward the central peak, always has a large half-width also indicating a possible overlap with a hidden peak. Moreover the spectral line between the central and Brillouin peaks never reaches the base line, defined in the next section, even with excellent finesse. This is seen in Figure 6 and also indicates a broad central relaxation peak.

# b-Baseline

The position of the base line in the experimental Brillouin spectra affects the degree which a Lorentzian equation will fit the experimental data, the value of the half-widths of the individual peaks and most importantly to our work, the value of the ratio  $J_{V}$ . As mentioned in the theory, this ratio should only measure isotropic fluctuations in the dielectric constant so only that scattered light which

is vertically polarized should be measured, V<sub>V</sub>. Even so, part of this vertically polarized light is still due to anisotropic fluctuations and is often seen as broad frequency shifts which cannot be resolved with an interferometer [56]. When possible, this scattered light from anisotropic fluctuations should be selectively removed in the spectral analysis. For benzene, the selection of a baseline position is even more difficult than for other liquids since there exists a significant amount of vertically polarized light due to anisotropic scattering that cannot be resolved by a Fabry-Perot scanning interferometer. Thus this light, referred to as the Rayleigh "wing" [57] since it extends out to 250 cm<sup>-1</sup> when analyzed by Raman spectroscopy, exists in the whole Brillouin spectrum as a flat background above a dark current base line, Figure 6.

This long flat background is very evident in spectra of benzene taken at small mirror separations of 2 mm, since at this separation the Brillouin peaks are then very close to the central peak. We take this flat background as our spectral base line when measuring the ratio  $J_{\rm V}$  and curve fitting the peaks to various shapes. Increasing the mirror separation "moves" the Brillouin peaks away from the central peak until they begin to overlap the Brillouin peaks of the next order. At this point of overlap the spectral base line increases in height above the dark current and the experimental ratio  $J_{\rm V}$  decreases.

Two different methods can be employed to determine when overlap occurs in a benzene spectrum if the ratio  $J_{t}$ cannot be used. The first method uses the fact that the horizontally polarized spectra, H,, has no detectable peaks in the Brillouin spectra and thus has a constant intensity above the dark current for both changing mirror separations and changing scattering angles. A ratio of this constant horizontally polarized intensity to the vertical polarized intensity of the spectral base line defined above, has a consistent value until the Brillouin peaks of consecutive orders begin to overlap; then the ratio changes, Table 1. This allows a quantitative evaluation of overlap between the Brillouin peaks. A second method, although more qualitative, determines the distance the Brillouin peaks extend out from their maximum value before a difference from the spectral base line is not detectable. Unfortunately this value for the extension of the Brillouin peaks decreases with increasing mirror separation because the free spectral range changes. Even so, this method still appears to indicate when overlap occurs and agrees with the first method.

#### c-Peak Areas

The areas under the three peaks are determined by tracing over each boundary with a planimeter. A ratio of the areas from the central and the two Brillouin peaks will

determine the ratio  $J_v = \frac{I_c}{2I_B}$ . For the lower boundary

Identification of When Brillouin Peak Overlap Occurs Table 1.

Interferometer Mirror Separation in cm	0.469	0.569	0.669	0.769	0.804	696.0
Intensity of Depolarized Spectra Intensity of Spectral Base Line	0.640	0.640 0.657 0.634	0.634	0.641	0.640	0.599 Peak Overlap
One-Half Separation Between Consecutive Brillouin Peaks in 10 <sup>9</sup> Hz	9.26	69.9	4.77	3.40	3.05	1.99
Brillouin Peak Extension in 10 <sup>9</sup> Hz	3.00-	2.67-	2.44	2.23-2.13	2.18	Peak Overlap

of the peaks the spectral base line is extended under the peak, whereas another line is drawn at one half the distance between peaks to separate them horizontally. When solutions of high molecular weights and/or high concentrations are used, the Brillouin peaks are expanded electronically by exactly three or ten fold in an attempt to obtain an area comparable to the central peak thus decreasing the large error present in measuring very small peak areas. A ten fold expansion is shown in Figures 18, 19, 20 for a polystyrene solution in benzene.

## 5-Spectral Analysis

## a-Solvents

# (1) Mirror Separation

The interferometer mirror separation should be selected to avoid the overlap of any peaks and also to insure that a correct set of Brillouin peaks are associated with a specific Rayleigh peak. Both those conditions can be met by taking a series of spectra at various mirror separations and plotting the relative Brillouin peak separation, the peak separation divided by the free spectral range, against the mirror separation, Figure 11.

This graph for benzene extrapolates through zero with a slope of 0.413. Thus any mirror separation less than 1.20 cm will make the Brillouin peaks closest to the Rayleigh peak the correct set of peaks. With benzene, this is double checked by recognizing the asymmetry in the Brillouin peak and

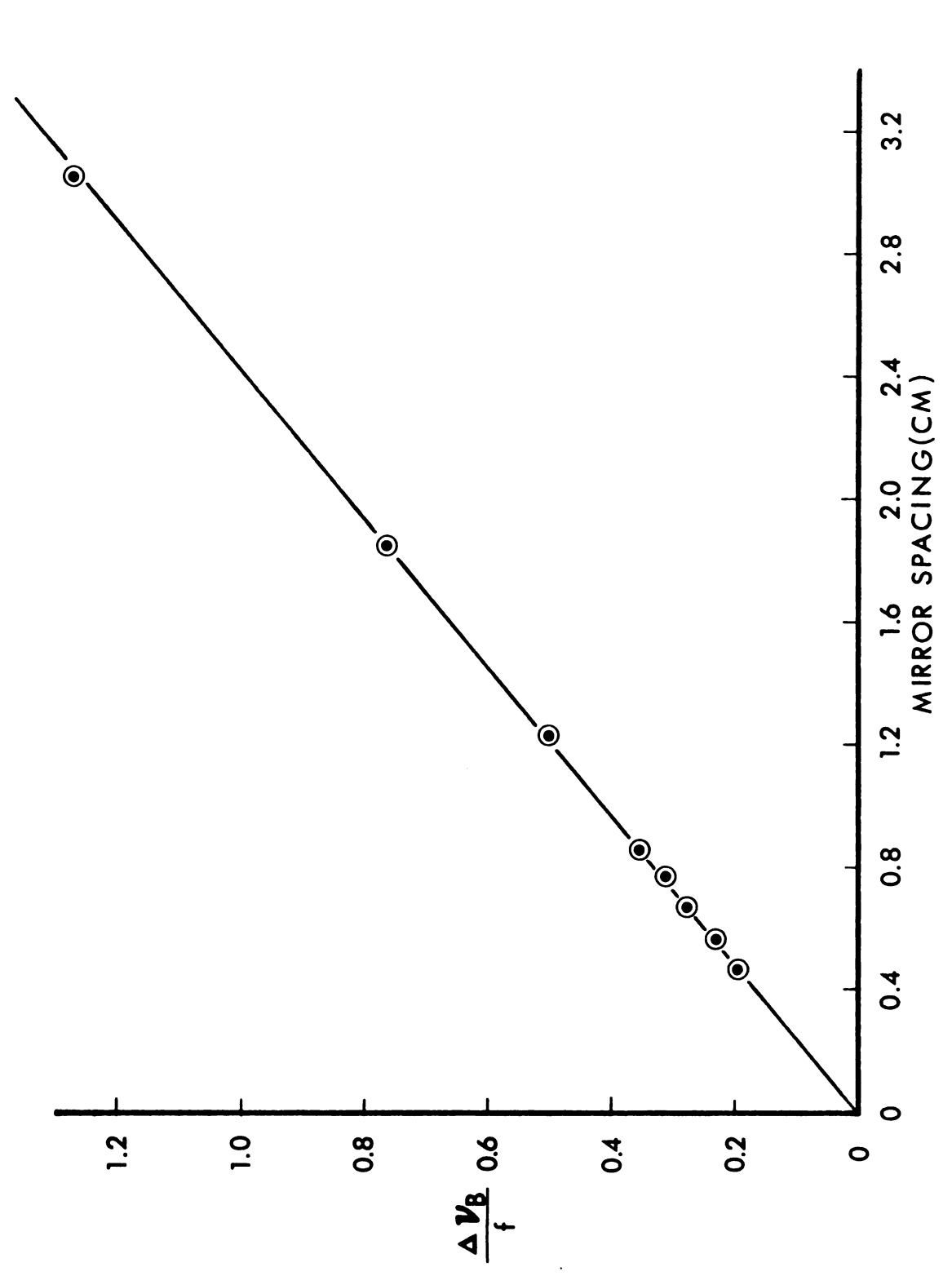


Figure 11. Relative Dependence of Brillouin Peak Separation on Interferometer Mirror Spacing for Benzene

noting that the side with the more slowly decreasing slope is always toward the side of the correct Rayleigh peak. Finally, a specific mirror setting is chosen to give equal spacing between all peaks and thus allows minimum overlap. The optimum mirror separation we have chosen for benzene is It is noted that in early measurements which have a low finesse, the Brillouin peaks are shifted or "pulled" toward the central peak because of an overlap with the central peak [18, 58, 59]. Therefore some authors have recommended that the mirror separations should be selected to allow an equal distance between Rayleigh and Brillouin peaks to minimize this effect. We have found with a finesse of 45, this "pulling" effect due to peak overlap is not evident as seen by the linear dependence of the Brillouin peak splitting on mirror separation in Figure 11. Thus a correct velocity of sound in a liquid or solution can be obtained even with a close proximity of the Rayleigh and Brillouin peaks.

#### 2-Angular Measurements

The frequency shift of the Brillouin peaks  $\Delta V$ , increases with an increasing scattering angle  $\Theta$ , as given in the following equation.

$$\Delta V = \frac{2v_s}{\lambda/n} \sin(\Theta/2)$$
 84

Thus we are probing higher frequency pressure fluctuations

by increasing the scattering angle and therefore can measure the velocity of sound at different frequencies. A plot of the relative Brillouin frequency shift against angle for benzene in Figure 12 shows a straight line. If the dispersion in the sound velocity had been large enough in our range of frequencies, we would detect a slight upward curvature, since for benzene the velocity dispersion is positive. This dispersion has been detected in other liquids using Brillouin scattering [60].

The half-width of the Brillouin peak is also angular dependent. According to hydrodynamic theory [39] the half-width is equal to the product of the velocity of sound and the amplitude absorption coefficient,

$$\Gamma_{1/2}^{B} = 2 \alpha v.$$
 85

When the absorption coefficient is derived from Stokes equation, assuming an ideal liquid with no relaxations, the half-width then has the following form.

$$\Gamma_{1/2}^{B} = \frac{1}{\rho_{0}} \left[ \frac{4}{3} \, \boldsymbol{\eta}_{s} + \, \boldsymbol{\eta}_{B} + \frac{\boldsymbol{\lambda}'}{c_{p}} \, (\boldsymbol{\gamma} - 1) \right] k^{2} ;$$

$$k^{2} = \frac{8\pi^{2}n^{2}}{\boldsymbol{\lambda}_{0}^{2}} (1 - \cos \theta)$$

When Mountain's theory for light scattering from a relaxing liquid is used instead, the half-width of the Brillouin

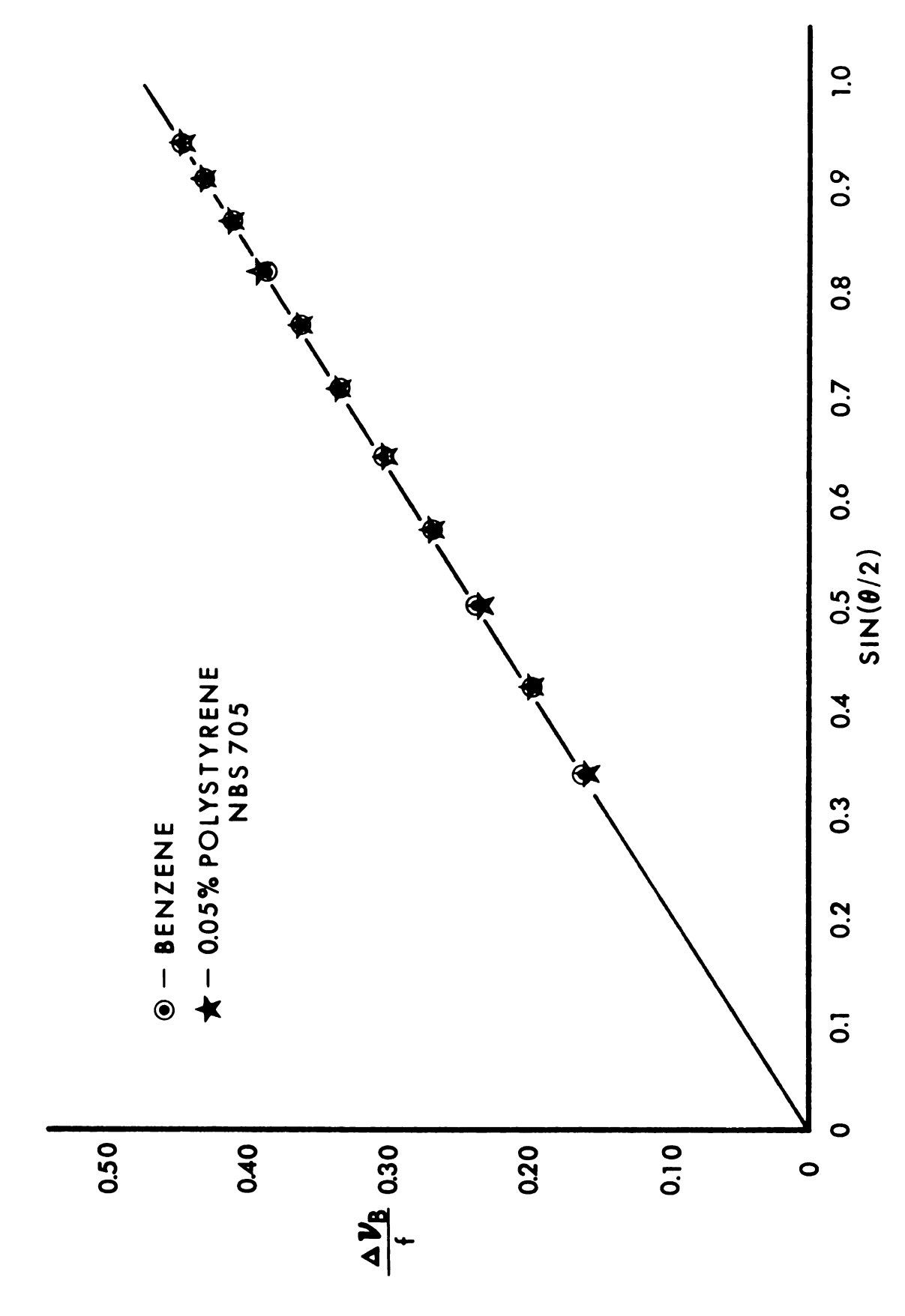


Figure 12. Relative Brillouin Peak Separation for Benzene and a Polystyrene Solution

peak is

$$\Gamma_{1/2}^{B} = \frac{1}{\rho_{0}} \left[ \frac{4}{3} \, \boldsymbol{\eta}_{s} + \, \boldsymbol{\eta}_{B} + \frac{\boldsymbol{\lambda}'}{c_{p}} \, \left( \boldsymbol{\gamma} - \frac{v_{o}^{2}}{v^{2}} \right) \right] k^{2} 
+ \left[ \frac{v_{\infty}^{2} - v_{o}^{2}}{1 + v^{2} \, \boldsymbol{\tau}^{2} k^{2}} \right] \cdot \left[ 1 - \frac{\boldsymbol{\lambda}' \boldsymbol{\tau}_{k}^{2}}{\rho_{o}^{c_{v}}} \right] k^{2} .$$

Thus the Brillouin peak half-width is not linearly dependent on the square of the scattering vector k. When we plot the true Brillouin half-width  $\Gamma_{1/2}$  against (1-cos  $\theta$ ) for the simplified non-relaxing case, we should obtain a zero intercept and constant slope. But the intercept is not zero and the slope of the experimental line is not a constant (Figure 13), since benzene is actually a relaxing liquid.

A least squares line is fit to the data for the non-relaxing case and has an intercept of about 60% of the half-width at a 90 degree scattering angle. Even though the data have a large error present, it is still evident that a simple theory does not give a zero intercept, indicating that an extra relaxing component is present as Mountain suggests in his theory.

The experimental ratio  $J_{\rm V}$  for benzene has a very small angular dependence as seen in Figure 14. It appears to increase only a small amount at angles greater than 90 degrees, although the increase is within experimental error, while there is a definite decrease at the lower angles. Since for smaller scattering angles, the Brillouin peaks would

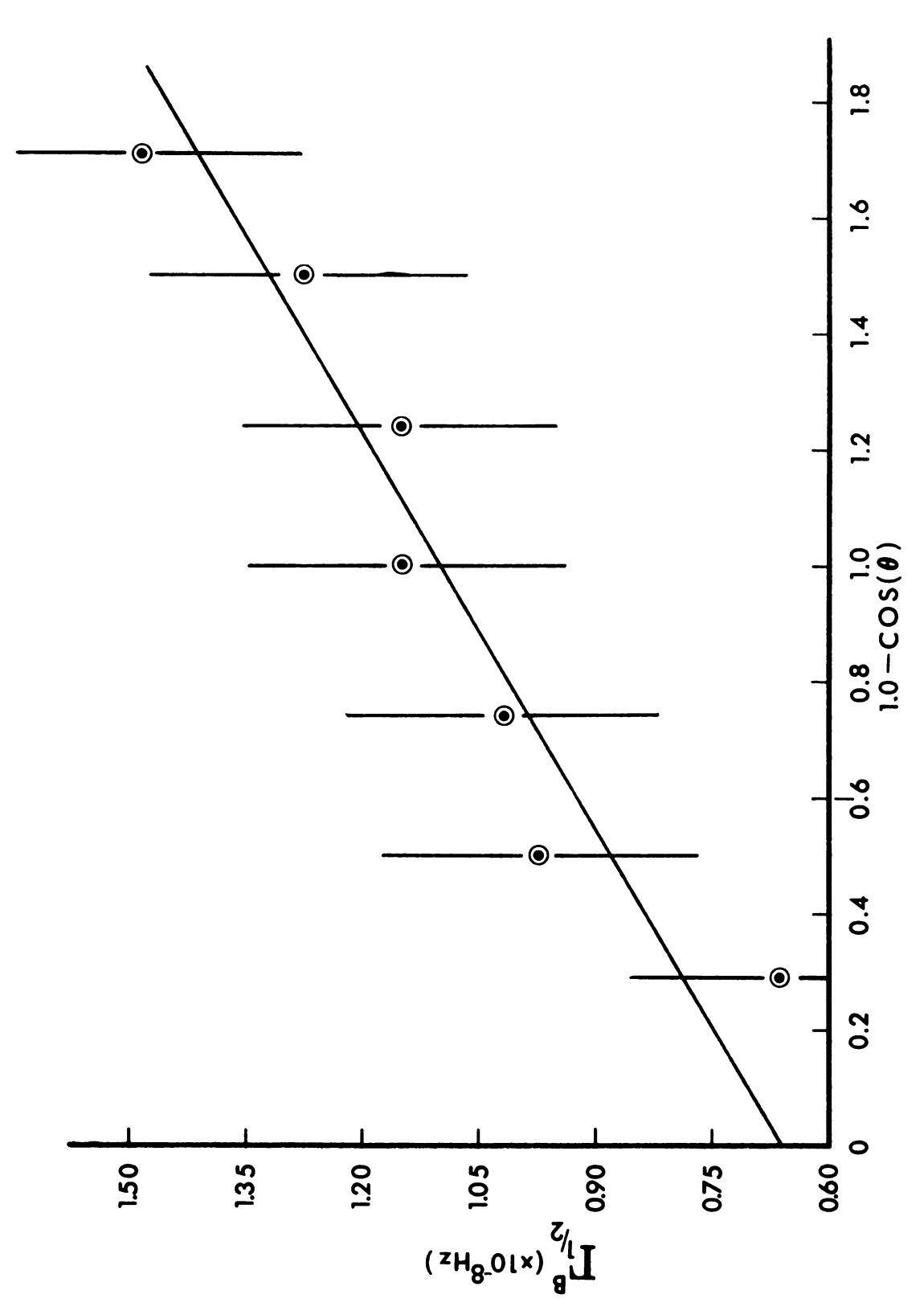


Figure 13. Angular Dependence of Brillouin Half-Widths

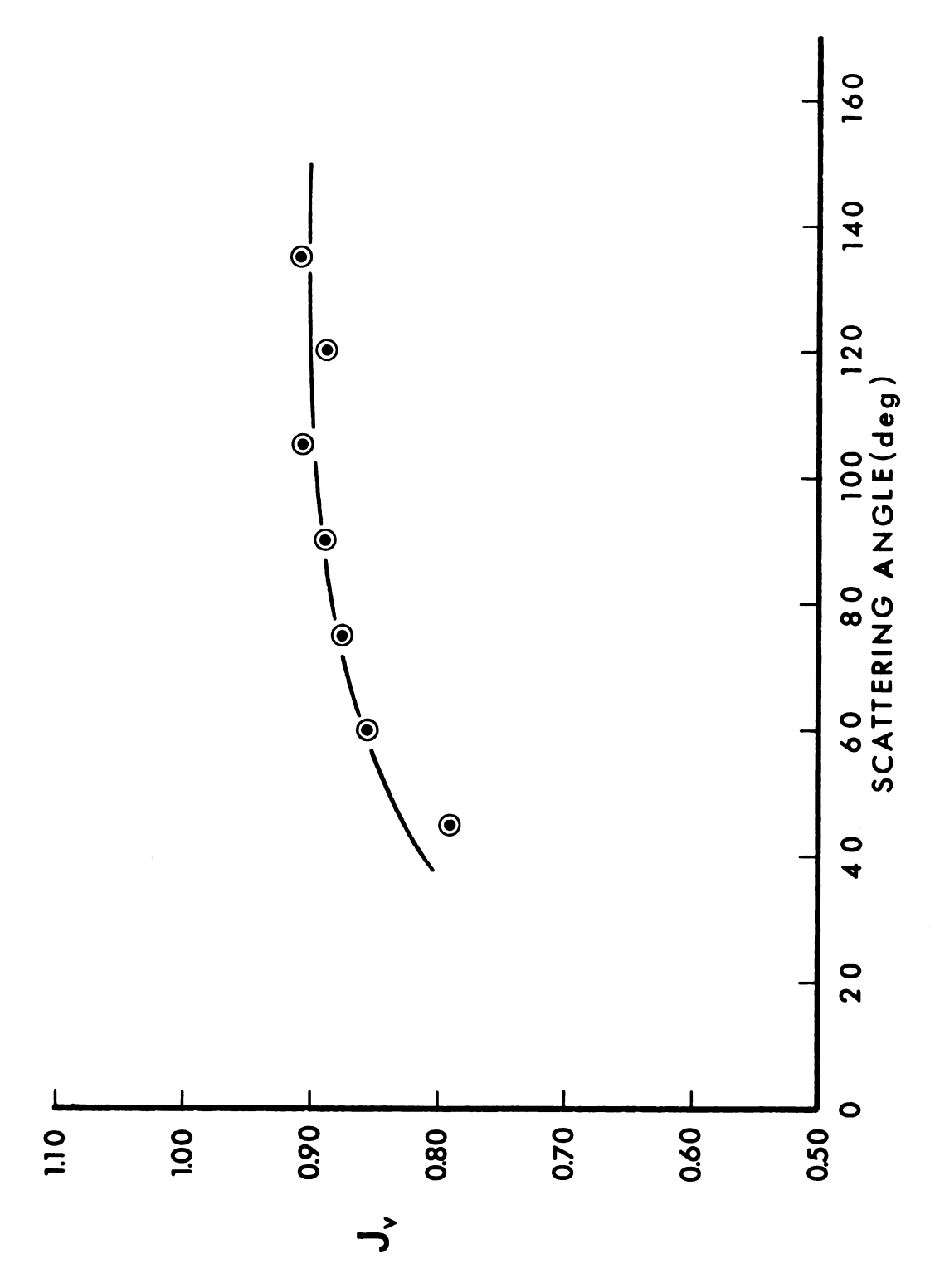


Figure 14. Angular Dependence of the Scattering Ratio  ${\mathtt J}_{{\mathtt V}}$  for Benzene

increasingly overlap this hidden peak and add part of it to their areas, the ratio  $\mathbf{J_v}$  should decrease with a decreasing scattering angle. This would also appear to confirm a Mountain line under the central peak.

#### 3-Polarization Measurements

The Brillouin spectra for benzene, when examined above the spectral base line defined previously, have identical intensity ratios when they are analyzed using incident vertically polarized light and either a vertical polaroid or no polaroid immediately in front of the detector. Thus the Brillouin spectra of benzene we have analyzed are due only to vertically polarized light as is assumed by the theory for light scattering from isotropic fluctuations in a liquid.

For a horizontally oriented analyzing polaroid with the incident light polarization vector either vertical or horizontal there is no indication of any resolvable peaks in the spectra [61] even with a scale intensity expansion of 100 times. This further confirms that the Brillouin spectra we use arises only from vertically polarized light.

#### 4-Experimental Values

The experimental values we have measured and calculated for benzene are listed in Table 2 along with values given by other authors for comparison. The velocity of sound is an average taken at seven different scattering angles as

shown in Figure 12 and is accurate to the extent that the Rayleigh and Brillouin peaks are sufficiently separated. To reduce this error to less than 0.1% requires a finesse of about 20, whereas our finesse for benzene is 45. A lower finesse appears to be the main reason for the lower values encountered in earlier velocity measurements by other authors.

The half-width of the Brillouin peaks measured at half-height are corrected for instrumental effects by subtracting the broadening due to the instrumental response as measured by the width of the Rayleigh peak. The half-widths of both peaks are very sensitive to alignment and reach a minimum value with good alignment, but because of the sensitivity to alignment the precision and reproducability of these values are low.

The relaxation time  $T_{\rm M}$  is derived from Mountain's dispersion equation 36 for a 90 degree scattering angle and 514.5 nm incident light. The zero frequency sound velocity  ${\rm v_O}$  is taken from acoustic measurements [20] while the infinite frequency velocity  ${\rm v_O}$  is calculated according to equations 37 and 38 with the assumption that only a single, dominant relaxation process affects the bulk viscosity. A value for the relaxation time calculated by O'Connor et.al. [62],  $T = 0.55 \times 10^{-10}$  sec. appears to be too small since this results in a half-width for the Mountain line of

 $<sup>\</sup>Gamma$  = 13.4 x 10<sup>9</sup>Hz, exceeding the Brillouin peak splitt-1/2

ing,  $\Delta V = 8.94 \times 10^9$  Hz, and is not consistent with

experimental observations of a flat spectral base line. Our value for  $\tau_{\rm M}$  appears small enough so that the half-width of the Mountain line  $\tau_{\rm 1/2}^{\rm M} = 5.35 \times 10^9 \, \rm Hz$  does not exceed the Brillouin peak splitting, but is large enough to slightly overlap the Brillouin peaks and not allow the spectral line between the Rayleigh and Brillouin peaks to reach the spectral base line. Also the slight dissymmetry in the Brillouin peaks indicates that some overlap exists.

A relaxation time for the bulk viscosity is also calculated according to acoustic theory [20], using the equations

$$\tau_{A} = \frac{\frac{a \pm \sqrt{a^{2} - 4\Omega^{2}}}{2\Omega^{2}}}{\frac{2\Omega^{2}}{\rho_{O}(v^{2} - v_{O}^{2})}}$$

$$a = \frac{\Omega^{2} \eta_{O}^{1}}{\rho_{O}(v^{2} - v_{O}^{2})}$$
87

The components in equation  $\underline{87}$  are the frequency of the Brillouin peaks  $\Omega=2\pi\Delta V$ , the shear viscosity  $\boldsymbol{\eta}_{0}^{'}$ , the density  $\rho_{0}$ , the velocity of sound at zero frequency  $v_{0}$ , and the velocity at the measured frequency. The calculated relaxation time from literature values [20],  $\boldsymbol{\tau}_{A}=1.46\times 10^{-10} \mathrm{sec}$  is in good agreement with the value calculated from Mountain's theory.

A third method for calculating the relaxation time [20] uses the half-width of the Brillouin peak to first determine the sound absorption coefficient  $\alpha$ , from equation 85. The absorption coefficient can be divided into three parts

according to the three main energy relaxation processes.

$$\alpha = \alpha \eta_s + \alpha \eta_B + \alpha_{\lambda'}$$

The last term on the right side depends on the contribution from the thermal conductivity  $\alpha_{\chi}$ , and is very small for most liquids and solids in comparison to the other two terms. The first and second terms due to the shear viscosity  $\alpha_{\eta}$  and to the bulk viscosity  $\alpha_{\eta}$ , respectively, are approximately equal in size. Since the absorption coefficient due to the shear viscosity has been measured by Fabelinskii [20] using acoustic methods as  $\alpha_{\eta} = 2.5 \times 10^3 \text{ cm}^{-1}$ , the absorption coefficient due to the bulk viscosity can be calculated if the Brillouin half-width is known. We obtain  $\alpha_{\eta} = 3.32 \times 10^3 \text{ cm}^{-1}$  and from the following equation also determine the relaxation time.

$$\alpha \boldsymbol{\eta}_{B} = \frac{\Omega^{2}}{2\rho_{O} v_{O}^{3}} \cdot \frac{\boldsymbol{\eta}_{O}'}{1 + \Omega^{2} \boldsymbol{\tau}_{B}^{2}}$$
89

The calculated value  $T_B = 2.63 \times 10^{-10}$  sec. agrees with a value calculated by Fabelinskii [20] in the same manner, namely  $T = 2.4 \times 10^{-10}$  sec., but is larger than either value calculated from Mountain's theory or from acoustic theory.

Each of these values for the relaxation time is used in Mountain's equation  $\underline{29}$  to calculate the ratio  $J_v$  for benzene. In order to use his equation, the half-width of the Mountain

peak must be less than the Brillouin splitting so that the intensity of the Mountain peak plus that of the Rayleigh peak can be experimentally separated from the Brillouin peaks. This requirement implies that the value of the product of the relaxation time, scattering vector and the velocity is greater than unity, or  $\tau \cdot k \cdot v \ge 1$ . Using the relaxation time defined from Mountain's dispersion equation, we calculate  $\tau \cdot k \cdot v = 5.44$ , thus satisfying the requirement that this product is not less than unity. The calculated ratios using the different relaxation times are  $J_{v}(\tau_{M}) = 0.961$ ,  $J_{v}(\tau_{A}) = 0.966$ ,  $J_{v}(\tau_{B}) = 0.990$ . These values show only a small variation of the ratio  $\boldsymbol{J}_{\boldsymbol{v}}$  using the various relaxation times, but all are slightly larger than the measured value  $J_v = 0.888$ . Since the experimental measurements include part of the Mountain peak in the Brillouin peak due to overlap whereas the theoretical calculations assume complete separation, the experimental value for  $\boldsymbol{J}_{\boldsymbol{v}}$  should be smaller than the theoretical value. The percentage of the Brillouin peak comprised by the Mountain peak due to overlap is thus about 3.72%, a reasonable value since the Mountain peak overlaps the Brillouin peaks by only a small amount. In conclusion, a relaxation peak appears to be present, but its intensity and width can only be approximated because it overlaps three other peaks simultaneously.

#### b-Solutions

## (1) - Peak Widths and Frequency Shifts

Dilute solutions of polystyrene in benzene, less than 0.25%, do not appear to effect either the peak widths

Table 2. General Physical Constants of Benzene

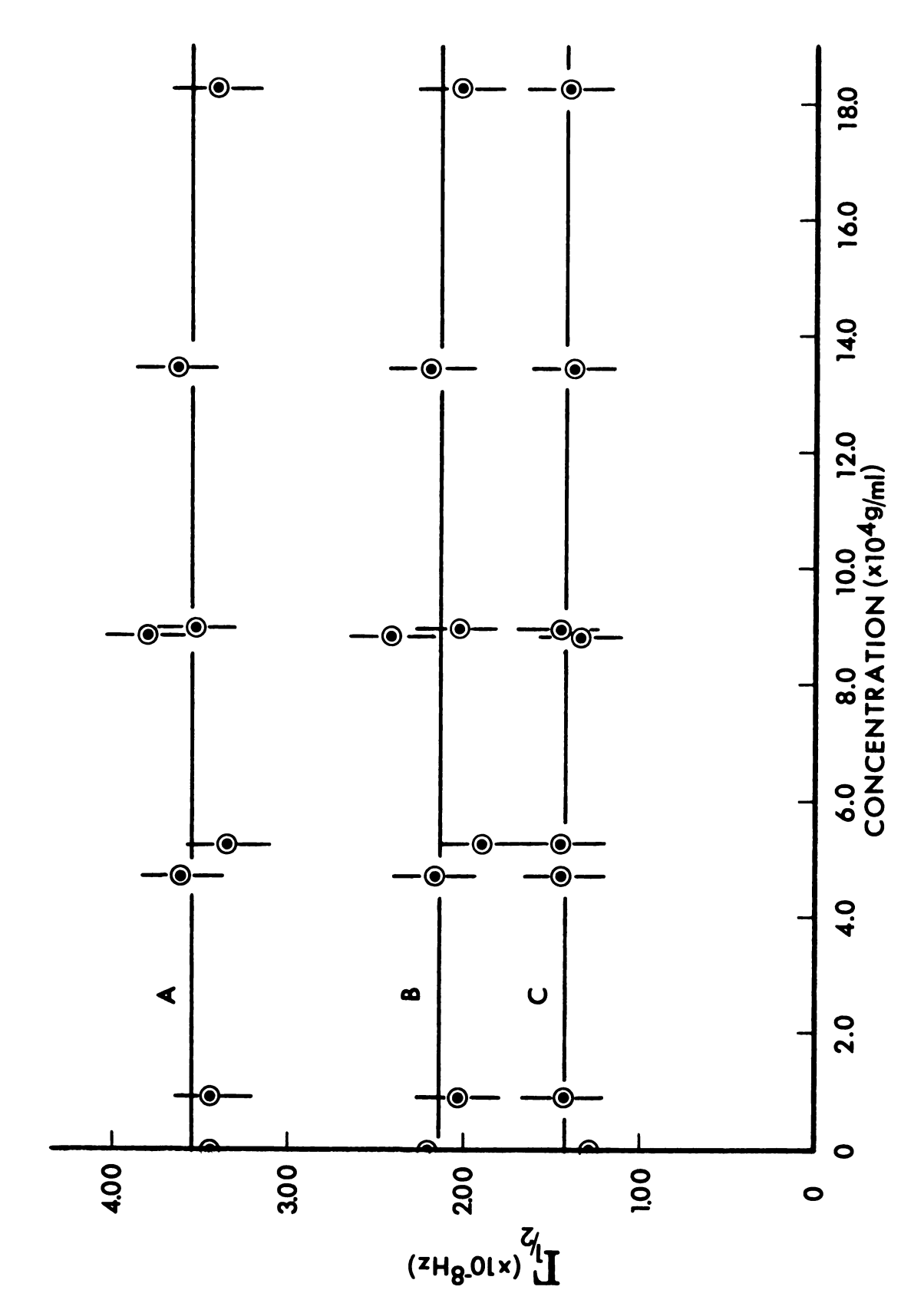
· · · · · · · · · · · · · · · · · · ·	
Our Value(22.6°C)	Literature Values
0.888 <u>+</u> .020	0.86(1)0.80(2)0.84 <u>+</u> .5(3)
0.961	0.79(2)
8.93x10 <sup>9</sup> Hz	-
1312m/sec	-
1533m/sec	1470 (4),1500 (3),1546 (5)
1540m/sec	-
1.42×10 <sup>8</sup> Hz <u>+</u> .20×10 <sup>8</sup> Hz	1.74×10 <sup>8</sup> (6)
5.35×10 <sup>9</sup> Hz	-
$3.32 \times 10^3 \text{cm}^{-1}$	
1.37×10 <sup>-10</sup> sec	$0.54 \times 10^{-10} (2)$
1.46x10 <sup>-10</sup> sec	$2.5 \times 10^{-10} (4)$
$2.63 \times 10^{-10} $ sec	$2.4 \times 10^{-10} (4)$
	Value (22.6°C)  0.888±.020  0.961  8.93×10 <sup>9</sup> Hz  1312m/sec  1533m/sec  1540m/sec  1.42×10 <sup>8</sup> Hz  ±.20×10 <sup>8</sup> Hz  5.35×10 <sup>9</sup> Hz  3.32×10 <sup>3</sup> cm <sup>-1</sup> 1.37×10 <sup>-10</sup> sec  1.46×10 <sup>-10</sup> sec

#### References

- 1-G. A. Miller, F. I. San Fillippo, D. K. Carpenter, Macromolecules 3 125 (1970)
- 2-C. L. O'Connor, J. P. Schlupf, J. Acoust. Soc. 40 663 (1966)
- 3-H. Z. Cummins, R. W. Gammon, J. Chem. Phys. <u>44</u> 2785 (1966)
- 4-I. L. Fabelinskii, "Molecular Scattering of Light," Plenum Press (1968)
- 5-S. L. Shapiro, M. McClintock, D. A. Jennings, R. L. Barger, I. E.E.E. J. Quant. El. QE-2 89 (1966)
- 6-R.Y. Chiao, P. A. Fleury, "Physics of Quantum Electronics," McGraw-Hill, New York (1966).

or the frequency shifts in Brillouin spectra. This effect has been confirmed for the central peak for other solutions using self-beat spectroscopy [60]. As seen in Figure 15 for increasing polystyrene concentrations, neither the Brillouin nor the Rayleigh peaks have half-widths that change even though over this range of concentrations, the central peak increased in intensity by five times. These peak half-widths are sensitive to instrumental alignment and so also represent a direct measure of our ability to reproduce a spectrum. However, the difference in the half-widths, the actual Brillouin half-width  $\Gamma_{1/2}$ , appears to be less susceptible to errors than either of the peaks. Also the Brillouin frequency shift, which should be a good test to determine if concentration effects are present because of its better accuracy, does not change over this same concentration range.

Since neither of these parameters vary with concentration, we can assume  $v_0$ ,  $v_\infty$  and  $\tau$  are also unaffected, and so any coupling between concentration fluctuations and pressure fluctuations is zero to a first order approximation, as Miller has assumed during the derivation of his theory. This allows us to use the much simpler equation of Miller 67, instead of the very complex equations of Mountain. Of course in a different case this simplified assumption might fail, for instance when the macromolecules have low molecular weights or small values of  $(\partial n/\partial C_2)$  thus requiring higher concentrations for good measurements. Also, Mountain's equations are based on a thermal relaxation of the bulk viscosity so liquids with a



Concentration Dependence of Rayleigh and Brillouin Peak Half-Widths for Polystyrene in Benzene-(A) Brillouin, (B) Rayleigh, (C) True Brillouin Half-Width Figure 15.

structural relaxation or highly ordered structure like water, dimethylsulfoxide, etc. can not be used, nor can anisotropic liquids such as liquid crystals. Accordingly we are limited to a narrow range of liquids when we seek to apply Mountain's and Miller's theories since several conditions must first be met. Primarily the solvent must dissolve the solute without absorbing light at the incident wave-length. Next the solute must not affect the properties of the solvent when in solution at a low concentration yet scatter sufficient light to be detectable. Finally the solvent can only have one dominant relaxation mechanism and that must be a thermal relaxation mechanism.

## 2- Molecular Weight Determination

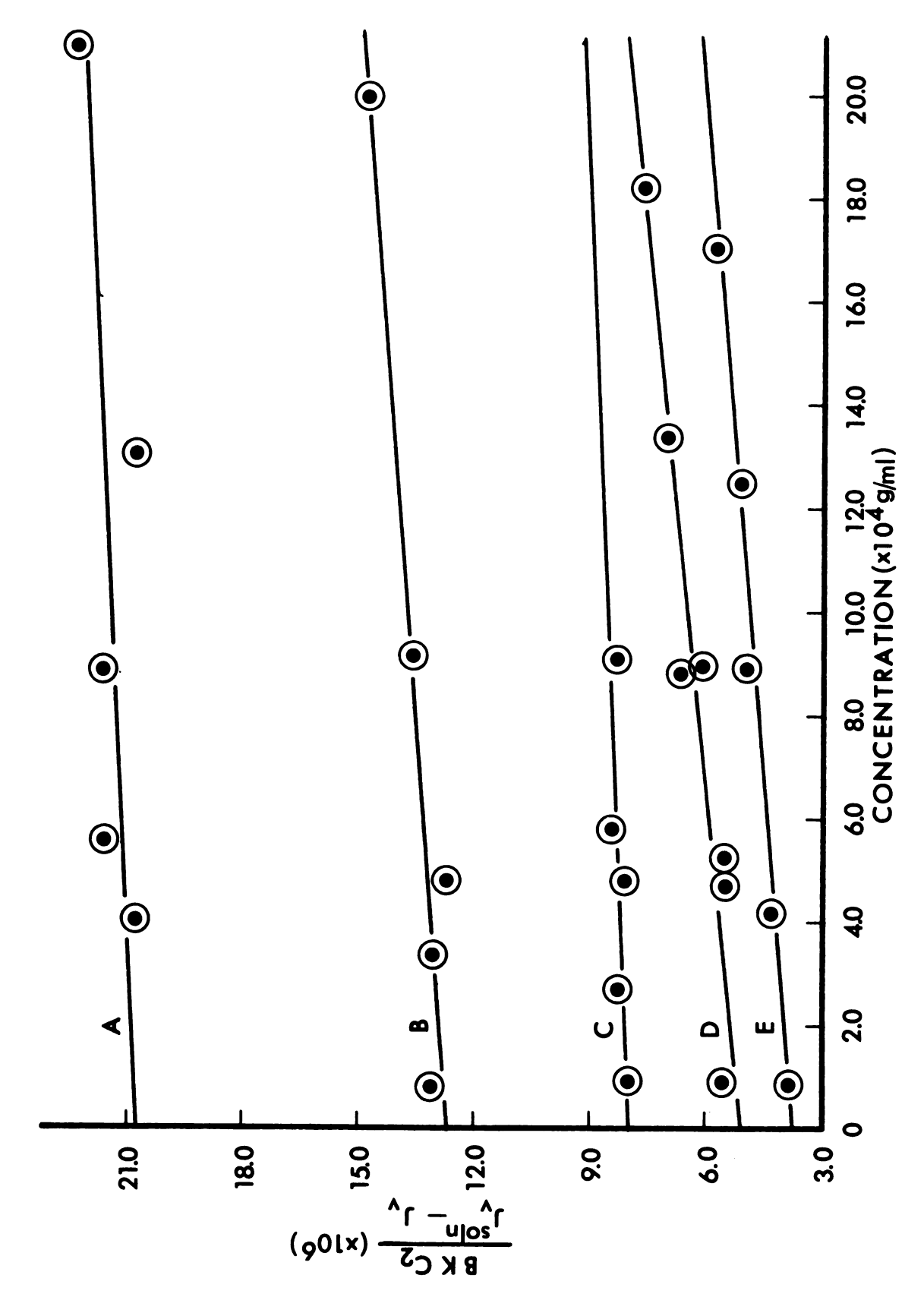
Weight average molecular weights are obtained from Brillouin scattering with an equation derived by Miller and modified with a factor  $P(\theta)$ .

$$\frac{BKC_2}{J_W \text{soln.} - J_W} = \frac{1}{M_W P(\Theta)} + 2A_2C_2$$
 90

For macromolecules with molecular weights less than about  $10^6$  g/mole, the factor P( $\theta$ ) is set equal to one for all scattering angles, with negligible error. The value of  $J_{_{\mbox{\bf V}}}$  for pure benzene is the average value given earlier while the values of the other parameters used in the calculation are listed in Table 4. A plot using equation  $\underline{90}$  to derive the molecular weights from Brillouin spectra for five poly-

styrenes of different molecular weights. four with narrow distributions, is shown in Figure 16. Each different concentration was filtered to eliminate dust, degassed, and sealed in a cylindrical cell. Then the Brillouin spectrum was observed at a 90 degree angle using a vertically polarized incident wave-length of 514.5 nm. A least squares computer calculation was used to determine the best line and the weight average molecular weights calculated from the intercept at zero concentration. The final values are given in Table 3 along with values from regular elastic light scattering and viscosity measurements which are ultimately derivable from elastic light scattering. The molecular weights from Brillouin scattering are comparable with other methods although at present this method appears to have a lower precision. The variation in the measured values are due both to difficulties in making up very small concentrations and in aligning a very sensitive instrument to obtain reproducable spectra.

Macromolecules with molecular weights greater than  $10^6$  g/mole require the use of the interference factor  $P(\theta)$  to obtain correct experimental molecular weights at a finite scattering angle. Unfortunately this factor cannot be calculated without first assuming a probable shape for the macromolecule such as a rod or a random coil, since an assumed shape will modify the final calculation. The data are used instead in a double extrapolation plot to both zero concentration and zero angle with a modified Zimm plot. With this procedure no assumed shape is necessary, since the factor  $P(\theta)$  is unity at the zero scattering angle.



Molecular Weight Measurements of Polystyrene in Benzene (A)  $\overline{M}_{W}=48,000$ , (B)  $\overline{M}_{W}=78,400$ , (C)  $\overline{M}_{W}=124,000$ , (D)  $\overline{M}_{W}=194,000$ , (E)  $\overline{M}_{W}=260,000$ Figure 16.

Table 3. Molecular Weight Measurement of Polystyrenes

Type	M <sub>W</sub> (Brillouin)	M_W (Viscosity)	M <sub>W</sub> (Source)	M W/M	A <sub>2</sub> × 10 <sup>4</sup> m <b>l</b> /g
Dow S-3	48,000	49,000	I	1	3.1
Dow S-102	78,400	89,400	82,500	1.05	5.3
Dow S-6	124,000	117,000	1	ı	1.5
NBS-705	194,000	1	179,300	1.07	7.1
NBS-706	260,000	1	257,800	2.1	5.5
Pressure Chemical *Data of Miller	1,850,000 ler	1	2,000,000	1.20	4.2

Table 4. Parameters Used in Molecular Weight Measurements

~~				
Parameter	Units (	Value 514.5nm,22.6°C)	Ref.	Miller's Value (632.8nm,25°C)
C <sub>P</sub>	cal/m -°C	0.3612	2	0.3616
(T6\n <b>6</b> )	1/°C	-6.42x10 <sup>-4</sup>	1,3	$-6.27 \times 10^{-4}$
( <b>3</b> n/3C)	cm/gm	0.108	4	0.102
đ	gm/m <b>l</b>	0.87096	4	_
γ	-	1.439	5	1.431
x	-	0.046	3	0.046
f	-	0.09979	-	0.09977
R	cal/mole-°C	1.987	-	-
ĸ	cm <sup>3</sup> /gm	0.05881	-	0.0542
J <sub>O</sub>	-	0.888	_	0.86
В	-	0.5237	-	0.59
вк	$cm^3/gm$	0.03079	-	0.02759

## References

- 1-G. A. Miller, F. I. San Fillippo, D. K. Carpenter, Macromolecules 3 125 (1970)
- 2-G. D. Oliver, M. Eaton, H. M. Huffman, J. Am. Chem. Soc. 70 1502 (1948)
- 3-D. J. Coumou, E. L. Mackor, J. Hijmans, Trans.Faraday Soc. 60 1539 (1964)
- 4-J. Brandrup, E. H. Immergut, "Polymer Handbook", J. Wiley, New York, (1966)
- 5-C. L. O'Connor, J. P. Schlupf, J. Acoust.Soc. 40 663 (1966)

Since  $J_{v}$  for benzene has a slight angular dependence as seen in Figure 14, the angular values for  $J_{v}$  are used instead of the average value determined at a scattering angle of 90 degrees.

Because of the large scattering associated with the macromolecule we selected, very low concentrations of polymer were used and the Brillouin peaks in the spectra were expanded tenfold for a more accurate detection of their intensities, as seen in Figures 18, 19, 20, Since these spectra were recorded while a constant intensity of the central peak was maintained, an increase in scattering is seen as the opposite of the true situation, a decrease of the Brillouin peak intensity. A close examination of the Figures 18, 19, 20 for a 0.038% polystyrene solution in benzene with a molecular weight of 1.85 x 10<sup>6</sup> g/mole shows only a very small overlap of Rayleigh and Brillouin peaks at 45°, even though the ratio J, is greater than twelve. Also the Brillouin peaks are significantly smaller at 45 degrees than at a 135 degree scattering angle, about twofold, indicating a definite dissymmetry in the scattering envelope and a definite need for an extrapolation to zero scattering angle. In comparison with the change in the ratio J, of pure benzene over the same angles, the benzene changes are barely noticeable in Figure 14, and then they change in the opposite direction due to increased overlap of the relaxation peak. The data for a macromolecule with molecular weight greater than 10<sup>6</sup> gms/mole are plotted in Figure 17 according to a

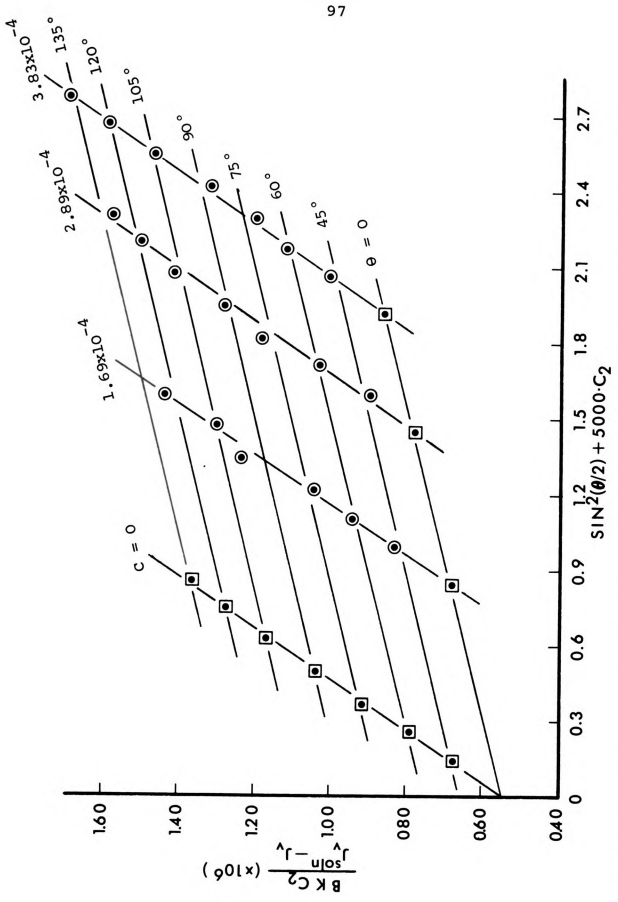


Figure 17. Molecular Weight Measurement of Polystyrene in Benzene.  $ar{M}_W=1.85 imes 10^6$ 

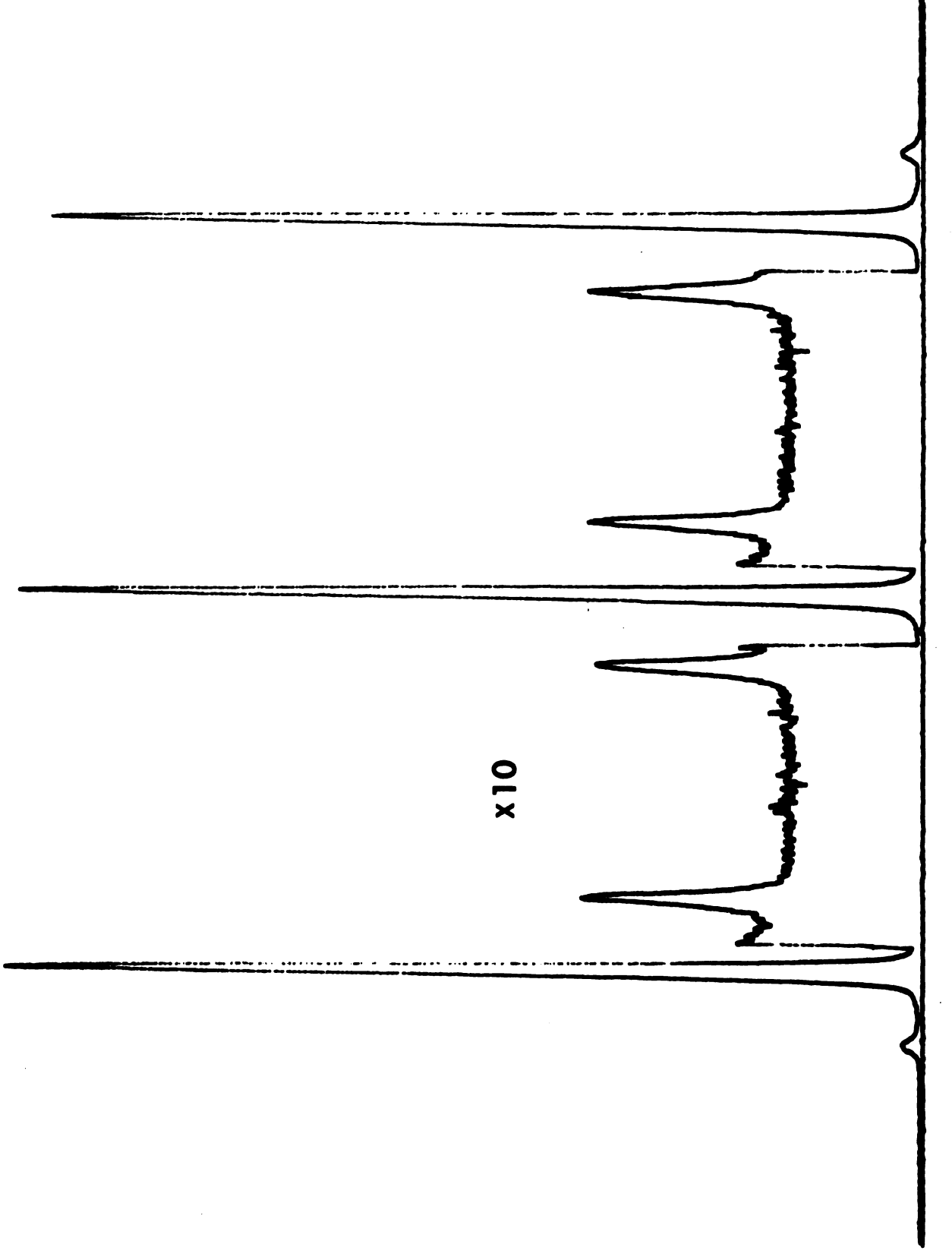


Figure 18. Brillouin Spectrum of Polystyrene in Benzene at 45 Degrees Scattering Angle,  $c_2 = 0.038\%, \, \overline{M}_W = 1.85 \, \times 10^6$ 

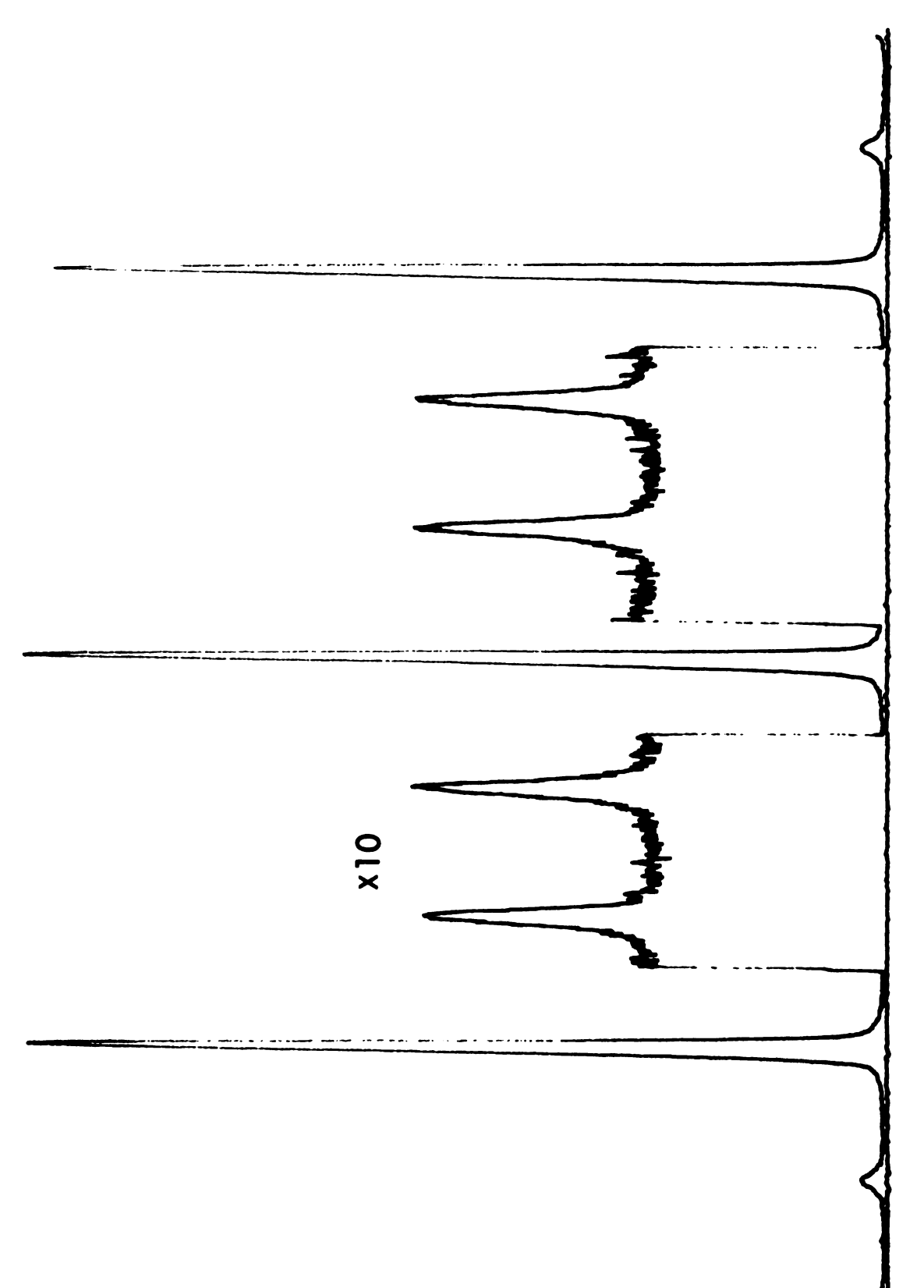


Figure 19. Brillouin Spectrum of Polystyrene in Benzene at 90 Degrees Scattering Angle,  $c_2 = 0.038\%$ ,  $\overline{M}_W = 1.85 \times 10^6$ 

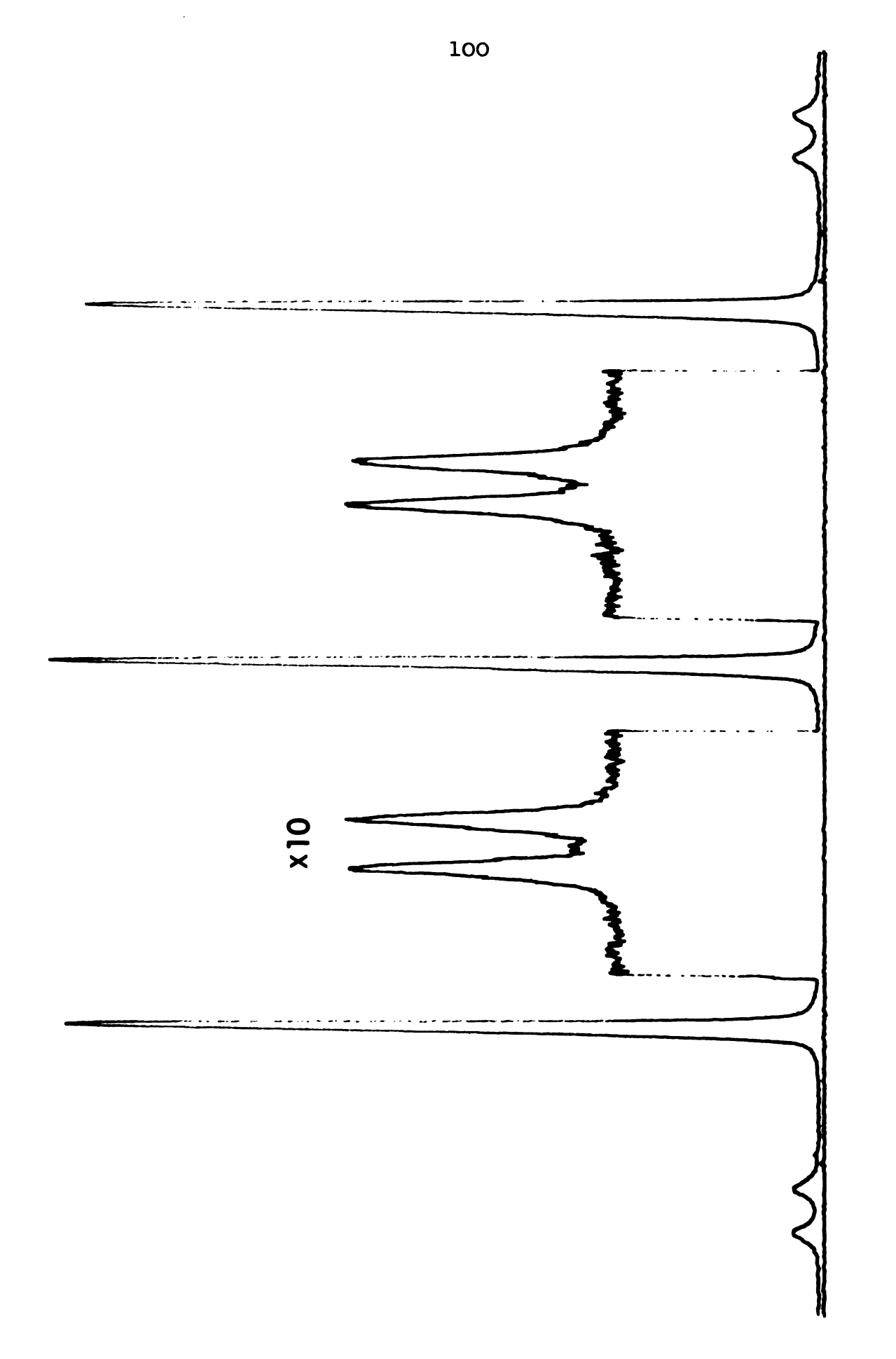


Figure 20. Brillouin Spectrum of Polystyrene in Benzene at 135 Degrees Scattering Angle,  $c_2 = 0.038\%, \overline{M}_W = 1.85 \times 10^6$ 

modified Zimm plot with the molecular weight determined from the intercept for zero concentration and zero scattering angle. These solutions and pure benzene were measured in the Brewster cell because back reflections occurring in standard light scattering cells interfered with accurate measurements.

## 6-Discussion

The accurate determination of light scattered from a solution of macromolecules or a pure liquid is difficult to measure at present using Brillouin spectroscopy. This method is based on the ability of a Fabry-Perot interferometer to resolve three peaks due to scattered light when the separation between these peaks is only about 0.15 cm<sup>-1</sup>. The very high resolution necessary for this separation can be obtained but because it is very high, the inability to consistently reproduce identical Brillouin spectra often causes a significant error in the final calculations. This error is due primarily to the interferometer drifting out of alignment because of very small disturbances. Even with this persistent drifting, we can obtain a reproducability of about 5% over long periods of time like a year, with some measurements such as the J, ratio for benzene. Much more sensitive parmeters, such as peak half-widths, necessarily have larger errors present.

A redesigned light scattering cell, the Brewster cell, partially solved an old problem of reflected light from the cell surfaces which has to be accounted for in most scattering measurements. The main source of reflected light is easily seen in Brillouin spectra taken at an angle other than 90 degrees as originating from incident light reflected from the back surface of the scattering cell at the exit window. Extraneous scattering from other cell surfaces is still present although all are much smaller in intensity than the direct back reflections and have been further reduced to an insignificant amount in our measurements by painting the outside of the cell a flat black.

Solvents and solutions must be free of large dust particles and remain in that condition during the scattering measurements. Thus elaborate cleaning and filtering procedures are necessary to obtain reproducable and meaningful data. With very dilute solutions, a concentration measurement should be made at the point of filling the sample cell since in some cases the macromolecule may be absorbed on any surface the solution has contacted. Conversely, solvent evaporation may have occurred as appears to be present during our procedure changing the original concentration.

The selection and measurement of light scattered specifically from isotropic fluctuations is very important since this is the only part described by current theory. In Brillouin spectra of benzene, only vertically polarized light is detected and from this part the nonresolvable component due to anisotropic fluctuations, the Rayleigh "wing", is separated and eliminated from the measurements. Calculations

using Mountain's equations to determine the ratio  $J_{tr}$  indicate our selection of a base line is correct since the measured and calculated ratios show a much closer agreement than previously used methods. The small remaining difference is resolved by assuming that the Mountain line due to an internal relaxation process overlaps the Brillouin peaks and leads to a lower experimental ratio. If the base line is located at any position lower than the spectral base line we have previously defined, the experimental ratio J. would decrease and not approach the value calculated from Mountain's equations. Thus the base line cannot be selected as the dark current nor can the base line be selected as an imaginary line drawn at 4/3 of the depolarized intensity as other research papers predict [17]. Another method often used when very low finesse and large peak overlap is present is to derive a base line from the best fit of three Lorentzian equations to the experimental spectra. Since the peaks only approximately fit a Lorentzian shape, this method will only give an approximate base line and values of J. and peak half-widths with very large errors [20].

The velocity of sound in benzene obtained from our measurements appears to be slightly larger than the general range of values. We can further substantiate this value of 1533 m/sec at 22.6° C by noting that no dispersion has been detected over the range of frequencies we can measure, even though a positive dispersion could be detected with this method.

When the velocity of sound for benzene is plotted against frequency over many orders of magnitude, an "S" shaped curve results which shows negligible velocity dispersion in the limits of very low and very high frequencies. We appear to be at the high end and close to the calculated maximum value of 1540 m/sec at 22.6° C, therefore only a very small positive dispersion is still possible.

The relaxation time appears to be of the correct order of magnitude, but because it has only a small effect on our calculations, an attempt to resolve the ambiguity between the different values is not useful for our measurements. With Brillouin scattering, we can determine if a given value for the relaxation time is too small since the Mountain line due to the relaxation should extend beyond the Brillouin peaks and be readily visible in an experimental spectra. Unfortunately we can judge only qualitatively if it is too large by examining the amount of dissymmetry in the Brillouin peaks.

The Brillouin spectra of solutions appear to require concentrations of at least an order of magnitude smaller than is necessary with regular photometric light scattering measurements. This is both an advantage and a disadvantage, since smaller quantities of solute are necessary, but the concentrations are much harder to determine accurately. This disadvantage appears to be one of the larger sources of error in our solution measurements of macromolecules.

If the solute in a relaxing liquid significantly affects the liquid parameters  $v_0$ ,  $v_\infty$ , and  $\boldsymbol{7}$  as noted in Mountain's

theory, the theory developed by Miller for the determination of the molecular weights of macromolecules requires modification. Any changes in these parameters will be reflected by changes occurring in the Brillouin peak with changing concentrations, such as broadening of the peak half-widths or by frequency shifts. We have found no such changes in our experimental resolution, indicating that Miller's theory is valid for our solvent, solute, and for our concentration range.

The molecular weights of macromolecules obtained from Brillouin scattering are consistent with other values measured by viscosity or regular photometric light scattering although they appear to have a lower precision. The angular measurements from the largest macromolecules are more consistent than those at different concentrations, indicating that a large percentage of the final error may be due to the concentration determination. Also the variation in the second virial coefficients with different macromolecules can be attributed to errors in concentration determinations.

# B-Viscosity

The molecular weight of a macromolecule is determined by measuring the increased viscosity of a solution of this macromolecule over the viscosity of the pure solvent. When a capillary viscometer is used, this method is a standard procedure which can be used to further evaluate molecular weights obtained with Brillouin light scattering, Table 3.

### 1-Constant Temperature Bath

A constant temperature water bath was constructed from a large battery jar placed inside a plywood box and insulated with two inches of foamed polystyrene, Figure 21. The bath temperature was controlled with a Yellow Springs model 72 proportional controller which reduced the temperature variation to ±.003° C. The temperature was accurately determined to better than 0.01° C with a calibrated mercury thermometer that had been standardized against a platinum resistance thermometer.

### 2-Viscometer

The capillary dilution viscometer, Cannon-Ubbelode model 50K414, was first studied to determine if kinetic energy corrections were necessary in the viscosity calculations. The elution time for a fixed volume of two liquids with different known viscosities was measured and substituted into the following equation to determine the constants [66].

$$\eta = \alpha \rho_0 \left( t_0 - \frac{\beta}{\alpha t_0} \right)$$

Using water and benzene as the two liquids, the constants at 30.00° C, with  $\rho_{O}$  the density, are

$$\alpha = 3.70 \times 10^{-3} \frac{\text{poise-ml}}{\text{gm-sec}}$$
, and  $\beta = 1.25 \frac{\text{poise-ml}-\text{sec}}{\text{gm}}$ .

For an elution time  $t_0$  of order 200 sec. or more, the second

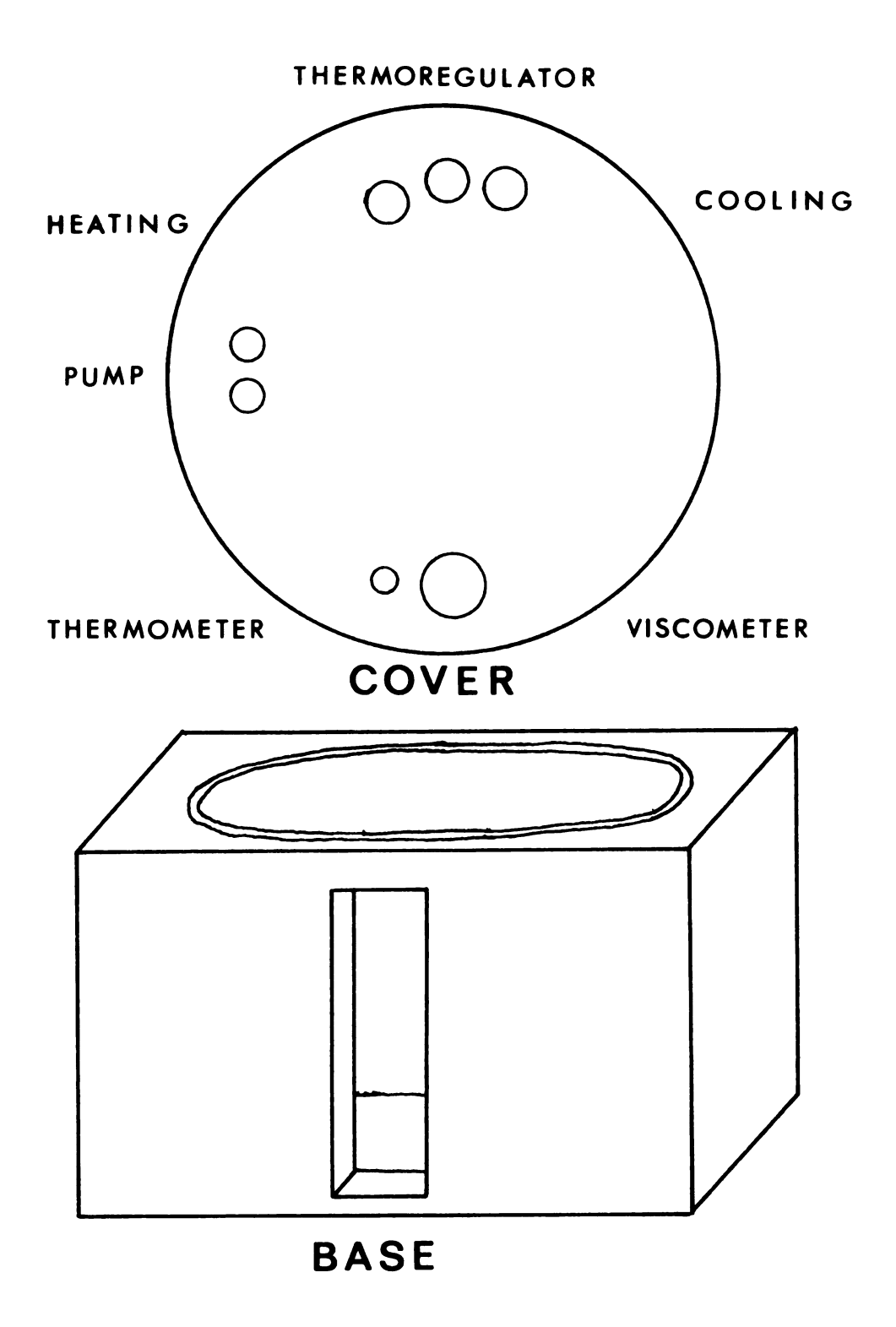


Figure 21. Constant Temperature Water Bath

term in equation <u>91</u> is 0.86% or less of the first term. This value is small enough to be neglected without serious error when determining the viscosity of a liquid, indicating that kinetic energy corrections are not necessary when an error of about 1% can be tolerated.

### 3-Solutions

All solutions and solvents were filtered through a small fritted glass filter of pore size 40-60 microns attached to the viscometer in order to eliminate dust or large particles. The elution times for both the solvent and solutions were constant to within 0.1 sec. even after cleaning the viscometer, indicating that no large dust particles were present nor were macromolecules absorbed on the capillary walls.

The increased viscosity of a liquid due to an added macromolecule is measured in terms of a relative viscosity  $\eta_{\rm rel}$ , and a specific viscosity  $\eta_{\rm sp}$ , with the assumption that the solution is dilute and the density of the solution is equal to that of the solvent. The following equations are then used by substituting the elution time  $t_0$  for the pure solvent and t for the solution.

$$\eta_{\text{rel}} = {}^{\text{t}}/{}^{\text{t}}_{\text{O}}$$
 ;  $\eta_{\text{sp}} = {}^{(\text{t-t}_{\text{O}})}/{}^{\text{t}}_{\text{O}}$   $\underline{92}$ 

To obtain the limiting viscosity number [  $\eta$ ], the viscosity number  $\eta_{\rm sp}/c_2$  is plotted against  $c_2$  using the Huggins equation.

$$\eta_{\text{sp/c}_2} = [\eta] + k_1 [\eta]^2 c_2$$

Simultaneously the data is plotted with the Kraemer equation.

$$\frac{\mathbf{k}_{n} (\mathbf{\eta}_{rel})}{\mathbf{c}_{2}} = [\mathbf{\eta}] + \mathbf{k}_{2} [\mathbf{\eta}]^{2} \mathbf{c}_{2}$$
 94

The common intercept  $[\eta]$  of both equations is then used in the Mark-Houwink equation along with values of k and a from elastic light scattering measurements.

$$[ \mathbf{\eta} ] = K \overline{M}_{w}^{a}$$
 95

For narrow molecular weight polystyrenes in benzene at  $30.0^{\circ}$  C, the constants are  $K = 9.7 \times 10^{-5}$  dl/gm, a = 0.74. [64].

The molecular weights obtained from these viscosity measurements are listed in Table 1 along with the values for Brillouin scattering and other sources for comparison. As a check on the viscosity measurements, we note that  $k_1 - k_2 = 0.50$  for a macromolecule in a good solvent. Our values for this difference are in excellent agreement and the plots shown in Figures 22, 23, and 24 are all straight lines without deviations at either end. Also the relative viscosity  $\pmb{\eta}_{\rm rel}$ , is within the range of 1.1 to 1.9, thus allowing an accurate measurement of the relative viscosity changes.

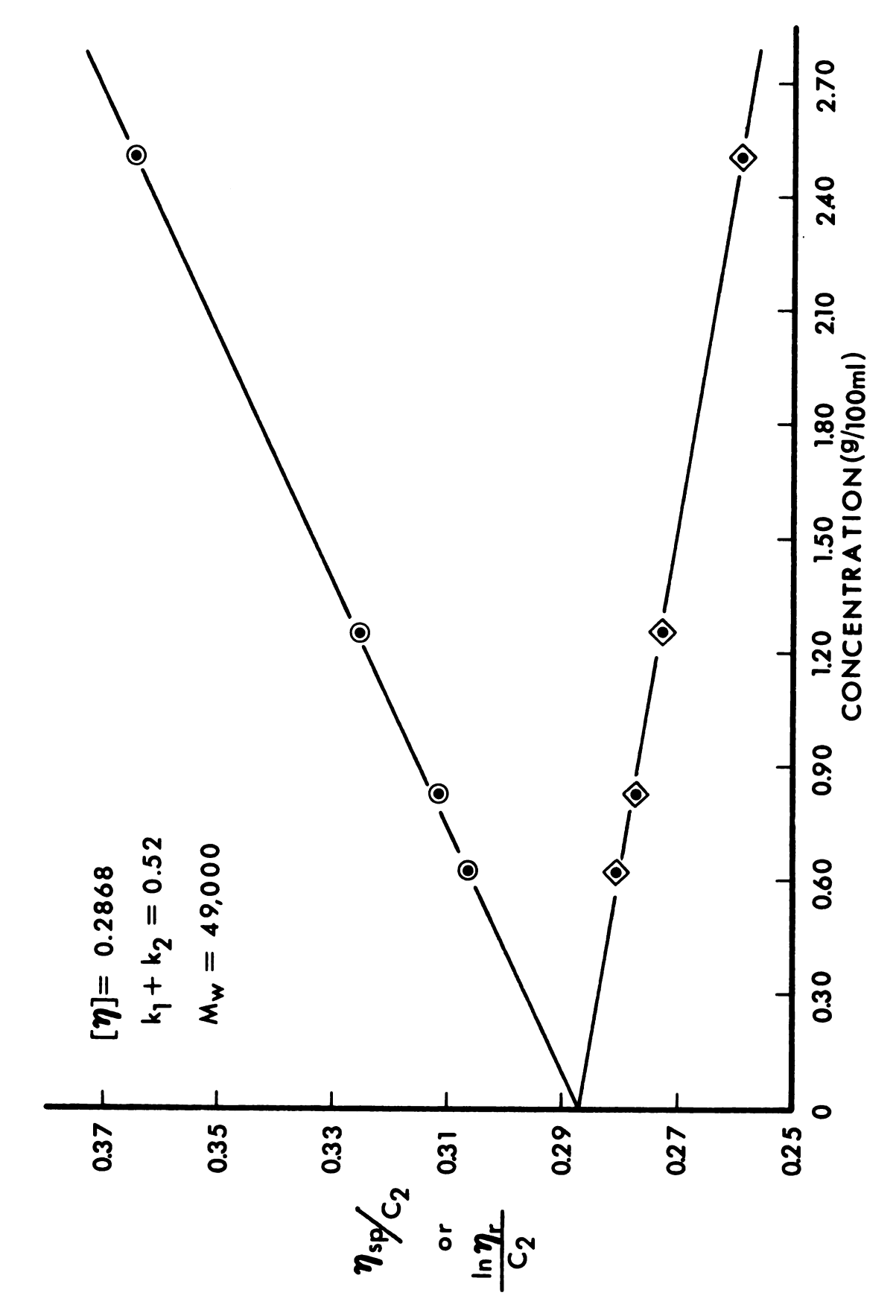


Figure 22. Viscosity of Polystyrene in Benzene at 30.0° C

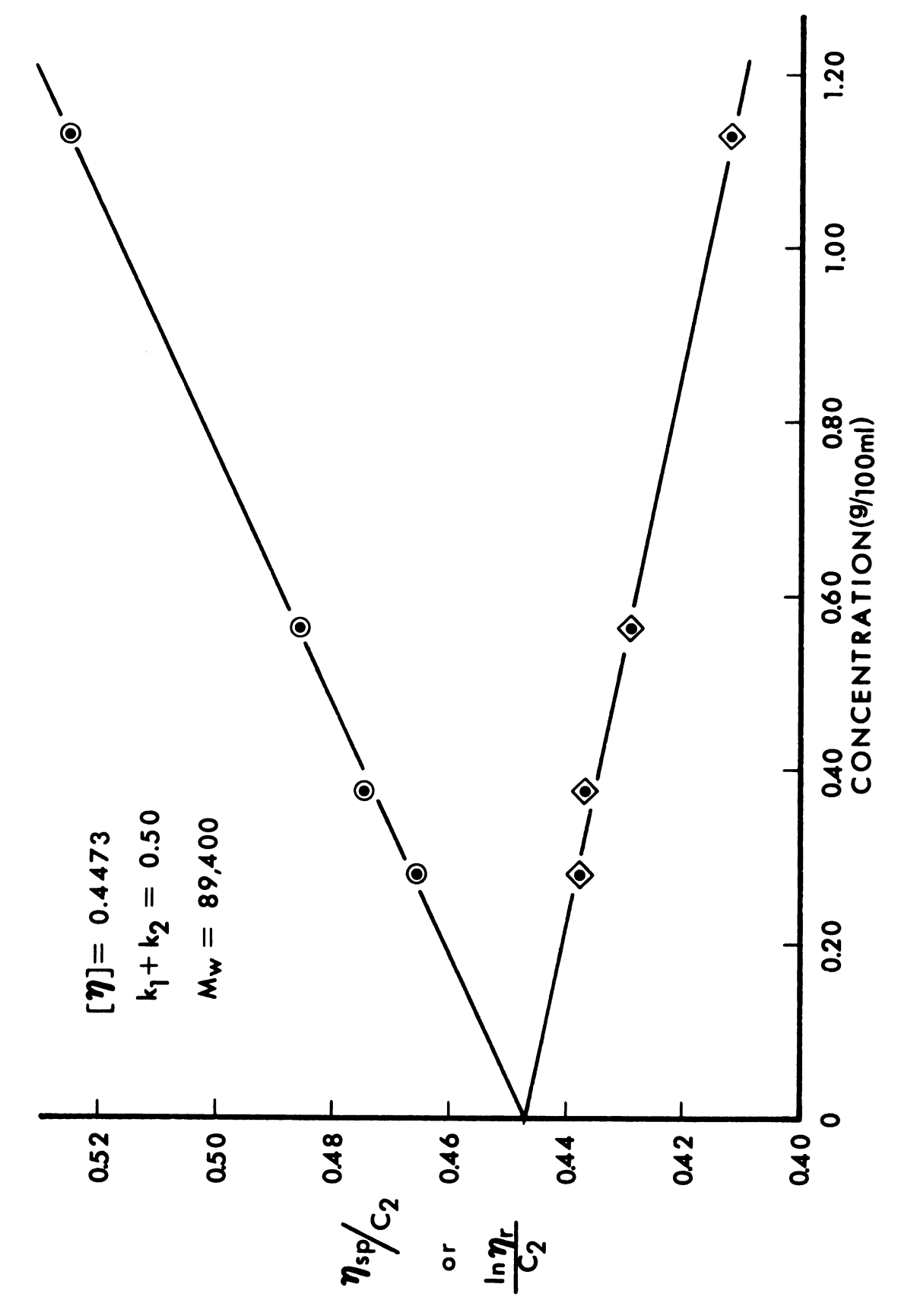


Figure 23. Viscosity of Polystyrene in Benzene at 30.0° C

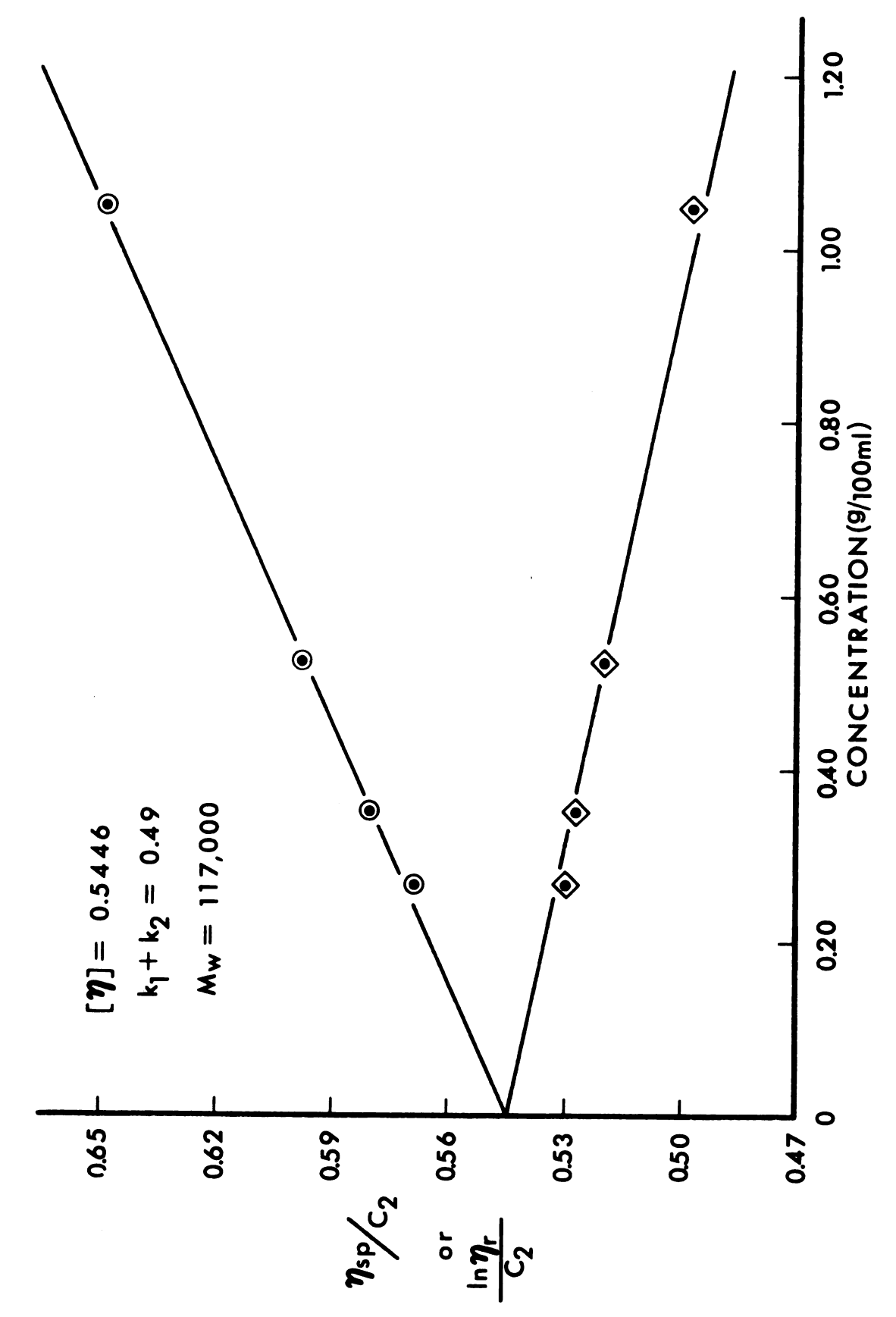


Figure 24. Viscosity of Polystyrene in Benzene at 30.0° C

## IV-Summary and Conclusions

The thermodynamic theory of Miller for measuring the molecular weight of macromolecules in solution was examined by first developing an instrumental alignment procedure to experimentally separate the Rayleigh and Brillouin peaks.

This procedure achieved a minimal peak overlap over the range of scattering angles from 45 to 135 degrees for a single interferometer mirror separation.

Brillouin spectra were taken and the isotropically scattered light was identified, separated and measured. A good correspondence was found between the ratio  $J_{\rm V}$  for the experimental measurements and the calculations from Mountain's theory for a thermally relaxing liquid, indicating that the correct spectral base line was selected. Also an extra relaxation peak, the Mountain line, was tentatively identified and the relaxation time, which is related to its half-width, was calculated by three different methods.

Macromolecular solutions were measured with Brillouin scattering and it was found that for dilute solutions of polystyrene in benzene the solute did not affect the solvent parameters  $\mathbf{v}_0$ ,  $\mathbf{v}_\infty$ , and  $\boldsymbol{\tau}$  to any measurable extent. The consistency of these parameters in a solution is critical for applying accurately Miller's thermodynamic theory. Also an extensive cleaning and filtering procedure was developed to give consistent scattering measurements from sample solutions.

The Brillouin spectra of six macromolecules with different molecular weights were experimentally measured and then their molecular weights were calculated using Miller's theory. The values compared well with other techniques obtained using photometric light scattering and viscosity measurement, although a lower precision was noted. Also the concentrations needed for measurement were found to be about an order of magnitude smaller than those needed for photometric measurements. Accurate angular measurements for scattering from large macromolecules required the design of a new scattering cell and simultaneous extrapolation of the measurements to zero concentration and zero scattering angle.



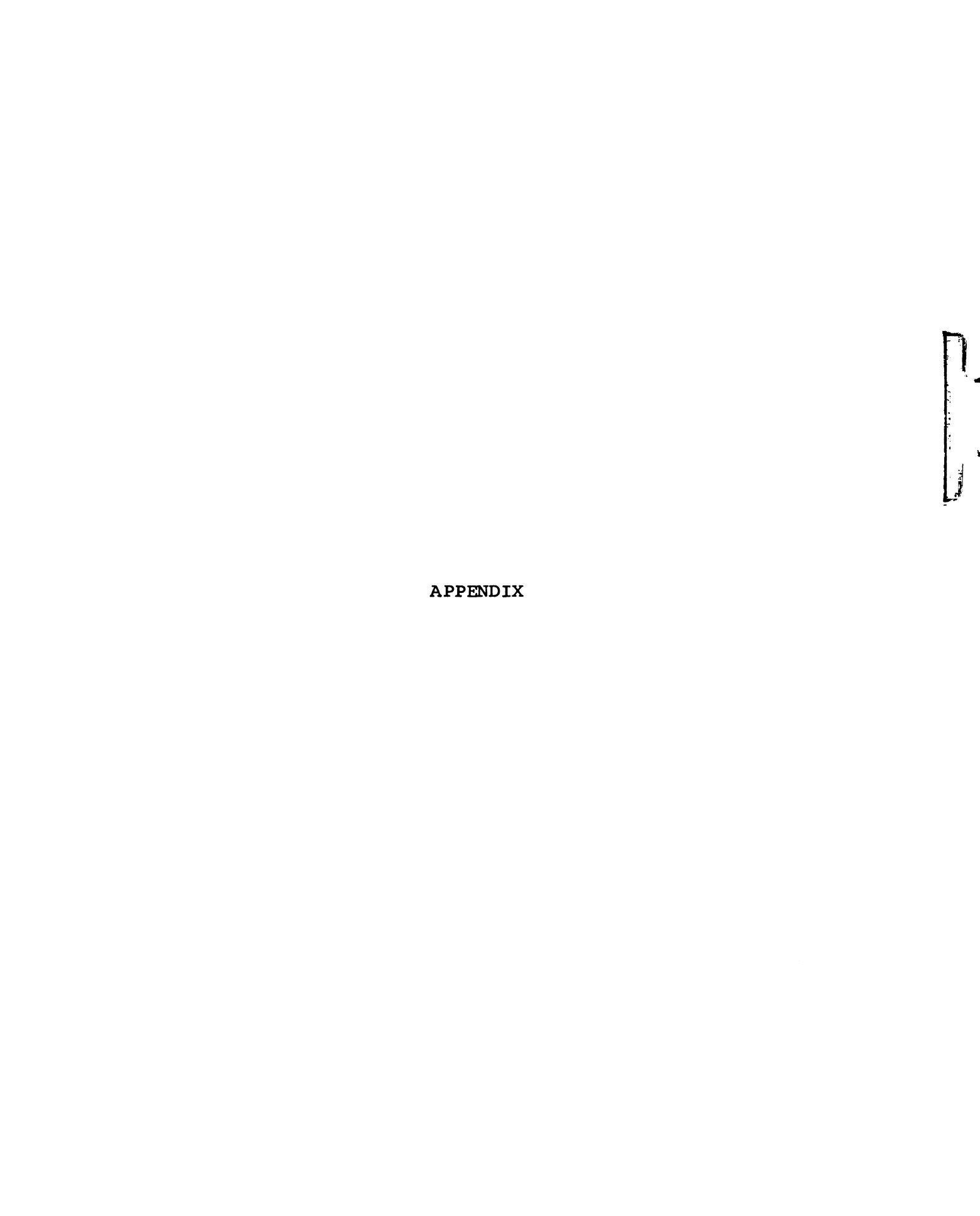
# Bibliography

- 1 J. Tyndall, Phil. Mag. 37 384 (1869)
- 2 J. W. Strutt, Phil. Mag. <u>41</u> 447 (1871)
- 3 J. W. Rayleigh, Phil. Mag. 42 81 (1881)
- 4 J. W. Rayleigh, Phil. Mag. 47 375 (1899)
- 5 A. Einstein, Ann. Physik. 33 1275 (1910)
- 6 L. Brillouin, Ann. Physique (Paris) 17 88 (1922)
- 7 E. Gross, Nature <u>126</u> 201 (1930)
- 8 G. G. Sukhotina, M. I. Shakhparonov, Moscow Univ. Chem. Bull. 21 5 (1966)
- 9 P. Debye, J. App. Phys. <u>15</u> 338 (1944); J. Phys. Chem. <u>51</u> 18 (1947)
- 10 B. H. Zimm, J. Chem. Phys. <u>16</u> 1099 (1948)
- 12 A. Javan, W. J. Bennet, Jr., D. R. Herriott, Phys.Rev. Lett. 6 106 (1961)
- 13 R. Y. Chiao, B. P. Stoicheff, J. Opt. Soc. Amer.
  54 1286 (1964)
- 14 G. Benedek, T. Greytak, I.E.E.E. <u>53</u> 1623 (1965)
- 15 G. A. Miller, C. S. Lee, J. Phy. Chem. 72 4644 (1968)
- 16 G. A. Miller, J. Phys. Chem. 71 2305 (1967)
- 18 H. W. Leidecker, J. T. La Macchia, J. Acoust. Soc. Amer. 43 143 (1968)
- 19 L. Fishman, R. D. Mountain, J. Phys. Chem. <u>74</u> 2178 (1970)
- 20 I. L. Fabelinskii, "Molecular Scattering of Light," Plenum Press, New York, (1968)
- 21 G. Dezelic, Pure and Applied Chem. 23 327 (1970)

- 22 L. D. Landau, G. Placzek, Z. Phys. Sowjetunion 5 172 (1934)
- 23 H. Z. Cummins, R. W. Gammon, J. Chem. Phys. <u>44</u> 2785 (1966)
- 24 J. Frenkel, "Kinetic Theory of Liquids," Dover, New York 1946, p.235
- 25 R. D. Mountain, T. A. Litovitz, J. Acoust. Soc. <u>42</u> 516 (1967)
- 26 R. Figgins, Contemp. Phys. 12 283 (1971)
- 27 H. N. W. Lekkerkerker, W. G. Laidlaw, Phys. Rev. <u>5A</u> 1604 (1972)
- 28 R. D. Mountain, Rev. Mod. Physics 38 205 (1966)
- 29 H. L. Frish, Physics 2 209 (1966)
- 30 B. J. Berne, J. P. Boon, S. A. Rice, J. Chem. Phys. <u>47</u> 2283 (1967)
- 31 W. S. Gornall, C. S. Wang, C. C. Yang, N. Bloembergen, Phys. Rev. Lett. <u>26</u> 1094 (1971)
- 32 L. von Hove, Phys. Rev. <u>95</u> 249 (1954)
- 33 L. I. Komarov, I. Z. Fisher, Soviet Physics J.E.P.T. 16 1358 (1963)
- 34 D. J. Coumou, E. L. Mackor, J. Hijmans, Trans. Faraday Soc. 60 1539 (1964)
- 35 H. F. P. Knapp, W. S. Gornall, B. P. Stoicheff, Phys. Review <u>166</u> 139 (1968)
- 36 R. D. Mountain, J. Res. N.B.S. 70A 207 (1966)
- 37 W. S. Gornall, G.I.A. Stegeman, B. P. Stoicheff, R. H. Stolen, V. Volterra, Phys. Rev. Lett. <u>17</u> 297 (1966)
- 38 N. C. Ford, Jr., G. B. Benedek, N.B.S. Pub. 273 (1966) p.157
- 39 K. F. Herzfeld, T. A. Litovitz, "Absorption and Dispersion of Ultrasonic Waves," Academic Press, New York, (1959)
- 40 G. A. Miller, J. Phys. Chem. <u>71</u> 2305 (1967)
- 41 P. Debye, J. Phys. Colloid Chem. <u>51</u> 18 (1947)
- 42 J. E. Piercy, G. R. Hanes, J. Acoust. Soc. Amer. <u>49</u> 1001 (1971)

- 43 M. A. Leontovich, J. Phys. U.S.S.R. 4 499 (1941)
- 44 S. M. Rytou, Sov. Phys. J.E.P.T. 6 130,401,513 (1958)
- 45 L. D. Landau, E. M. Lifshitz "Electrodynamics of Continuous Media," Addison-Wesley, Reading, Mass., 1960 Chapt. 14
- 46 A. B. Bhatia, E. Tong, Phys. Rev. 173 231 (1968)
- 47 C. Chung, S. Yip, Phys. Rev. 4A 928 (1971)
- 48 H. N. W. Lekkerkerker, J. P. Boon, Phys. Lett. <u>39A</u> 9 (1972)
- 49 H. Morawetz, "Macromolecules in Solution," Interscience, New York, 1965, Chapt. VI
- 50 P. J. Flory, J. Chem. Phys. <u>17</u> 303 (1949)
- 51 S. J. Gaumer, Ph.D. Thesis, Michigan State University, East Lansing, Michigan, 1972.
- 52 V. Met, Laser Techn., Sept. 45 (1967)
- 53 M. Born, E. Wolf, "Principles of Optics," Pergamon Press, Oxford, Great Britain, (1965)
- 54 H. K. Yuen, Ph.D. Thesis, Michigan State University, East Lansing, Michigan 1973
- 55 C. J. Montrose, V. A. Solovyev, T. A. Litovitz, J. Acoust. Soc. Amer. 43 117 (1968)
- 56 S. Gewurtz, W. S. Gornall, B. P. Stoicheff, J. Acoust. Sol. 49 994 (1971)
- 57 E. Zamir, N. D. Gershon, A. Ben-Reuven, J. Chem. Phys. 55 3397 (1971)
- 58 D. P. Eastman, A. Hollinger, J. Kenemuth, D. A. Rank, J. Chem. Phys. <u>50</u> 1567 (1969)
- 59 W. H. Nichols, C. R. Kunsitis-Swyt, S. P. Singal, J. Chem. Phys. <u>51</u> 5659 (1969)
- 60 R. Y. Chiao, P. A. Fleury, "Physics of Quantum Electronics," J. Wiley, 1966, p.241
- 61 G. I. A. Stegeman, B. P. Stoicheff, Phys. Rev. Lett. <u>21</u> 202 (1968)

- 62 C. L. O'Connor, J. P. Schlupf, J. Acoust. Soc. Amer. 40 663 (1966)
- 63 J. B. Kinsinger, "Viscosity," Encyclopedia of Polymer Science, C 1971, vol.14, p.717
- 64 R. H. Boundy, R. F. Boyer, "Styrene, its Polymers, Copolymers and Derivatives," Reinhold, New York, 1952
- 65 D. E. Nordhaus, J. B. Kinsinger, "Brillouin Spectroscopy of Macromolecular Solutions," J. Polymer Sci. (to appear)



## Appendix

The alignment procedure for the Brillouin spectrophotometer is divided into three parts which are to be done sequentially: (1) alignment of the two optical paths, (2) alignment of the interferometer and (3) alignment of the lenses and pinholes. Each of these sections is often divided into an initial adjustment to locate approximate settings and positions, then a fine alignment to achieve the best finesse. A two step procedure of this type is necessary since a slight misalignment of one component may be masked with the subsequent introduction of other components and resulting in a low finesse.

This instrument is very sensitive to alignment, especially the interferometer, so the fine adjustments must be done very carefully; even then parts (2) and (3) are often redone after taking each spectrum. The alignment is affected by small building vibrations, room temperature variations and mechanical slippage of the micrometer screws resulting in distorted spectra and large decreases in finesse, as from 50 to 30 or less in a very short time. Efforts were made during the design to reduce building vibrations by placing all the components on an acoustically isolated table. Large temperature variations in the room were reduced by keeping the room doors closed during experimental runs and attaching a permanent sealing strip around the doors. This sealing strip also reduced the amount of dust entering

the room. Even with these precautions the average time required for one good spectral run was about 2.5 hours because frequent realignments were still necessary.

This instrument has two parallel tracks, one containing the laser and movable mirror and the other an alignment laser, angular adjustment table, collecting lens, interferometer, resolving lens, and detector. For best results all optical components are cleaned before use since they readily accumulate dust and grease from the air in the room. In the following stepwise alignment procedure, the initial positions of each component are shown in Figure (1).

# Alignment of Optical Paths

- 1 Locate the argon laser approximately parallel to the long edge of the table top and adjust the beam height to 25 cm above the table surface.
- 2 Align the beam height of the argon laser so it is parallel to the surface of the table by passing the beam through two pinholes 3mm in diameter and 25cm high placed at both ends of an optical rail which is located at the other end of the table from the laser.
- 3 Remove the pinholes and place the movable front surfaced mirror on the optical rail, then adjust the height of the mirror so the argon laser beam strikes the approximate center of the mirror.

- 4 Place the alignment laser in the second track so that the beam height is also 25 cm above the table surface and approximately in line with the "dovetail" optical rails inside the two light tight boxes. Both the alignment beam and optical rails should be parallel to the long edge of the table top.
- 5 Take two pinholes 2 mm in diameter, labeled No.1 and No.2, and adjust their heights to 25 cm above the table surface when they are placed on the optical rails inside the light tight boxes.
- 6 Place one pinhole on the optical rail near the photomultiplier tube (PMT) and adjust the alignment laser to pass the beam through this pinhole.
- 7 Place the other pinhole on the rail in front of the first and adjust its height to that of the alignment beam. Check that both pinholes are perpendicular to the alignment beam and not twisted at an angle.
- 8 Reverse the positions of the two pinholes and repeat step No.7 until both pinholes are identical in height, 25 cm above the table top, and passing the alignment beam into the center of the PMT.
- 9 Remove pinhole No.1, place it inside and in the front of the front box, then adjust the alignment laser to pass the beam through both pinholes.
- 10 Remove pinhole No.2, place it inside and in the back of the front box, then adjust the position of the optical rail so the alignment beam passes through both pinholes.

- 11 Remove both pinholes and place them at opposite ends of the rear optical rail, then adjust the position of this rail until the alignment beam passes through both pinholes. Replace pinhole No.l inside and in the front of the front box. At this point the alignment beam and both optical rails should be parallel.
- 12 Set the Bridgeport rotary table to zero degrees by turning into this setting with a clockwise movement.
- 13 Adjust the center position of the Bridgeport table to coincide with the alignment beam by placing a sharp needle at its center and moving the Bridgeport table laterally until the needle bisects the alignment beam as seen by the shadow of the needle on the pinhole in the front box.
- 14 Adjust the permanent pinholes, 1 mm in diameter, at each edge of the Bridgeport table to pass the alignment beam. These steps set the height of the incident beam and at the same time establish the zero scattering angle so that any other angle can be selected with a precision of  $\pm$  3 sec. of arc.
- 15 Rotate the Bridgeport table to 90 degrees and then place the collimating tube containing the adjustable pinholes at each end into the front end of the front box.
- 16 Adjust the position of this tube so the front pinhole is about 8 cm from the center of the Bridgeport table.

17 - Close each adjustable pinhole located on the ends of the collimating tube in turn, center them on the alignment beam, and then open them fully.

# Alignment of the Interferometer

- 1 Place two special pinholes 4 mm in diameter into the front and back of the interferometer body after uncoupling the front and back bellows which connect the interferometer to the boxes. Adjust the interferometer body and its platform to pass the alignment beam through these pinholes.
- 2 Remove the special alignment pinholes from the interferometer body, replace the bellows, place the rear interferometer mirror in the approximate position to be used and place pinhole No.l in the front of the front box.
- 3 Adjust the body of the interferometer so the reflected beam passes through the pinhole on the optical rail in the front box.
- 4 Place both front and back mirrors in the interferometer at a spacing for the desired spectral range and again adjust the body of the interferometer to allow the main reflected beam from the front mirror to pass through the pinhole on the optical rail in the front box. Both steps No.3 and No.4 need to be only approximate adjustments.
- 5 Place the interferometer in the scan mode at a rate of about one spectral order per five seconds, place the

cover on the interferometer and hold a white card in back of the back interferometer mirror to examine the transmitted beam, then adjust the micrometer screws to align the interferometer mirrors so they are parallel. Initially only a bright line is seen extending from about the center of the original optical path to an outside edge. This line points in the direction that the mirrors are spreading apart and thus indicates which direction the mirrors must be adjusted to realign them parallel. As the mirrors are adjusted closer to parallel, this line decreases in length until it finally forms a series of diffuse concentric circles.

- 6 Adjust the body of the interferometer to reflect the alignment laser beam through the front pinhole then readjust the micrometer screws to obtain parallel interferometer mirrors. Repeat this procedure twice so that the two following critical concitions are met: first the interferometer mirrors are perpendicular to the alignment beam and second, the mirrors are parallel to each other.
- 7 Remove the white card and place a long focal length lens (100 cm) in back of the interferometer so its focal plane is about 3 cm in front of the face of the PMT.
- 8 Adjust this lens so the alignment beam passes through the rear pinhole in its focal plane.
- 9 Remove the pinhole in the front box and place a white card about 10 cm behind the rear lens. The main alignment beam is then seen on the white card as a bright spot with a slight halo, both of which are surrounded by

unfocused concentric rings at increasing distances from the center.

- 10 Adjust the body of the interferometer so the halo about the central spot of the alignment laser is symmetrical, then readjust the micrometer screws to give a symmetrical ring pattern. This halo is a back reflection due to the incident beam first striking the front mirror, being reflected to the front alignment laser mirror and reflected again down the original path. In this way we can achieve an excellent interferometer alignment by using the double reflected beam as an exact check.
- 11 Remove both the rear pinhole and the white card in back of the rear lens. Place the card at the focal point of this lens and realign the mirrors parallel as judged by the focused rings which are symmetrical and converge on a central spot.
- 12 The rear interferometer mirror appears to be driven slightly off axis by the piezoelectric crystal, therefore during the scan over about five spectral orders, the mirrors should be aligned so the first two orders are slightly unsymmetrical in one direction, the third order is symmetrical about the central spot and the last two are slightly unsymmetrical in the opposite direction. Only the three central orders are used in the analysis.

## Alignment of Lenses and Pinholes

- 1 Place a lens of focal length 50 cm in the front box so its focal point is located at the center of the scattering volume. An exact placement is not necessary within ± 2 cm since the divergence angle of the scattered light is very small.
- 2 Replace pinhole No.1 on the optical rail in front
  of this front lens.
- 3 Adjust the front lens so the reflected alignment beam from the front and back surfaces of the lens passes through the pinhole as well as the reflected beam from the interferometer mirrors.
- 4 Remove pinhole No.1 and finely adjust the front lens so the rings on the white card in the rear of the back box converge symmetrically on the central spot.
- 5 Remove this white card and replace it with a pinhole of 2mm in diameter which blocks out all transmitted light
  except that from the central spot at the focal point of the
  back lens and center it exactly on the central spot from the
  alignment beam.
- 6 Adjust the front pinhole in the collimating tube to 1 mm in diameter and the second pinhole to 2 mm in diameter. This is easily done by inserting a wire of that specific size in the adjustable pinhole then closing down the pinhole until it strikes the wire.

- 7 Place a large adjustable pinhole, 1 cm in diameter between the front lens and the front interferometer mirror.
- 8 Close both front and rear light-tight boxes, place the scattering cell in position and align it in the crossed beams from both lasers.
- 9 Turn off the alignment laser and the room lights, open the shutter in front of the PMT and begin to take the Brillouin spectra.

The usual instrumental settings used for scattering from pure benzene are listed below for reference.

Laser - 400 mw at 5145A°, single mode.

PMT - 1,200 vts

PMT Cooling - -10°C

Preamp. Head - 0 to  $10^{-9}$  amps

Damping - 30% of maximum

Voltage Supression - 0.0 vts

Recorder - 0 - 100 mv scale

fast chart speed
lowest damping

